

**AN *IN VITRO* INVESTIGATION OF NOVEL QUINOLONE DERIVATIVES ON
SELECTED PHARMACOLOGICAL TARGETS FOR DIABETES MELLITUS AND
ASSOCIATED COMPLICATIONS**

A thesis submitted in fulfilment of the requirements for the degree of

Master of Science (Pharmacy)

By

Omobolanle Opeyemi Ayodele

November 2022



RHODES UNIVERSITY
Where leaders learn

ACKNOWLEDGEMENTS

I would like to express my sincere appreciation to God Almighty for the strength, mercy and grace to pursue this research and see it through.

My profound gratitude goes to my supervisor Dr N Sibiya for his advice, guidance, innovative and immense contribution to the success of this work. I will also like to thank my co-supervisors, Prof SD Khanye and Prof MM Mothibe, for their contribution to the success of this work.

I am sincerely grateful to the Rhodes University Postgraduate Funding Office for its financial support.

I wish to thank my parents, Prof. SM Ayodele and Mrs EE Ayodele and my siblings, Oluwakemi and Boluwatife, for their prayers, support and encouragement throughout my research journey.

Finally, I want to thank my colleagues and friends, especially Williams, for his support and encouragement throughout this journey.

May God Almighty reward you all abundantly.

TABLE OF CONTENT

ACKNOWLEDGEMENTS	i
LIST OF FIGURES	vii
LIST OF TABLES	xii
ABSTRACT.....	xiii
LIST OF ABBREVIATIONS.....	xv
CHAPTER 1: LITERATURE REVIEW	1
1.1 INTRODUCTION	1
1.2 GLUCOSE HOMEOSTASIS	2
1.2.1 Carbohydrate digestion and absorption	3
1.2.2 Insulin	4
1.2.2.1 Insulin secretion	4
1.2.2.2 Insulin signalling.....	6
1.3 DIABETES MELLITUS	8
1.3.1 Type 1 diabetes mellitus	8
1.3.2 Type 2 diabetes mellitus	9
1.3.3 Aetiology of diabetes mellitus complications.....	9
1.3.4 Diabetes mellitus complications	10
1.3.4.1 Microvascular complications	10
1.3.4.1.1 Diabetic retinopathy.....	10
1.3.4.1.2 Diabetic nephropathy	11
1.3.4.1.3 Diabetic neuropathy	11
1.3.4.2 Macrovascular complications	12
1.4 LINK BETWEEN DIABETES MELLITUS AND CARDIOVASCULAR DISEASES.....	12

1.5	MANAGEMENT OF DIABETES MELLITUS AND CARDIOVASCULAR DISEASES	15
1.5.1	Diabetes mellitus.....	15
1.5.1.1	Insulin therapy	16
1.5.1.2	Sulphonylureas.....	16
1.5.1.3	Meglitinides	17
1.5.1.4	Biguanides.....	17
1.5.1.5	Thiazolidinediones.....	18
1.5.1.6	Alpha-glucosidase inhibitors	18
1.5.1.7	Sodium-glucose co-transporter 2 (SGLT2) inhibitors	19
1.5.1.8	GLP-1 receptor agonist.....	19
1.5.1.9	DPP4 inhibitors.....	19
1.5.2	Cardiovascular disease.....	21
1.5.2.1	Antihypertensives	21
1.5.2.2	Anti-lipidaemias.....	21
1.5.2.3	Antiplatelets	22
1.6	EMERGING ALTERNATIVE ANTIDIABETIC AGENTS	22
1.6.1	Quinolones as potential antidiabetic agents.....	22
1.6.1.1	Classification of quinolones.....	23
1.6.1.1.1	First-generation quinolones	23
1.6.1.1.2	Second-generation quinolones	24
1.6.1.1.3	Third-generation quinolones.....	25
1.6.1.1.4	Fourth-generation quinolones	25
1.6.1.2	Effect of quinolones on glucose homeostasis	28
1.6.1.3	Effect of quinolones on glucose uptake by target cells.....	29

1.6.1.4	Insulinotropic effects of quinolones.....	30
1.6.1.5	Quinolone interaction with other anti-hyperglycaemic agents	32
1.6.1.6	Clinical studies.....	32
1.6.1.7	Emergence of quinolone derivatives as an antidiabetic agent	34
1.7	QUINOLONE COMPOUNDS OF INTEREST IN THIS STUDY.....	36
1.8	JUSTIFICATION OF THE STUDY	38
1.9	AIM.....	38
1.10	OBJECTIVES	38
1.10.1	Cell-free assays	38
1.10.2	Cell-based assays	39
CHAPTER 2: MATERIALS AND METHODOLOGY		40
2.1	CHEMICALS.....	40
2.2	EQUIPMENT.....	40
2.3	SYNTHESIS AND CHARACTERISATION OF QUINOLONE DERIVATIVE COMPOUNDS.....	41
2.3.1	Synthesis of ethyl 6-acetyl-4-oxo-1,4-dihydroquinoline-3-carboxylate.....	41
2.3.2	Synthesis of ethyl 6-acetyl-1-ethyl-4-oxo-1,4-dihydroquinoline-3-carboxylate	41
2.3.3	Synthesis of quinolinyl-chalcone hybrids.....	41
2.4	PREDICTING THE DRUG-LIKENESS AND GASTROINTESTINAL ABSORPTION OF THE QUINOLONE DERIVATIVES.....	42
2.5	CELL-FREE ASSAY	42
2.5.1	Preparation of compounds for in vitro testing	42
2.5.2	Antidiabetic assays.....	43
2.5.2.1	Alpha-amylase inhibition assay	43
2.5.2.1.1	Enzyme kinetics and mode of α -amylase inhibition.....	44

2.5.2.2	Alpha-glucosidase inhibition assay.....	45
2.5.2.2.1	Enzyme kinetics and mode of inhibition of α -glucosidase	46
2.5.2.3	DPP4 inhibition assay	47
2.5.2.4	Protein tyrosine phosphatase 1B inhibition assay.....	48
2.5.2.5	Aldose reductase inhibition assay.....	49
2.5.3	Cardio-protective activity assay.....	50
2.5.3.1	Factor Xa inhibition assay	50
2.5.3.2	HMG-CoA reductase assay.....	51
2.5.4	Antioxidant activity assay.....	51
2.5.4.1	DPPH radical scavenging activity assay.....	51
2.5.4.2	Ferric reducing antioxidant power (FRAP) assay.....	52
2.6	CELL-BASED ASSAY	53
2.6.1	Preparations of compounds.....	53
2.6.2	Cell culture and differentiation	53
2.6.3	Glucose uptake assay	54
2.6.4	Cell viability assay	54
2.7	DATA AND STATISTICAL ANALYSIS	55
CHAPTER 3:	RESULTS	56
3.1	DRUG-LIKENESS AND GASTROINTESTINAL ABSORPTION OF THE QUINOLONE DERIVATIVES	56
3.2	CELL-FREE ASSAY	58
3.2.1	Antidiabetic assays.....	58
3.2.1.1	Alpha-amylase inhibition assay	58
3.2.1.1.1	Alpha-amylase kinetics study	59
3.2.1.2	Alpha-glucosidase inhibition assay.....	61

3.2.1.2.1	Alpha-glucosidase kinetics study.....	62
3.2.1.3	DPP4 inhibition assay	64
3.2.1.4	Protein tyrosine phosphatase inhibition assay	65
3.2.1.5	Aldose reductase inhibition assay	66
3.2.2	Cardio-protective activity assay.....	68
3.2.2.1	Factor Xa (FXa) inhibition assay.....	68
3.2.2.2	HMG-CoA reductase inhibition assay	70
3.2.3	Antioxidant assays	71
3.2.3.1	DPPH inhibition assay	71
3.2.3.2	Ferric reducing antioxidant power (FRAP) assay.....	73
3.3	CELL-BASED ASSAY	74
3.3.1	Glucose uptake assay	74
3.3.2	Cell viability assay.....	75
CHAPTER 4:	DISCUSSION.....	77
CHAPTER 5:	CONCLUSIONS, LIMITATIONS AND FUTURE STUDIES.....	91
REFERENCES	93
APPENDICES	116

LIST OF FIGURES

- Figure 1.1:** An illustration of insulin secretion. Increased blood glucose concentration stimulates the GLUT2 transporter on the pancreatic beta cell to transport glucose into the cell. Glucokinase converts glucose to glucose-6-phosphate, which is oxidized, resulting in an increase in levels of ATP. Subsequently, the K_{ATP} channel closes, and the Ca^{2+} channel opens, resulting in the influx of calcium ions into the islet cells. Subsequent events lead to an increase in insulin secretion (20-23). 5
- Figure 1.2:** Insulin signalling pathway illustration. Insulin binds to the insulin receptor leading to the phosphorylation of IRS in tyrosine, activating PI3K and Akt, which stimulates GLUT4 translocation to the cell membrane, hence GLUT4 transports glucose into the skeletal muscle.... 7
- Figure 1.3:** The link between DM and CVD involving hypertension, dyslipidaemia and insulin resistance (83-100)..... 15
- Figure 1.4:** An illustration of fluoroquinolone's mechanism of action in the pancreatic beta-cell. Fluoroquinolones have been demonstrated to block the ATP-sensitive potassium channel. The closure of ATP-sensitive channels results in a subsequent L-type voltage-gated calcium channel opening, resulting in the influx of calcium ions in the islet cells. Subsequent events lead to an increase in insulin secretion (156). 29
- Figure 1.5:** A fluoroquinolone derivative known as quinolinoylguanidine. This compound has a carbonylguanidine group at position 2 (red), an ethoxy group at position 4 (blue), and a fluorine atom at position 6 (green). 35
- Figure 1.6:** Substituted benzimidazole quinolone derivatives synthesised from ciprofloxacin (a) and levofloxacin (b) by reacting o-phenylenediamine with the carboxylic group of ciprofloxacin and levofloxacin. The resulting intermediates were transformed through the Mannich reaction to produce substituted benzimidazole quinolones. These compounds exhibited inhibitory activity against alpha-glucosidase at 200 $\mu\text{g/mL}$ 36
- Figure 1.7:** Structure of the quinolone derivatives investigated for their antidiabetic and cardio-protective properties. The quinolone scaffold is drawn in red, and it is substituted with an ethyl group at position 1 (green), an ethyl ester group at position 3 (blue) and a substituted chalcone moiety at position 6 (black). 37

Figure 3.1: The BOILED-Egg model showing the location of the quinolone derivatives on the model. The yellow region represents BBB penetration, while the white region represents GIT absorption..... 57

Figure 3.2: The inhibition of alpha-amylase activity by quinolone derivatives and acarbose at different concentrations. The data are presented as mean \pm SD represented with error bars, (n = 3), and the asterisk (*) represents the statistical difference between the test compounds and the control at $p < 0.05$ 58

Figure 3.3: Michaelis-Menten curve showing the mode of inhibition of alpha-amylase in the presence (blue) and absence (red) of an inhibitor. The curve was generated by plotting maltose concentration against substrate concentration ranging from 0.25 to 4.0 mM. From the curve, V_{max} and K_m were generated – QD4 at 120 $\mu\text{g/mL}$ $V_{max} = 0.3739$ and $K_m = 0.3155$ while control's $V_{max} = 0.4340$ and $K_m = 0.1604$ 60

Figure 3.4: Lineweaver-Burk plot of the reaction of alpha-amylase in the presence (blue) and absence (red) of an inhibitor. The plot was generated by plotting the reciprocal of the reaction velocity (1/V) against the reciprocal of the substrate concentrations (1/S). From the plot, a mixed-type inhibition of alpha-amylase by QD4 can be deduced because as K_m increases, V_{max} decreases, and the data set lines intersect, but not on the x-axis or y-axis..... 60

Figure 3.5: The inhibition of alpha-glucosidase activity by quinolone derivatives and acarbose at different concentrations. The data are presented as mean \pm SD represented with error bars, (n = 3), and the asterisk (*) represents the statistical difference between the test compounds and the control at $p < 0.05$ 61

Figure 3.6: Michaelis-Menten curve showing the mode of inhibition of alpha-glucosidase in the presence (blue) and absence (red) of an inhibitor. The curve was generated by plotting *p*-nitrophenyl concentration against substrate concentration ranging from 0.125 to 4.0 mM. From the curve, V_{max} and K_m were generated – QD1 at 120 $\mu\text{g/mL}$ $V_{max} = 8.244$ and $K_m = 2.158$ while control's $V_{max} = 8.268$ and $K_m = 1.505$ 63

Figure 3.7: Lineweaver-Burk plot of the reaction of alpha-glucosidase in the presence (blue) and absence (red) of an inhibitor. The plot was generated by plotting the reciprocal of the reaction velocity (1/V) against the reciprocal of the substrate concentrations (1/S). From the plot,

competitive inhibition of alpha-glucosidase by QD1 can be deduced because as K_m increases, V_{max} remains constant, and the data set line intersect on the y-axis..... 63

Figure 3.8: The inhibition of DPP4 by quinolone derivatives at different concentrations and sitagliptin at IC_{50} concentration. The data are presented as mean \pm SD represented with error bars, (n = 3), and the asterisk (*) represents the statistical difference between the test compounds and the control at $p < 0.05$ 64

Figure 3.9: The inhibition of PTP1B by quinolone derivatives and sodium orthovanadate at different concentrations. The data are presented as mean \pm SD represented with error bars, (n = 3), and the asterisk (*) represents the statistical difference between the test compounds and the control at $p < 0.05$ 66

Figure 3.10: The inhibition of aldose reductase activity by quinolone derivatives and quercetin at different concentrations. The data are presented as mean \pm SD represented with error bars, (n = 3), and the asterisk (*) represents the statistical difference between the test compounds and the control at $p < 0.05$ 67

Figure 3.11: The inhibition of FXa by quinolone derivatives at different concentrations and GGACK dihydrochloride. The data are presented as mean \pm SD represented with error bars, (n = 3), and the asterisk (*) represents the statistical difference between the test compounds and the control at $p < 0.05$ 69

Figure 3.12: The inhibition of HMG-CoA reductase by quinolone derivatives and pravastatin at different concentrations. The data are presented as mean \pm SD represented with error bars, (n = 3), and the asterisk (*) represents the statistical difference between the test compounds and the control at $p < 0.05$ 70

Figure 3.13: DPPH radical scavenging activity by quinolone derivatives and ascorbic acid at different concentrations. The data are presented as mean \pm SD represented with error bars, (n = 3), and the asterisk (*) represents the statistical difference between the test compounds and the control at $p < 0.05$ 72

Figure 3.14: Ferric reducing antioxidant power of quinolone derivatives and ascorbic acid at different concentrations. The data are presented as mean \pm SD represented with error bars, (n = 3),

and the asterisk (*) represents the statistical difference between the test compounds and the control at $p < 0.05$ 73

Figure 3.15: Media glucose concentration after exposing C2C12 cells to quinolone derivatives at 15, 30 and 60 $\mu\text{g/mL}$ for 24 hours. The data are presented as mean \pm SD represented with error bars, ($n = 3$). The horizontal line at 23.5 mmol/L represents the media glucose concentration at time = 0 hours. 74

Figure 3.16: Media glucose concentration after exposing HepG2 cells to quinolone derivatives at 15, 30 and 60 $\mu\text{g/mL}$ for 24 hours. The data are presented as mean \pm SD represented with error bars, ($n = 3$), and the asterisk (*) represents the statistical difference between the test compounds and the control at $p < 0.05$. The horizontal line at 6.4 mmol/L represents the media glucose concentration at time = 0 hours..... 75

Figure 3.17: Percentage cell viability for C2C12 cell lines after 24 hours of exposure to quinolone derivatives at 15, 30 and 60 $\mu\text{g/mL}$. The horizontal line at 100% represents the control. The data are presented as mean \pm SD represented with error bars, ($n = 3$). 76

Figure 3.18: Percentage cell viability for HepG2 cell lines after 24 hours of exposure to quinolone derivatives at 15, 30 and 60 $\mu\text{g/mL}$. The horizontal line at 100% represents the control. The data are presented as mean \pm SD represented with error bars, ($n = 3$). 76

Figure 4.1: Structure of sitagliptin, a known DPP4 inhibitor. The trifluoromethyl (CF_3) group on the structure is essential for binding to DPP4 side chain residue Ser209 and Arg358 in the S_2 extensive subsite, while the amine group (NH_2) forms a strong salt bridge with Glu205 and Glu206 on the binding site. 82

Figure 4.2: Structures of the three main classes of aldose reductase inhibitors. Fidarestat is a cyclic imide derivative, quercetin is a polyphenolic compound, and epalrestat is a carboxylic acid derivative..... 85

Figure 4.3: The structure of GGACK dihydrochloride, a potent FXa inhibitor. The amide moiety of the inhibitor is required for bonding with the S_1 subsite of clotting FXa..... 87

Figure 4.4: Statin pharmacophore essential for binding to the active site of HMGR..... 88

Figure 4.5: The basic structure common to the four quinolone derivatives. On this structure are ketone groups (blue), aromatic rings (red), carboxylate group (green), aliphatic chains and hydrogen bond acceptors that aided the moderate inhibitory effect exhibited by the quinolone derivatives. 90

LIST OF TABLES

Table 1.1: Summary of anti-hyperglycaemic agents used clinically, including their mechanism of action, examples and side effects (107-133).....	20
Table 1.2: Summary of some quinolones, which includes their generation, structure, antimicrobial spectrum activity, and common side effects (143-152).....	26
Table 3.1: Predicted Lipinski's rule of 5 parameters for the quinolone derivatives.....	56
Table 3.2: The IC ₅₀ concentrations for the quinolone derivatives and acarbose obtained from the alpha-amylase inhibitory assay.	59
Table 3.3: The IC ₅₀ concentrations for the quinolone derivatives and acarbose obtained from the alpha-glucosidase inhibitory assay.	62
Table 3.4: The IC ₅₀ concentrations for the quinolone derivatives obtained from the DPP4 inhibitory assay.	65
Table 3.5: The IC ₅₀ concentrations for the quinolone derivatives and quercetin obtained from aldose reductase inhibitory assay.....	67
Table 3.6: The IC ₅₀ concentrations for the quinolone derivatives obtained from FXa inhibitory assay.....	69
Table 3.7: The IC ₅₀ concentrations for the quinolone derivatives and pravastatin obtained from HMG-CoA reductase inhibitory assay.....	71
Table 3.8: The IC ₅₀ concentrations for the quinolone derivatives and ascorbic acid obtained from DPPH radical scavenging assay.....	72

ABSTRACT

Background

Diabetes mellitus (DM) is a group of endocrine and metabolic disorders characterised and identified by the presence of hyperglycaemia over a long period and, to an extent, accompanied by hyperlipidaemia. CVD has been reported to be the leading cause of mortality in patients with DM. Several antidiabetic agents are available for managing DM, but these agents are not for curative therapy and present with undesirable side effects. In addition, these agents become less effective as the patient's condition progresses to complete beta-cell failure. Therefore, developing newer antidiabetic agents with minimal undesirable side effects, prolonged efficacy and protection against the development of DM complications are necessary. This study was conducted to identify potential novel antidiabetic agents with cardiovascular-protective activity. The compounds of interest for the study were quinolone derivatives since quinolones have been reported to have an antihyperglycaemic effect.

Methodology

In this study, the novel quinolone derivatives were referred to as QD1, QD2, QD3 and QD4. The drug-likeness and gastrointestinal absorption (GIT) of the quinolone derivatives were predicted by generating Lipinski's rule of 5 parameters and a BOILED-Egg model using the SwissADME web tool. The therapeutic targets that the quinolone derivatives were screened against include alpha-amylase, alpha-glucosidase, dipeptidyl peptidase-4 (DPP4), protein tyrosine phosphatase 1B (PTP1B), aldose reductase, pancreatic lipase, 3-hydroxy-3-methylglutaryl coenzyme A reductase (HMGR), and clotting factor Xa (FXa). The antioxidant activity of the quinolone derivatives was also investigated using a 2,2-diphenyl-1-picrylhydrazyl (DPPH) radical scavenging assay and ferric reducing antioxidant power (FRAP) assay. In each assay, reference compounds were used to validate the protocols used, and the assays were carried out in triplicates. The data obtained from reading the absorbance/fluorescence of the product formed were used to calculate percentage inhibition. Enzyme kinetics studies for alpha-amylase and alpha-glucosidase inhibition were conducted using Michaelis-Menten and Lineweaver Burk plots.

Furthermore, the quinolone derivatives were investigated for their effect on glucose uptake. In this study, separate preparations of C2C12 myoblasts and HepG2 cells in a 24-well plate were exposed to quinolone derivatives for 24 hours, after which glucose uptake and cell viability were assessed.

Results

From Lipinski's rule of 5 parameters and a BOILED-Egg model generated, we could predict that the quinolone derivatives are “druggable” and can be absorbed in the GIT. The results from the assays conducted on selected therapeutic targets showed that the quinolone derivatives exhibited good inhibitory activity against alpha-amylase and alpha-glucosidase. While the inhibitory activity exhibited against DPP4, aldose reductase, pancreatic lipase, HMGR and clotting FXa was moderate. No inhibitory activity was exhibited on PTP1B. The quinolone derivatives also exhibited moderate antioxidant activity. Furthermore, the glucose uptake assay showed that the quinolone derivatives have no substantial effect on glucose uptake when compared to the control group and the cell viability assay showed that the quinolone derivatives are non-cytotoxic.

Conclusion

The investigated quinolone derivatives exhibited a promising effect on DM and its associated complications. Therefore, to enhance the potency of the investigated compounds, their structural features should be modified to contain moieties that can aid their binding to the active site of the enzymes implicated in DM.

LIST OF ABBREVIATIONS

ACE	Angiotensin converting enzyme
ADME	Absorption, distribution, metabolism and excretion
ADP	Adenosine diphosphate
AGEs	Advance glycation endproducts
AMC	7-Amino-4-methylcoumarin
AMPK	Adenosine-5'-monophosphate-activated protein kinase
ANOVA	Analysis of variance
Apo B	Apolipoprotein B
ARB	Angiotensin II receptor blocker
ATM	Ataxia telangiectasia mutated
ATP	Adenosine triphosphate
BBB	Blood brain barrier
cAMP	Cyclic adenosine monophosphate
CF ₃	Trifluoro carbon
COX-1	Cyclooxygenase 1
CVD	Cardiovascular disease
CYP450	Cytochrome P450
DAG	Diacylglycerol
DCM	Dichloromethane
DM	Diabetes mellitus
DMEM	Dulbecco's modified eagle's medium
DMF	Dimethylformamide

DMSO	Dimethyl sulfoxide
DNSA	3,5-Dinitrosalicylic acid
DPP4	Dipeptidyl peptidase-4
DPPH	2,2-Diphenyl-1-picrylhydrazyl
DTT	Dithiothreitol
EDTA	Ethylenediaminetetraacetic acid
ESI-HRMS	High-resolution electrospray ionization mass spectrometry
FBS	Fetal bovine serum
FDA	Food and drug administration
Fe ³⁺ -TPTZ	Ferric-tripyridyltriazine
FRAP	Ferric reducing antioxidant power
FXa	Factor Xa
GIP	Glucose-dependent insulinotropic polypeptide
GIT	Gastrointestinal tract
GLP-1	Glucagon-like peptide-1
GLUT2	Glucose transporter type 2
GLUT4	Glucose transporter type 4
GPIIb/IIIa	Glycoprotein IIb/IIIa
HbA1c	Haemoglobin A1c
HDL-C	High-density lipoprotein cholesterol
HMG-CoA	3-Hydroxy-3-methylglutaryl coenzyme A
HMGR	3-Hydroxy-3-methylglutaryl coenzyme A reductase
IC ₅₀	Concentration of drug that reduces enzyme activity by 50%
IDF	International diabetes federation

IRS	Insulin receptor substrate
K_m	Michaelis constant
LADA	Latent autoimmune diabetes in adults
LDL	Low-density lipoprotein
Log P	Octanol-water partition coefficient
MEM	Minimum essential medium eagle
MeOH	Methanol
NADPH	Nicotinamide adenine dinucleotide phosphate
NO	Nitric oxide
PAI-1	Plasminogen activator inhibitor-1
PBS	Phosphate buffer solution
PI3K	Phosphatidylinositol-3-kinase
PKC	Protein kinase C
p NPG	P -nitrophenyl- α -D-glucopyranoside
p NPP	P -nitrophenyl phosphate
PPAR	Peroxisome proliferator-activated receptor
PTP1B	Protein tyrosine phosphatase 1B
QD1	Quinolone derivative 1
QD2	Quinolone derivative 2
QD3	Quinolone derivative 3
QD4	Quinolone derivative 4
RAAS	Renin-angiotensin- aldosterone system
ROS	Reactive oxygen species
SD	Standard deviation

SGLT1	Sodium glucose co- transporter 1
SGLT2	Sodium glucose co-transporter 2
T1DM	Type 1 diabetes mellitus
T2DM	Type 2 diabetes mellitus
TLC	Thin layer chromatography
TPA	Tissue plasminogen activator
TPTZ	2,4,6-Tris(2-pyridyl)-s-triazine
TRIS HCl	TRIS hydrochloride
TXA ₂	Thromboxane A ₂
UTI	Urinary tract infection
VLDL	Very low-density lipoprotein
V _{max}	Maximum velocity
WHO	World Health Organisation

CHAPTER 1: LITERATURE REVIEW

1.1 Introduction

Diabetes mellitus (DM) is a group of endocrine and metabolic disorders characterised and identified by the presence of hyperglycaemia over a long period and, to an extent, accompanied by hyperlipidaemia (1). DM is one of the major endocrine disorders found in every population and region of the world. Studies have reported that the number of people diagnosed with DM is steadily rising. According to the World Health Organization (WHO), in the year 2000, the worldwide estimate of adults between ages 20-79 years living with DM was 150 million, while the International Diabetes Federation (IDF) estimation was 151 million (2, 3). As of 2021, the estimated cases tripled to approximately 537 million adults. Low- and middle-income countries accounted for about 79.4% of the adult population living with DM. It was further estimated that by 2030 and 2045, the adult population of 643 million and 783 million, respectively, would be living with DM if preventative interventions were not implemented (2, 3). IDF estimated that in 2021, about 1.2 million children and adolescents (0-19 years) have diabetes mellitus type 1, and there were about 4.2 million deaths due to DM (3). South Africa has the highest number of patients with DM in Africa, estimated at 4.6 million people aged 20-79 (4).

DM is diagnosed when haemoglobin A1c (HbA1c) is $\geq 6.5\%$ or fasting plasma glucose concentration is ≥ 126 mg/dL, or two-hour plasma glucose is ≥ 200 mg/dL during an oral glucose test, or random plasma glucose concentration is ≥ 200 mg/dL (5). Symptoms of DM include polyuria, polydipsia, and polyphagia. Uncontrolled hyperglycaemia can lead to acute complications, including diabetic ketoacidosis and non-ketotic hyperosmolar coma and long-term complications, including foot ulcer, stroke, cardiovascular disease (CVD), nephropathy, neuropathy, and retinopathy (6). One of the leading causes of death in DM patients is CVD, a condition affecting the heart or blood vessels (7). However, not all patients with DM have the same risk of developing CVD. The risk of developing CVD increases with DM duration and comorbidities, which include hypertension, obesity, and dyslipidaemia. Therefore, targeting cardiovascular risk factors in patients with DM is critical in minimising the long-term cardiovascular complications of the disease. DM is managed with lifestyle modifications and

antidiabetic agents. There are different existing antidiabetic agent classes, ranging from oral antidiabetic agents that includes metformin to injectables such as insulin and liraglutide. Although these different classes of antidiabetic agents have been beneficial, they have undesirable side effects and reduced effectiveness long term. Therefore, there is a necessity to develop and evaluate potential novel compounds. Clinical and laboratory studies have reported that fluoroquinolone affects glucose homeostasis, and the extent to which disturbance in glucose homeostasis occurs varies among the different fluoroquinolones. An example of a fluoroquinolone that has been withdrawn from clinical use is gatifloxacin, and this is because of its severe hypoglycaemic effect (8). This, therefore, suggest that these agents possess properties that can be leveraged.

In this study, the effort was directed at the *in vitro* investigation of the effect of novel quinolone derivatives on selected therapeutic targets for DM and CVD for potential beneficial antidiabetic properties and associated cardiovascular pharmacological targets. It is envisaged that the novel quinolone derivatives could address the shortcomings associated with conventional treatments of DM and associated CVD. Additionally, considering the burden exerted in DM, it is therefore important that promising compounds are investigated in an effort to expand the treatment regimen to patients.

1.2 Glucose homeostasis

Glucose is a carbohydrate that is an essential source of energy and is constantly required by most tissues and organs. The monosaccharide is mainly obtained from the diet, however, it can be synthesised *de novo* by the liver and kidney (9, 10). Although glucose is an important metabolic substrate, blood glucose concentration has to be maintained within a narrow limit to avoid hyperglycaemia or hypoglycaemia. Glucose homeostasis is a process that involves maintaining blood glucose concentration within a narrow limit to achieve a steady-state level through intestinal glucose absorption, hepatic glucose production, pancreatic hormone secretion and peripheral glucose uptake (10). Achieving and maintaining a steady-state level of blood glucose concentration occurs through a balance among several factors, which include the rate of consumption and intestinal absorption of carbohydrates, glucose utilisation by peripheral tissues and release or removal of glucose by the liver (10, 11). The disturbance in glucose homeostasis may lead to hyperglycaemia, which inevitably leads to DM.

1.2.1 Carbohydrate digestion and absorption

The digestion of carbohydrates begins in the oral cavity. During mastication, the salivary gland serous cell synthesises and secretes the salivary alpha-amylase enzyme, which hydrolyses the α -1,4 bonds of starch to dextrans (12). Only about 5% of carbohydrates are broken down in the oral cavity due to limited exposure of starch to the salivary alpha-amylase. Also, digestion of carbohydrates does not occur in the stomach due to a high acidic environment which inactivates alpha-amylase. Hence, further digestion of carbohydrates occurs in the small intestine. In the small intestine, acinar cells of the pancreas secrete pancreatic alpha-amylase, which further breaks down dextrin into α -limit dextrans, maltose and maltotriose. The final stage of carbohydrate digestion is carried out by the brush border enzymes. The brush border enzyme includes maltase (digests maltose to glucose), isomaltase (digests α -1,6 bonds of α -limit dextrin to produce maltose), sucrase (digests sucrose to glucose and fructose), lactase (digest lactose to glucose and galactose) and trehalase (digests trehalose to glucose) (13-15). The undigested carbohydrates in the small intestine are passed into the large intestine, where they are subjected to colonic bacterial digestion.

Once carbohydrate digestion is completed in the small intestine, the end products, glucose, fructose and galactose, are absorbed and transported through the intestinal mucosal cells into the portal circulation. The carbohydrate absorption from the intestine lumen occurs through active and facilitative transport (16). Glucose and galactose are actively transported from the brush border membrane of the small intestine mucosal cell by sodium-glucose transporter (SGLT-1). The glucose transport is driven by a sodium gradient across the apical cell membrane generated by the sodium/potassium (Na^+/K^+ ATPase) pump located in the basolateral membrane of the enterocyte (17, 18). The Na^+/K^+ ATPase pump generates the sodium gradient by transporting 3 Na^+ ions out of the cell and 2 K^+ ions into the cell, creating a low intracellular sodium concentration. Two Na^+ ions bind to the outer face of the SGLT-1 transporter, which results in a conformational change permitting subsequent glucose binding. Following another conformational change involving the rotation of the receptors, the two Na^+ ions and the glucose molecule are transferred to the cytoplasmic side of the membrane, which then leads to the release of glucose first, followed by the Na^+ ions. The Na^+ ions are transported from high to low concentration and, at the same time, thus allowing the carrier to transport glucose against its concentration gradient which is maintained by the subsequent release of Na^+ ions (16-18). The absorption of glucose after a meal raises the blood

glucose concentration, and this is referred to as postprandial hyperglycaemia. In diabetic patients, postprandial hyperglycaemia is more pronounced. Therefore, the inhibition of carbohydrate digestion by inhibiting alpha-amylase and alpha-glucosidase in the gut is beneficial in controlling postprandial hyperglycaemia in diabetic patients. The inhibition of these enzymes leads to a decrease in glucose absorption, resulting in decreased blood glucose concentration. A known inhibitor of alpha-amylase and alpha-glucosidase used in managing DM is acarbose. Acarbose inhibits carbohydrate digestion and glucose absorption in the gastrointestinal tract (GIT), resulting in decreased blood glucose concentration. However, the clinical use of acarbose is limited due to its side effect, which includes flatulence and diarrhoea (19). Since the inhibition of alpha-amylase and alpha-glucosidase has a therapeutic effect and it is beneficial in managing DM, the quinolone derivatives were investigated for their inhibitory effect on these enzymes.

1.2.2 Insulin

The pancreas secretes hormones that play a crucial role in regulating blood glucose concentration. The hormones secreted by the pancreas to avoid fasting hypoglycaemia and postprandial hyperglycaemia are insulin, glucagon and amylin. Insulin and glucagon have an opposite effect. In this literature review, the focus is primarily on insulin.

1.2.2.1 Insulin secretion

Insulin is an anabolic protein that contains two polypeptide chains with 51 amino acids. When there is an increase in the postprandial blood glucose concentration, glucose activates insulin secretion (Figure 1.1) from the islets of Langerhans beta cells of the pancreas through a process called glucose-stimulated insulin secretion (20). This process occurs when glucose transporter 2 (GLUT2), located on the surface of the beta-cells, allows the glucose molecule to enter the cells through facilitated diffusion. Glucose is phosphorylated to glucose-6-phosphate (prevent glucose diffusion from the cell) by the enzyme glucokinase (21, 22). Glucokinase is also a glucose sensor that plays a central role in regulating glucose homeostasis. An increased oxidative metabolism due to increased blood glucose concentration leads to an increase in the adenosine triphosphate/adenosine diphosphate (ATP/ADP) ratio in the mitochondria. The increase in the ratio of ATP/ADP closes the ATP-sensitive potassium channel (K_{ATP}) (22). K_{ATP} channel closure

leads to a decrease in K^+ efflux, resulting in depolarisation of the plasma membrane. Subsequently, the sodium channel and voltage-dependent T-type calcium channel open, allowing the influx of Na^+ and calcium ion (Ca^{2+}), respectively, into the cell, causing further depolarisation. The increase in intracellular Ca^{2+} and activation of protein motors and kinases trigger the fusion of insulin-containing vesicles with the plasma membrane, facilitating the exocytosis of the insulin-containing vesicle content (23).

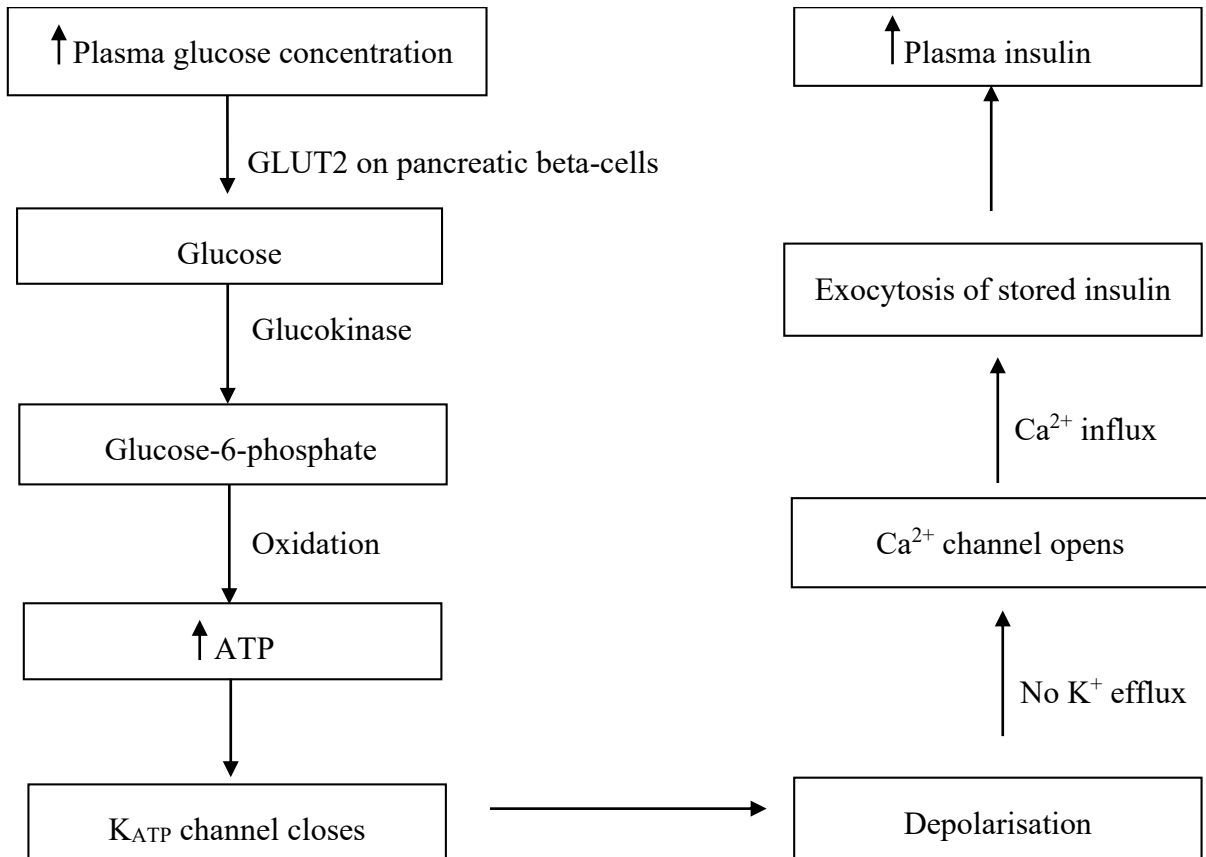


Figure 1.1: An illustration of insulin secretion. Increased blood glucose concentration stimulates the GLUT2 transporter on the pancreatic beta cell to transport glucose into the cell. Glucokinase converts glucose to glucose-6-phosphate, which is oxidized, resulting in an increase in levels of ATP. Subsequently, the K_{ATP} channel closes, and the Ca^{2+} channel opens, resulting in the influx of calcium ions into the islet cells. Subsequent events lead to an increase in insulin secretion (20-23).

Insulin secretion is also stimulated by the interaction of glucose-dependent insulintropic polypeptide (GIP) and glucagon-like peptide-1 (GLP-1) with their receptor. GIP and GLP-1 are gut-derived peptide hormones known as incretins. They are secreted by K cells in the upper small

intestine and enteroendocrine L cells in the distal intestine, respectively, upon oral ingestion of carbohydrates (24). Incretins are nutrient-dependent. When GIP and GLP-1 interact with their receptor in the pancreas, they increase cAMP concentration, which in turn increases intracellular Ca^{2+} concentration, thus enhancing the exocytosis of insulin-containing vesicles (25). Incretins are responsible for 50 to 70 % of insulin released (26). Incretins stimulate glucose-dependent insulin release and inhibit glucagon, increasing the insulin concentration required for hormonal regulation of blood glucose concentration, and this is known as the “incretin effect” (27). However, this effect is short-lived due to the degradation of incretins by dipeptidyl peptidase-4 (DPP4). DPP4 is a glycoprotein enzyme that is widely expressed throughout the body and abundantly expressed in endothelial cells (28, 29). It is attached to the intravascular portion of vascular endothelial cells and also exists in a soluble circulating form (30). DPP4 is a serine protease that cleaves proline or alanine dipeptides from the N-terminus of polypeptides (28).

Targeting the incretin system through the use of a GLP-1 receptor agonist such as liraglutide and a DPP4 inhibitor such as sitagliptin serves as a beneficial therapeutic target in the management of DM. This is because insulin secretion is enhanced, and glucagon release is inhibited (31, 32). Therefore, DPP4 inhibition has been found to extend glycaemic control. Since DPP4 inhibition is beneficial in managing DM, quinolone derivatives were screened for their inhibitory effect on DPP4 activity.

1.2.2.2 Insulin signalling

Once insulin is released into circulation, an insulin-receptor complex with specialised receptors found on most cell membranes forms. This process is known as insulin signalling (Figure 1.2). Insulin forms an insulin-receptor complex with the tyrosine kinase receptor, which has two extracellular α subunit that binds insulin and two transmembrane β subunits with tyrosine kinase activity (33, 34). Insulin binds to the α subunit and transmits signals that activate the intracellular β subunit tyrosine kinase through the transphosphorylation of one β subunit on specific tyrosine residue, thereby enhancing the activity of kinase (35). Also, the tyrosine kinase receptor undergoes intramolecular autophosphorylation at other tyrosine residues, and the activated receptor phosphorylates tyrosine residues on intracellular substrates, which includes the insulin receptor substrate (IRS) family (36). Due to the phosphorylation of tyrosine, the insulin receptor substrate

interacts and activates phosphatidylinositol-3-kinase (PI3K), an enzyme that facilitates insulin-stimulated glucose uptake through GLUT4 translocation (37, 38). Protein tyrosine phosphatase (PTP) is an enzyme that can dephosphorylate and inactivate insulin receptors, thereby switching off insulin signalling leading to poor glucose uptake. PTP1B is an intracellular PTP involved in the negative regulation of insulin receptors, and an elevated expression of this enzyme has been reported in insulin-resistant patients (39). Inhibiting the PTP1B enzyme is a promising therapeutic target for managing DM. Inhibitors of PTP1B include vanadium compounds such as vanadate and pervanadate, which target PTP1B active sites and reduce PTP1B activity resulting in attenuation of insulin resistance (40-42). For this reason, PTP1B was selected as one of the targets of interest in this study. Insulin-stimulated glucose uptake is mainly limited to the skeletal muscle and adipose tissue. Accordingly, the skeletal muscle cell line was utilised to gain insights into the effect of quinolone derivatives on glucose uptake.

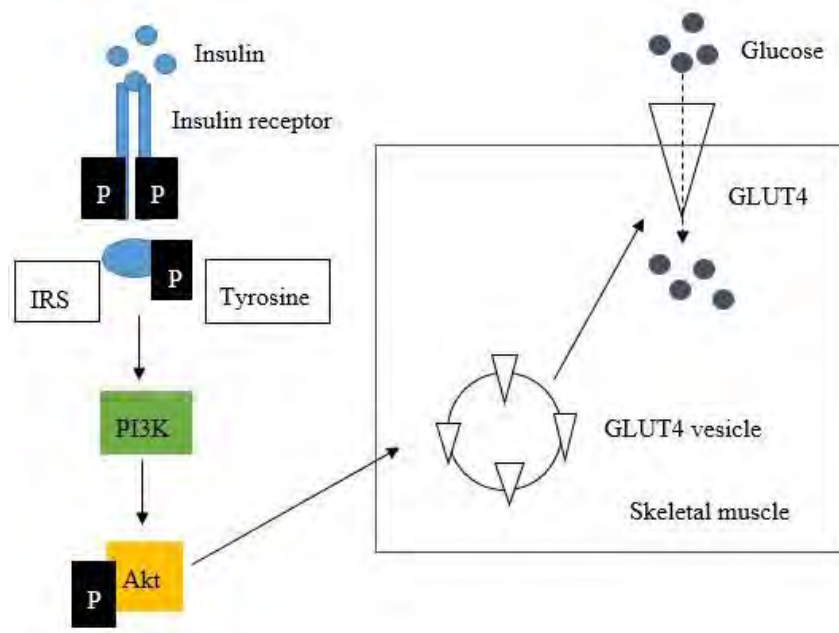


Figure 1.2: Insulin signalling pathway illustration. Insulin binds to the insulin receptor leading to the phosphorylation of IRS in tyrosine, activating PI3K and Akt, which stimulates GLUT4 translocation to the cell membrane, hence GLUT4 transports glucose into the skeletal muscle.

Furthermore, insulin regulates glucose homeostasis at many sites by reducing hepatic glucose production through decreased glycogenolysis (the breakdown of glycogen in the liver and skeletal

muscle) and gluconeogenesis (generating glucose from the non-carbohydrate substrate) (43, 44). The inability of the body to secrete insulin or respond to insulin leads to DM (2).

1.3 Diabetes mellitus

The two main types of DM are type 1 and type 2. Another type of DM includes gestational diabetes mellitus, which occurs during pregnancy due to metabolic and hormonal changes (45). In DM, insulin is either not secreted, too little is secreted, or there is normal insulin secretion, but the cells are not responsive, resulting in uncontrolled blood glucose concentration (2, 3).

1.3.1 Type 1 diabetes mellitus

Type 1 diabetes mellitus (T1DM), known as juvenile or insulin-dependent diabetes mellitus, is a condition in which the body produces no insulin or very little insulin, and beta-cells fail to respond to all insulinogenic stimuli (46). This is often due to an autoimmune reaction in which the pancreatic beta-cell that produces insulin is attacked and destroyed by the body's immune system. The destruction of the pancreas beta-cell is attributed to CD4⁺ and CD8⁺ T cells and macrophages infiltrating the islet of Langerhans (47). This autoimmune reaction is not fully understood, but studies suggest that environmental triggers, genetic susceptibility combinations, some dietary factors, and toxins are the primary determinants in the development of T1DM (48). In T1DM, a serological marker is identified in the form of autoantibodies against insulin (anti-insulin antibodies), pancreatic carcinoma, tyrosine phosphatase (anti-IA-2), and glutamic acid decarboxylase (anti-GAD antibodies). However, some patients do not produce these autoantibodies, but this does not rule out the diagnosis of T1DM (49). Amylin, a hormone co-secreted with insulin from the pancreas beta-cell, is also deficient in patients with T1DM. T1DM occurs mostly in children and childhood, although it can develop at any age. T1DM is one of the chronic childhood diseases diagnosed at around the age of 4-5 years, in their teens or early adulthood. The rapid rate of beta-cell destruction in children often presents with ketoacidosis, while in adults, they may maintain sufficient insulin secretion to prevent ketoacidosis for many years, which is known as latent autoimmune diabetes in adults (LADA) (50). T1DM represents about 10% of all DM cases globally, and its incidence rate is rising (2). Approximately 1.1 million

children and adolescents (0-19 years) have T1DM and each year, the number of newly diagnosed cases is about 128 900 (1-3).

1.3.2 Type 2 diabetes mellitus

Type 2 diabetes mellitus (T2DM), also known as non-insulin-dependent diabetes mellitus, is a condition in which the body does not respond to pancreatic insulin due to peripheral tissue resistance. This is primarily due to insulin receptors within cells being desensitised to insulin and impaired insulin ability to suppress hepatic glucose production (51). Consequently, glucose does not readily enter the insulin target tissues and, thus, leads to elevated blood glucose concentration. In addition to insulin receptor defects, insulin resistance can also be due to insulin receptor-signal transduction pathway defects, glucose transport and phosphorylation, and glycogen synthesis defect (52, 53). Over time, there is a pancreatic beta-cell failure, which leads to a decline in insulin production. Hence, insulin sensitivity and secretion defects coexist in T2DM (54). In T2DM, ketoacidosis is uncommon. T2DM has been linked to overweight and obesity, which aggravates insulin resistance (55). Genetics are also a major risk factor accounting for about 30-70% of T2DM. A high concentration of circulating free fatty acids in obesity leads to insulin resistance resulting in a reduction in insulin-stimulated glucose uptake due to the intracellular accumulation of lipids skeletal in muscle cells (56). T2DM is most common in adults, but children and adolescents can also be affected. T2DM accounts for about 90-95% of DM cases (2, 57).

1.3.3 Aetiology of diabetes mellitus complications

Sustained uncontrolled hyperglycaemia can lead to the onset and progression of DM complications over time. The development of DM complications can be linked to several factors, including advanced glycation end-products (AGEs) formation, activation of protein kinase C (PKC) and the polyol pathway. Prolonged hyperglycaemia causes glucose to form a covalent bond with proteins through a non-enzymatic reaction, resulting in the formation of AGEs, which disrupt molecular conformation and alter protein function by binding to intracellular and extracellular proteins (58). Although AGEs formation is a part of normal metabolism, excessive levels in tissues and circulation become pathogenic. The binding of AGEs to extracellular proteins can lead to extracellular matrix thickening and atherosclerosis, which induces cell death and cell

differentiation. AGEs can bind to cell surface receptors and induce reactive oxygen species (ROS) production (59). Ca^{2+} homeostasis may also be altered when AGEs bind to ryanodine, an intracellular protein, increasing CVD renal failure risk. The polyol pathway, which converts glucose to sorbitol by aldose reductase, can also be hyperactivated by hyperglycaemia (60). The activation of this pathway decreases nicotinamide adenine dinucleotide phosphate (NADPH), a precursor for glutathione synthesis, which is a major antioxidant. Due to a decrease in NADPH, reactive oxygen species (ROS) production increases. In uncontrolled DM, there is an increase in aldose reductase activity. Hence, there is an increase in the production of sorbitol, which leads to osmotic cell swelling production of ROS and AGEs, which causes peripheral tissue damage (60, 61). Aldose reductase inhibitors, such as epalrestat, used for treating diabetic neuropathy, reduce intracellular sorbitol accumulation. Therefore, in this study novel, quinolone derivatives were investigated for their aldose reductase inhibitory activity. Furthermore, hyperglycaemia leads to the accumulation of diacylglycerol (DAG) in cells which in turn induces the activation of PKC, a serine/threonine kinase (62). The activation of the PKC β in vascular cell result in angiogenesis, change in vascular permeability, cytokine activation, ROS production and inflammation (62, 63). In this study, quinolone derivatives were investigated for their potential antioxidant properties since ROS are implicated in the pathogenesis of severe diabetic complications.

1.3.4 Diabetes mellitus complications

The resulting DM complications are grouped into microvascular disease, which is damage to small blood vessels and includes retinopathy, neuropathy and nephropathy, while macrovascular disease, which is damage to the arteries, includes peripheral arterial diseases and coronary artery disease (64, 65).

1.3.4.1 Microvascular complications

1.3.4.1.1 Diabetic retinopathy

Diabetic retinopathy develops within 5-10 years after the onset of DM, and it causes lesions within the retina, which often leads to blindness (66). Diabetic retinopathy is categorised into non-proliferative and proliferative disease stages. The non-proliferative stage is the initial stage, where visual impairment is not observed. In this stage, hyperglycaemia leads to intra-mural pericyte death

and basement membrane thickness, altering the blood-retinal barrier and vascular permeability (67). The retinal capillaries begin to degenerate, resulting in ischaemia, followed by the release of angiogenic factors, which advance the disease into the proliferative stage. During the proliferative stage, macular oedema (fluid buildup in the macula of the retina) and neovascularisation (formation of new blood vessels) occurs, which further enhances visual impairment (68). Retina electrophysiology is also altered due to cell death within the neural retina, resulting in the inability to differentiate between colours (69).

1.3.4.1.2 Diabetic nephropathy

Diabetic nephropathy is the leading cause of end-stage renal disease in diabetic patients due to poor glycaemic control (70). Although some patients with good glycaemic control still develop diabetic nephropathy. Chronic hyperglycaemia results in haemodynamic abnormalities, which trigger an increase in systemic and intraglomerular pressure, oxidative stress, fibrosis, metabolic abnormalities, and renin-angiotensin system activation (71). Inflammation, fibrosis, and oxidative stress are the key links in the progression of diabetic nephropathy. Diabetic nephropathy is characterised by the thickening of the glomerular basement membrane, nodular glomerular sclerosis, kidney hypertrophy, proteinuria, mesangial expansion, and tubulointerstitial fibrosis, which leads to a decrease in glomerular filtration rate that occurs over time (72, 73). Furthermore, the development of nephropathy is a risk factor for cardiovascular complications (74).

1.3.4.1.3 Diabetic neuropathy

Diabetic neuropathy affects both the somatic and autonomic nervous systems due to segmental demyelination and axonal degeneration (75). It is clinically characterised by the thickening of the capillary basement membrane, endothelial hyperplasia, and nerve deterioration or damage observed in advanced neuropathy (67, 76). Damage to the higher central nervous system and spinal cord can also occur. Due to peripheral nerve damage affecting longer nerve fibers, the feet are affected more often than the hands (77). Furthermore, diabetic neuropathy contributes to wound healing impairment, erectile dysfunction, and CVD (78, 79).

1.3.4.2 Macrovascular complications

The leading cause of death in diabetic patients is macrovascular complications resulting from CVD (80). Macrovascular complications in a diabetic patient involve damage to large blood vessels, thus leading to coronary artery, cerebrovascular and peripheral vascular disease. Hyperglycaemia is a risk factor for developing CVD, and often CVD arises due to atherosclerosis. When there is dysfunction in the vascular endothelium, which is responsible for vascular homeostasis, atherosclerosis occurs. Thus, plaque formation due to fat, cholesterol, and other substances accumulates in and on the artery wall. The rupture and destabilisation of the plaque can block blood vessels, leading to stroke, peripheral artery disease, unstable angina, or myocardial infarction (67).

1.4 Link between diabetes mellitus and cardiovascular diseases

CVD is a major complication and the leading cause of mortality and morbidity in diabetic patients (81). The mortality rate in adult diabetic patients is 2-4 times higher than in those without DM. The development of CVD in diabetic patients, especially T2DM, can be linked to several factors often present in diabetic patients (Figure 1.3). These factors include endothelial dysfunction, neuropathy, coagulation enhancement and oxidative stress. Furthermore, DM comorbidities such as hypertension, obesity and dyslipidaemia increase the risk of developing CVD (82). Also, AGEs formation and PKC activation, as discussed earlier, increase the risk of CVD in diabetic patients (58-63).

DM and hypertension are often coexisting, with either one preceding the other. DM patients are twice as likely to develop hypertension than those without DM, while hypertensive patients have 2-3 times higher risk of developing DM than normotensive patients (83). Hypertension among diabetic patients is closely tied to the development of diabetic nephropathy. Hyperglycemia stimulates renal cells, producing humoral mediators, cytokines, and growth factors (84). The production of these factors is often responsible for structural alterations seen in the glomeruli of diabetic patients, including hyaline arteriosclerosis (primarily of the efferent arteriole), increased collagen deposition of the extracellular matrix, and increased permeability of the glomerular basement membrane (85). These structural changes increase filtration pressure and often lead to

microalbuminuria with a compensatory activation of the renin-angiotensin-aldosterone system (RAAS). Chronic activation of the RAAS often progresses to hypertension, placing added stress on the glomeruli and causing additional damage to the nephrons of diabetic patients (85, 86). If left untreated, diabetic nephropathy can progress to a nephrotic syndrome, characterised by proteinuria, a hypercoagulable state and hyperlipidemia, which may contribute to the increased risk of CVD seen in diabetic patients with renal dysfunction. Also, increased renin-angiotensin sympathetic system axis activities may cause insulin resistance by stimulating the angiotensin II type 1 receptor, which triggers increased ROS in adipocytes, skeletal muscle and cardiovascular tissue (85-88).

The risk of developing dyslipidaemia in diabetic patients is higher than in nondiabetic patients because there is an increase in the free fatty acid release in insulin-resistant fat cells (89). The secretion of apolipoprotein B (Apo B) and very low-density lipoprotein (VLDL) cholesterol is enhanced due to increased triglyceride production as a result of the high concentrations of free fatty acids. The increase in the concentration of triglyceride-rich lipoproteins leads to increased catabolism of high-density lipoprotein cholesterol (HDL-C), resulting in low HDL-C and a shift in the low-density lipoprotein (LDL) phenotype towards the small dense LDL (89, 90). Furthermore, hyperglycaemia enhances the glycosylation and oxidation of LDL and VLDL, resulting in the development of aggressive atherosclerosis. The decrease in the concentration of HDL and an increase in the concentration of LDL, VLDL and Apo B are risk factors for developing CVD (91). Dyslipidaemia is usually managed with statin, a 3-hydroxy-3-methylglutaryl coenzyme A (HMG-CoA) reductase inhibitor that blocks the cholesterol synthesis pathway. Due to the effect of DM on the cholesterol synthesis pathway, quinolone derivatives were investigated for their effect on HMG-CoA reductase (HMGR) activity.

Hyperglycaemia impairs the coagulation system by affecting the platelets, coagulation factors and fibrinolytic proteins. This can result in the formation of a thrombus or an embolus which leads to a CVD. Platelets play a vital role during fibrin clot production, from converting prothrombin to thrombin through to interaction with fibrin fibers and aggregation via glycoprotein IIb/IIIa (GPIIb/IIIa) receptors (92). Platelet activation leads to the release of arachidonic acid from the cell membrane, which is then converted to thromboxane A₂ (TXA₂) by cyclooxygenase 1 (COX-1) and TXA₂ synthase (93, 94). Antiplatelet such as aspirin irreversibly inhibit COX-1, thereby

inhibiting the synthesis of TXA₂. Also, platelet activation involves releasing of stored granule content, including ADP, which mostly stimulates platelet activation through P2Y₁₂ receptors (95). P2Y₁₂ inhibitor such as clopidogrel irreversibly antagonises the P2Y₁₂ receptor. TXA₂ and the released content of the storage granules further enhance additional platelet activation, hence initiating platelet aggregation through a fibrinogen cross-link with GPIIb/IIIa (92, 96). Hyperglycaemia and insulin resistance alter the platelet function by increasing the adhesion of platelets to the endothelial cell wall, increasing platelet activation and altering the fibrinogen/platelet interaction through increased expression of the P2Y₁₂ and GPIIb/IIIa receptors (92, 96, 97). Also, there is an increase in coagulation factors, including tissue factor, factor VII, thrombin and fibrinogen. The elevation of these coagulation factors results in an increase in clot formation and a denser fibrin network that is more resistant to fibrinolysis due to changes in clot structure (98). Insulin resistance also enhances the elevation of plasminogen activator inhibitor-1 (PAI-1), a fibrinolytic inhibitor that inhibits the conversion of plasminogen to plasmin by tissue plasminogen activator (TPA), hence reducing the fibrinolysis process (99, 100). Due to the effect of DM on the coagulation system, novel quinolone derivatives were also investigated for their anticoagulant activity by targeting clotting factor Xa.

Furthermore, hyperglycaemia and insulin resistance accelerates endothelial cell dysfunction, which alters the release of vasoactive molecules such as nitric oxide (NO) (92). NO has an important anti-atherosclerotic property. The reduction in NO release increases inflammation, oxidative stress, smooth muscle cell proliferation, expression of adhesion molecules and impairs vasodilation (101, 102). An increase in oxidative stress increases ROS, which accelerates LDL oxidation. Oxidised LDL infiltrates macrophages, and these macrophages develop into foam cells that are capable of secreting inflammatory cytokines, tumour necrosis factor- α and interleukin-6, which eventually form fatty streak, an atherosclerotic plaque precursor, which is a risk factor for developing CVD (103, 104).

Finally, DM management with thiazolidinediones, especially rosiglitazone, has been reported to increase the risk of cardiovascular events in diabetic patients. Rosiglitazone increases the number of atherogenic particles and the concentration of LDL cholesterol and triglycerides, which are risk factors for developing CVD (105).

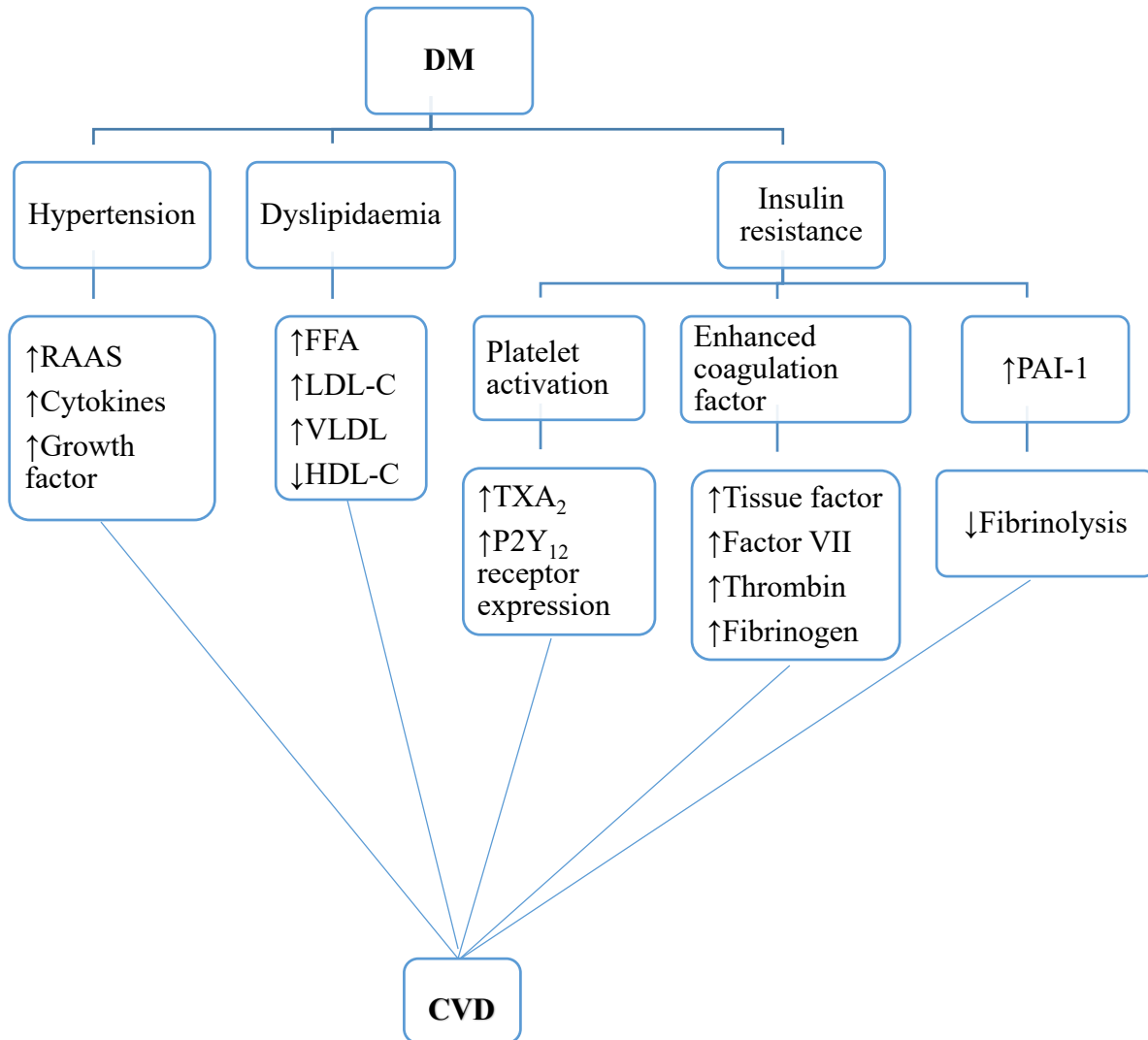


Figure 1.3: The link between DM and CVD involving hypertension, dyslipidaemia and insulin resistance (83-100).

1.5 Management of diabetes mellitus and cardiovascular diseases

1.5.1 Diabetes mellitus

DM is a life-long disease that has no cure. Hyperglycaemia can be controlled through lifestyle modifications (healthy diet and exercise) and medications to improve quality of life, decrease mortality, and decrease the risk of long-term complications associated with DM (106). Due to the progressive nature of DM, constant glycaemic control and therapeutic regimens adjustment are necessary as they can prevent the onset and progression of DM complications, including CVDs.

Before initiating single or combined treatment for patients, the patient should be assessed for possible risk factors, DM complications present, and a review of previous treatment. When pharmacological treatment is initiated for a patient, they are initially started on monotherapy. When a single agent can no longer provide glycemic control, adding a second or third medication will be more effective than switching to another single agent. All pharmacological treatment initiated should be combined with lifestyle interventions.

1.5.1.1 Insulin therapy

Insulin is the primary treatment for patients with T1DM, and it is also indicated for T2DM when glycaemic control is not achieved with oral antidiabetic medications (7). Insulin is mainly administered subcutaneously, and the types of insulin used clinically are short-acting insulin (regular), intermediate-acting insulin (isophane NPH insulin), rapid-acting insulin analogues (lispro, aspart, and glulisine), long-acting insulin analogue (glargine and detemir) for basal insulin replacement, and premixed insulin (contains both a basal and prandial insulin) (107). The short, intermediate, and rapid-acting insulins are referred to as bolus or prandial insulin because they cover meals and glycaemic excursions. Long-acting insulin is referred to as basal insulin because it regulates blood glucose concentration between meals by suppressing hepatic glucose production and maintaining near-normal glycaemic concentration during fasting. Premix insulin is preferred for T1DM to achieve adequate glycaemic control, while long-acting insulin is the preferred initial insulin therapy for T2DM. One of the adverse effects of insulin therapy is hyperinsulinemia which has been reported to increase the risk of developing CVD by enhancing inflammation, endothelial dysfunction and hypertension (108).

1.5.1.2 Sulphonylureas

The sulphonylureas are insulin secretagogues administered orally and indicated for T2DM. Sulphonylureas increase insulin release from the pancreas. When sulphonylureas bind to their receptor on pancreatic beta-cells, it leads to the closure of the K_{ATP} channel, thus inhibiting K^+ efflux and causing depolarisation of the cell membrane (109). Subsequently, the voltage-gated calcium channel opens, allowing Ca^{2+} influx and enhancing insulin release (110). Sulphonylureas also increase peripheral insulin sensitivity and reduction in hepatic glucose production. The

sulphonylurea effect is not specific to the pancreatic beta-cell only. It also binds to K_{ATP} channels in the cardiomyocytes and vascular smooth muscle cells, increasing the risk of developing CVD and increasing CVD mortality (111).

Sulphonylureas are divided into first and second-generation agents. The first-generation agents include tolazamide, chlorpropamide, tolbutamide, and acetohexamide. These agents have a slower onset of action, longer half-lives, and a higher risk of hypoglycaemia. The second-generation agent includes glimepiride, glyburide, gliclazide, glipizide, gliquidone, and glipizide. Second-generation agents are more potent and therefore preferred for managing DM (11). These agents reduce HbA1c by 1.5 – 2 %. Hypoglycaemia is the major side effect associated with sulphonylureas, and this is because they can stimulate insulin release even at basal blood glucose concentrations.

1.5.1.3 Meglitinides

Meglitinides are oral insulin secretagogues used in treating T2DM. Their mechanism of action is the same as that of sulphonylurea as they bind to a site adjacent to the sulphonylureas receptor in pancreatic beta-cell, stimulating insulin secretion from pancreas beta-cell (112). Meglitinides have a lower binding affinity for the sulphonylureas receptor; hence they are short-acting insulin secretagogues (113). Repaglinide and nateglinide are examples of meglitinides, and they may be used to replace sulphonylurea in patients who develop late postprandial hypoglycaemia. Meglitinides reduce HbA1c by 0.8 – 1% and have a lesser hypoglycaemic effect since it requires high blood glucose concentrations before stimulating insulin release. The major side effect associated with meglitinides is hypoglycaemia, but the incidence of hypoglycaemia is lower when compared to sulphonylureas (114).

1.5.1.4 Biguanides

The oral biguanide used clinically is metformin. Phenformin and buformin are also biguanides, but they have been withdrawn since they are associated with lactic acidosis (33). Biguanides act independently of the pancreas. Metformin enhances adenosine 5' monophosphate-activated protein kinase (AMPK) in the liver, causing hepatic glucose uptake and inhibiting hepatic gluconeogenesis and glycogenolysis (115). Metformin enhances hepatic and peripheral tissue sensitivity to insulin by enhancing tyrosine kinase activity (116). Metformin also decreases

triglyceride and LDL-C concentration, thus providing cardiovascular protection alongside its antidiabetic effect (117). Although metformin provides some cardiovascular protection, it has also been reported to increase the risk of CVD by accumulating homocysteine resulting from vitamin B₁₂ deficiency (118). Homocysteine is an amino acid converted to cysteine or recycled into methionine by the B vitamins, and high levels of homocysteine are a CVD marker. Vitamin B₁₂ deficiency results from the interference of metformin with calcium-dependent membrane action responsible for vitamin B₁₂ absorption from the GIT (119). Metformin is a first-line oral treatment for T2DM due to its efficacy, low cost, and manageable side effects. Metformin reduces HbA_{1c} by 1.5 – 2 % and can be used alone or in combination with therapy for uncontrolled DM. Due to the metformin weight loss effect, it is useful in treating an obese diabetic patient (120).

1.5.1.5 Thiazolidinediones

Rosiglitazone and pioglitazone are oral thiazolidinediones used clinically for treating T2DM, while troglitazone has been withdrawn due to severe hepatotoxicity resulting in liver failure. Thiazolidinediones bind to peroxisome proliferator-activated receptor (PPAR) gamma, leading to increased glucose transporter type 4 (GLUT 4) expression (121). When PPAR-gamma is activated, it alters the transcription of several genes involved in glucose and lipid metabolism. They also enhance hepatic and peripheral tissue sensitivity to insulin and decrease insulin resistance. Thiazolidinediones reduce HbA_{1c} by 1 – 1.5 %. Due to the activity of thiazolidinediones on the renal PPAR-gamma, there is an increase in sodium and fluid retention, leading to adverse effects, including heart failure and oedema (122).

1.5.1.6 Alpha-glucosidase inhibitors

The two oral agents in this class used for treating T2DM are acarbose and miglitol. They act by inhibiting pancreatic alpha-amylase and alpha-glucosidase enzymes found in the small intestine brush border. Alpha-glucosidase inhibitors prevent the breakdown of oligosaccharides and disaccharides into monosaccharides by the aforementioned enzymes (123). Although there is a delay in the absorption of these nutrients, they are not malabsorbed. Alpha-glucosidase inhibitors are usually used in the early stage of T2DM or in combination therapy for treating T2DM. The major side effects are gastrointestinal disturbance, including diarrhoea and flatulence (19).

1.5.1.7 Sodium-glucose co-transporter 2 (SGLT2) inhibitors

Canagliflozin, dapagliflozin, and empagliflozin are oral agents approved for clinically treating T2DM. SGLT2 inhibitors block glucose reabsorption in the proximal renal tubule into the bloodstream, increasing glucose excretion in the urine (124, 125). SGLT2 is responsible for about 90% of glucose reabsorption; hence inhibiting SGLT2 lowers the glucose concentration in T2DM patients. A major side effect associated with SGLT2 is urinary tract infection (UTI) (126).

1.5.1.8 GLP-1 receptor agonist

Liraglutide and exenatide are the two agents in this group. These agents are GLP-1 analogues with high resistance to DPP4 degradation and help restore GLP-1 activity. DPP4 is an enzyme that degrades gut-derived GLP-1 (127). GLP-1 receptor agonists are administered subcutaneously. GLP-1 receptor agonist enhances insulin secretion and suppresses high postprandial glucagon secretion, decreasing hepatic glucose production, slow gastric emptying, increasing satiety, and promoting weight loss (128). GLP-1 receptor agonists have also been shown to have cardiovascular benefits, which include reduced arrhythmias, improved left ventricle function, blood pressure, and reduced body weight and lipids (129). Side effects of these agonists include gastrointestinal tract (GIT) disturbances and local injection site reactions (130).

1.5.1.9 DPP4 inhibitors

The agents in this group are sitagliptin, vildagliptin, linagliptin, saxagliptin, and alogliptin. They inhibit DPP4, an enzyme that degrades active GLP-1 and GIP when released, thereby prolonging the half-life of endogenously produced GLP-1 and GIP (131). Furthermore, inhibition of DPP-4 reduces CVD risk by increasing postprandial lipid mobilisation and oxidation (132). There is an average of 0.5 – 0.9% reduction in HbA1c, and the major side effects of these inhibitors are upper respiratory tract infection, nasopharyngitis, and headache (133).

Table 1.1: Summary of anti-hyperglycaemic agents used clinically, including their mechanism of action, examples and side effects (107-133).

Anti-hyperglycaemic agents	Mechanism of action	Examples	Side effects
Insulin	Facilitates glucose uptake	Humulin Insulin glargine	Hyperinsulinemia
Sulphonylureas	Stimulate pancreatic beta-cell insulin secretion	Glimepiride Glyburide	Hypoglycaemia
Meglitinides	Stimulate pancreatic beta-cell insulin secretion	Repaglinide Nateglinide	Hypoglycaemia
Biguanides	Enhance hepatic glucose uptake and inhibits hepatic gluconeogenesis and glycogenolysis	Metformin	Weight loss
Thiazolidinedione	Decrease insulin resistance by increasing the sensitivity of insulin receptors to insulin	Pioglitazone Rosiglitazone	Heart failure Oedema
Alpha-glucosidase inhibitors	Delay the absorption of glucose by preventing the breakdown of oligosaccharides and disaccharides into monosaccharides	Acarbose, Miglitol	Diarrhoea Flatulence
SGLT2 inhibitors	Increase glucose excretion by blocking glucose reabsorption in the proximal renal tubule	Canagliflozin Dapagliflozin	Urinary tract infection (UTI)

GLP-1 receptor agonist	Enhance insulin secretion and slow gastric emptying	Liraglutide Exenatide	GIT disturbances
DPP4 inhibitors	Prevent the degradation of GLP-1 and GIP by inhibiting the DPP4 enzyme	Sitagliptin Saxagliptin	Headache Nasopharyngitis

1.5.2 Cardiovascular disease

As mentioned earlier on, DM can precipitate cardiovascular complications through several mechanisms. Therefore, CVDs prescription of CVD medications is common in diabetic patients. Different classes of drugs are available for managing CVD; the selected class will depend on the disease present and the patients’ comorbidities. The major classes used for managing CVD in diabetic patients are antihypertensive, anti-lipidaemia and antithrombotic.

1.5.2.1 Antihypertensives

The angiotensin-converting enzyme (ACE) inhibitors and angiotensin II receptor blockers (ARBs) are the two main classes of antihypertensive use in managing CVD in diabetic patients. ACE inhibitors prevent the conversion of angiotensin I to angiotensin II and also prevent the hydrolyses of bradykinin by inhibiting ACE, resulting in enhanced blood vessel dilation, which promotes the free flow of blood (134). The major side effect of ACE inhibitors includes cough and angioedema. ARB binds and blocks angiotensin II receptor type 1, preventing angiotensin II from binding to the receptor (135). Therefore, preventing vasoconstriction and sodium retention. The major side effect of ARBs includes dizziness and cough. ACE inhibitors and ARBs are used to treat hypertension, congestive heart failure and diabetic nephropathy.

1.5.2.2 Anti-lipidaemias

Statins are the main anti-lipidaemia drugs used to manage CVD in diabetic patients. Statins inhibit cholesterol synthesis by competitively inhibiting HMGR – an enzyme required for the production of mevalonate, which eventually produces cholesterol (136). The decrease in hepatic cholesterol

production leads to an increase in microsomal HMG-CoA reductase production and cell surface LDL receptor expression resulting in an increase in LDL-C clearance from the bloodstream, which subsequently leads to a reduction in the circulating LDL-C (136, 137). Statins are used for the treatment of atherosclerosis. The major side effect associated with statins is myalgia (138).

1.5.2.3 Antiplatelets

Aspirin and P2Y₁₂ inhibitors are the two antiplatelets used for managing CVD in diabetic patients. Aspirin irreversibly inhibits the COX-1 enzyme in platelets resulting in the inhibition of TXA₂ synthesis, a potent vasoconstrictor and platelet aggregant (139). P2Y₁₂ inhibitors antagonise the P2Y₁₂ receptor, resulting in the inhibition of platelet activation and aggregation (140). The major side effect includes an increased risk of excessive bleeding (141).

1.6 Emerging alternative antidiabetic agents

As alluded to previously, different classes of drugs are used clinically for managing DM and its associated complications. However, most of these drugs are expensive, and they have undesirable side effects and reduced efficacy over time, eventually leading to the use of combination therapy for effective management of glycaemic index. Therefore, there is a necessity for research into novel compounds which have lesser side effects, enhanced and prolonged efficacy and effectiveness against the development of DM associated CVD. The novel compounds investigated in this study are quinolone derivatives due to their effect on glucose homeostasis.

1.6.1 Quinolones as potential antidiabetic agents

Quinolone is an important pharmacophoric unit in synthetic antimicrobials that was discovered in the 1960s as a by-product during the synthesis of chloroquine (142, 143). Quinolones comprise a broad group of compounds with similar bicyclic core structures and unique mechanisms of action, but they differ in their potency. Mechanistically, quinolones inhibit DNA synthesis by inhibiting topoisomerase II (DNA gyrase) and topoisomerase IV (142). Hence, quinolones are bactericidal. Several quinolones and related compounds are effective against either gram-positive, gram-negative bacteria or both. The antimicrobial spectrum activity and potency of different quinolones

depend on the key strategic structural modification implemented on the quinolone structural motif. Some of the important modification includes: (i) the addition of a fluorine atom on carbon 6, which enhances the inhibition of topoisomerase II, (ii) the incorporation of a piperazine or methylpiperazine ring on carbon 7, which increases quinolone activity against all aerobic gram-negative bacteria and enhances activity against gram-positive bacteria, (iii) addition of fluorine atom on carbon 8 which increases absorption and provides a longer elimination half-life, (iv) appending a cyclopropyl ring on N₁ – enhances quinolone activity against aerobic gram-negative and gram-positive bacteria, (v) addition of a methoxy group on carbon 8 which enhances the specificity of quinolones for topoisomerase II and topoisomerase IV (144). Clinically, quinolones are classified into four generations based on their antimicrobial spectrum activity and potency. However, classifying the different quinolones into generations slightly differs depending on the country. Quinolones are widely used clinically because they possess broad-spectrum activity and are largely well-tolerated. They are mostly used to treat UTIs, respiratory tract infections, community-acquired and nosocomial pneumonia, sexually transmitted diseases and skin and soft tissue infection (142, 144). Clinical and laboratory studies have reported that fluoroquinolone affects glucose homeostasis. The extent to which disturbance in glucose homeostasis occurs varies among the different fluoroquinolones. Gatifloxacin is an example of fluoroquinolone withdrawn from the market due to its severe dysglycaemia effect (8).

1.6.1.1 Classification of quinolones

Like many other antibiotic classes, the classification of quinolones is based on when they were developed. Hence, they are classified into generations, as discussed below and shown in Table 1.2.

1.6.1.1.1 First-generation quinolones

The first quinolone discovered was nalidixic acid in 1962 by George Leshner and his colleagues. Nalidixic acid was discovered as a by-product during the synthesis of chloroquine – an effective antimalarial drug for treating malaria caused by *Plasmodium falciparum* (143). Although nalidixic acid is a naphthyridine and not a true quinolone, nalidixic acid became the backbone for developing other quinolones that are now widely used clinically (145). Other examples of quinolones in this group include oxolinic acid, cinoxacin, pipemidic acid, piromidic acid and flumequine. First-

generation quinolones are effective against aerobic gram-negative bacteria and are used clinically to treat uncomplicated UTIs. However, they are not very effective against aerobic gram-positive bacteria and anaerobic bacteria (144).

1.6.1.1.2 Second-generation quinolones

The second generation of quinolones was synthesised around the 1980s to improve their effectiveness of quinolones. The key modification to the initial structure involved adding a fluorine atom to the carbon 6 position and adding either a piperazine or methyl-piperazine ring to the carbon 7 position (146). Due to the fluorine atom at the C-6 position of the quinolone structure, the newly synthesised compounds were referred to as fluoroquinolones. The second-generation quinolones have a broad spectrum of antimicrobial activity, including enhanced activity against gram-negative bacteria such as *Pseudomonas* species and gram-positive bacteria such as *Staphylococcus aureus* (145, 146). Furthermore, this generation of antibiotics displays enhanced pharmacokinetics and pharmacodynamics properties. Even with the modifications made to this class of quinolones, the second generation is still ineffective against anaerobes.

The second-generation quinolones include norfloxacin and ciprofloxacin. Norfloxacin is the first fluoroquinolone to be synthesised, and its structure has a fluorine atom at C₆ and a piperazine ring at the C₇ position. Norfloxacin is indicated for bacterial enteritis, gonorrhoea and prostatitis (147). Ciprofloxacin is the most common quinolone used clinically to date, and it is listed as an essential medicine by the WHO. Ciprofloxacin was the first second-generation fluoroquinolone to show activity against other conditions apart from urinary tract infection. Ciprofloxacin structure has a fluorine atom at C₆, a piperazine ring at C₇ and a cyclopropyl ring at the N₁ position. Ciprofloxacin is indicated for urinary tract infections, gonorrhoea, typhoid fever, bone and joint infection, lower respiratory tract infection and febrile neutropenia (148). Other quinolones in this generation include lomefloxacin - fluorine substituent at C₆ and C₈ positions and methylpiperazine ring at C₇ position. Ofloxacin -fluorine substituent at C₆, methylpiperazine ring at C₇ and 1,4-benzoxazine motif formed via the C₈ and N₁ of the quinolone scaffold (145).

1.6.1.1.3 Third-generation quinolones

In an effort to increase the antibacterial spectrum, further key structural modifications were conducted to generate new quinolones with enhanced activity against gram-positive bacteria compared to the second generation. Additional modifications were implemented at position 7 and position 8. Third-generation quinolones include sparfloxacin and gatifloxacin. Sparfloxacin has an amino group at C₅, fluorine atom at C₆ and C₈, dimethylpiperazine ring at C₇ and cyclopropyl ring at N₁. Sparfloxacin is indicated for community-acquired pneumonia that does not respond to conventional therapy (148). Gatifloxacin has a fluorine atom at C₆, methylpiperazine ring at C₇, methoxy group at C₈ and cyclopropyl ring at N₁ position. Gatifloxacin is also indicated for community-acquired pneumonia and uncomplicated and complicated urinary tract infection (8, 148). However, gatifloxacin has been withdrawn from clinical use due to its ability to interfere with glucose homeostasis (149). Grepafloxacin structure has a methyl group at C₅, fluorine atom at C₆, methylpiperazine at C₇ and cyclopropyl ring at N₁ position. Similarly, grepafloxacin was indicated for community-acquired respiratory tract infection and gonorrhoea before being withdrawn from therapeutic use (148, 149).

1.6.1.1.4 Fourth-generation quinolones

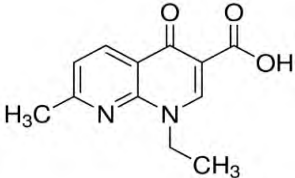
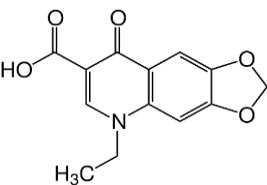
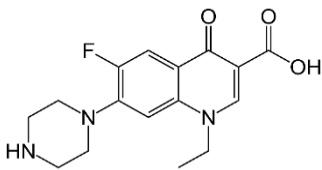
The fourth generation of quinolones was developed to have enhanced potency and broader spectrum activity, including anaerobic bacteria. The quinolone in this group includes moxifloxacin, gemifloxacin and trovafloxacin. Moxifloxacin is a fluoroquinolone with a structure that has a fluorine atom at C₆, a (4a*S*,7a*S*)-octahydro-6H-pyrrolo[3,4-*b*]pyridine-6-yl group at C₇, a methoxy group at C₈ and a cyclopropyl ring at N₁ position (148). Moxifloxacin has enhanced activity against gram-positive bacteria and anaerobes but lower activity against gram-negative bacteria such as *Pseudomonas* species and *Enterobacteriaceae* (150). Moxifloxacin is indicated for community-acquired pneumonia, acute bacterial sinusitis, bacterial conjunctivitis and uncomplicated skin infection. Moxifloxacin has also been listed in the WHO essential medicine list to manage multiple drug-resistant tuberculosis (144).

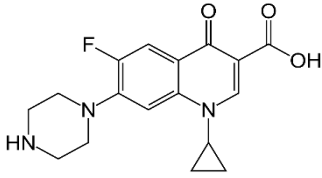
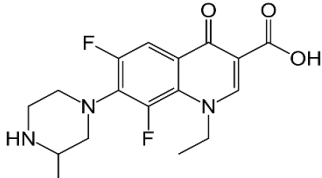
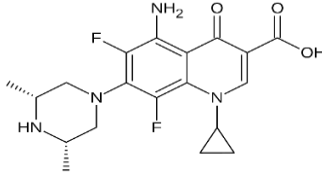
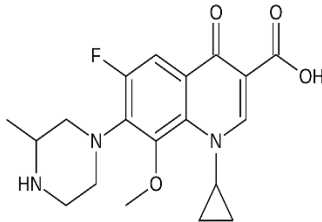
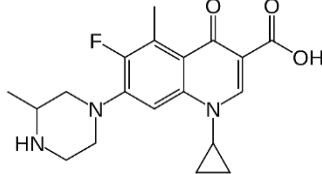
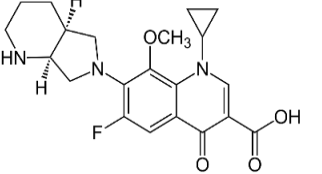
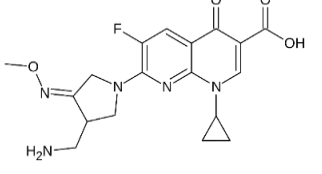
Gemifloxacin is the first fluoroquinolone that was synthesised with a pyrrolidine substituent in its structure. The structure of gemifloxacin has a fluorine atom at C₆, a 3-(aminomethyl)-4-methoxyiminopyrrolidin-1-yl group at C₇ and a cyclopropyl ring at N₁ position. The pyrrolidine

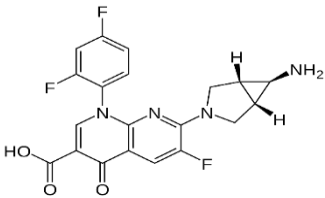
substituent enhances gemifloxacin activity against gram-positive and gram-negative bacteria and anaerobes (151). Gemifloxacin is indicated for acute bronchitis and mild to moderate community-acquired pneumonia.

Trovafloxacin is another fluoroquinolone antibiotic with a structure that has a fluorine substituent at C₆ and a 6-amino-3-azabicyclo[3.1.0]hex-3-yl group at C₇, and a 2,4-difluorophenyl ring at N₁ position. Trovafloxacin was reported to be more effective against gram-positive bacteria than gram-negative bacteria. It was mainly indicated for the treatment of both community-acquired and nosocomial pneumonia and was also used to treat complicated intra-abdominal and pelvic infections as well as complicated skin and soft tissues infection. However, trovafloxacin has been withdrawn from the market due to its hepatotoxic effect (152).

Table 1.2: Summary of some quinolones, which includes their generation, structure, antimicrobial spectrum activity, and common side effects (143-152).

Generation	Compound	Structure	Antimicrobial spectrum activity	Common side effects
First-generation	Nalidixic acid		Effective against gram-negative bacteria except for <i>Pseudomonas</i> species	Drowsiness
	Oxolinic acid			Headache
	Norfloxacin		Increased activity against all gram-	Nausea
				Diarrhoea
				Flatulence
				Lethargy
				Abdominal pain
				Dysgeusia
				Heartburn
				Muscle or joint pain
				Dizziness

Second-generation	Ciprofloxacin		negative bacteria	Rash Vomiting Restlessness Abdominal pain
	Lomefloxacin		Activity against some Gram-positive bacteria such as <i>Staphylococcus aureus</i>	Seizures Confusion Muscle or joint pain
Third-generation	Sparfloxacin		Enhanced activity against gram-negative and gram-positive bacteria	Indigestion Photosensitivity Tinnitus Headache
	Gatifloxacin			Dysglycaemia Insomnia Arthralgia Fever
	Grepafloxacin			Dry mouth Rash Abdominal pain
Fourth-generation	Moxifloxacin		High activity against gram-negative, gram-positive and anaerobic bacteria.	Hypoglycaemia Diarrhoea Prolong QT interval Heartburn
	Gemifloxacin			Neutropenia Photosensitivity Rash Diarrhoea

	Trovafloracin		Dizziness Hepatotoxicity Headache Abdominal pain
--	---------------	---	---

1.6.1.2 Effect of quinolones on glucose homeostasis

Glucose homeostasis is one of the physiological processes susceptible to disturbance when certain drugs are introduced into the body. Glucose regulation is achieved by the interplay among many tissues, including the small intestine, skeletal muscle, adipose tissue, and the pancreas, which is the key organ. These organs are crucial in glucose handling, and many conventional diabetic drugs act in these tissues. For example, sulphonylureas achieve their effect by stimulating pancreatic beta cells' insulin secretion (110). On the other hand, metformin achieves its glycaemic control by delaying intestinal glucose absorption, blocking hepatic glucose production and improving insulin sensitivity in target tissues (153). This, therefore, provides a clear indication that glucose homeostasis can be affected through the interaction of drugs with various tissues. Although these tissues have been key in developing anti-hyperglycaemic agents, certain drugs indicated for other ailments may also act on these tissues and produce hypoglycaemia or glycaemia. Examples of drugs that can produce glycaemic abnormalities include cardiovascular drugs, mental health agents, and antibiotics. There have been reports of fluoroquinolones influencing glucose homeostasis, specifically in diabetic and elderly patients (154). Gatifloxacin is an example of a fluoroquinolone withdrawn from the market due to its severe effect on glucose homeostasis. Studies have reported that drugs penetrating the cell membrane and chelating multivalent metal ions can induce intracellular magnesium deficiency. Magnesium deficiency has been linked to T2DM development. Also, in people with T2DM, magnesium deficiency can worsen insulin resistance. Fluoroquinolones are an example of quinolones that leads to magnesium deficiency, and this can be linked to its 3-carboxylic acid moiety, which has a metal-chelating activity (155).

On the other hand, quinolones can stimulate the pancreatic beta-cells to secrete insulin through a mechanism similar to sulphonylureas (Figure 1.4). In the pancreatic beta-cell, quinolones block the K^+_{ATP} channel, inhibiting K^+ efflux and causing cell membrane depolarisation (156). Subsequently, the voltage-gated Ca^{2+} channel opens, allowing Ca^{2+} influx, which enhances the exocytosis of insulin granules resulting in insulin release into the extracellular space. The extent

of the hypoglycaemic effect produced by quinolones will differ since different quinolones have different affinities for pancreatic beta-cell (156, 157). Quinolones such as temafloxacin and gatifloxacin have a greater affinity for the pancreatic beta-cell. Therefore, they may exert a more significant hypoglycaemic effect than other fluoroquinolones (158). In order to have a comprehensive view of the effect of quinolones on glucose homeostasis, the direct effect on glucose uptake by the target cells, the effect on insulin secretion, interaction with antidiabetic drugs and clinical studies that have been conducted to determine the effect of quinolone on glycaemic control will be discussed.

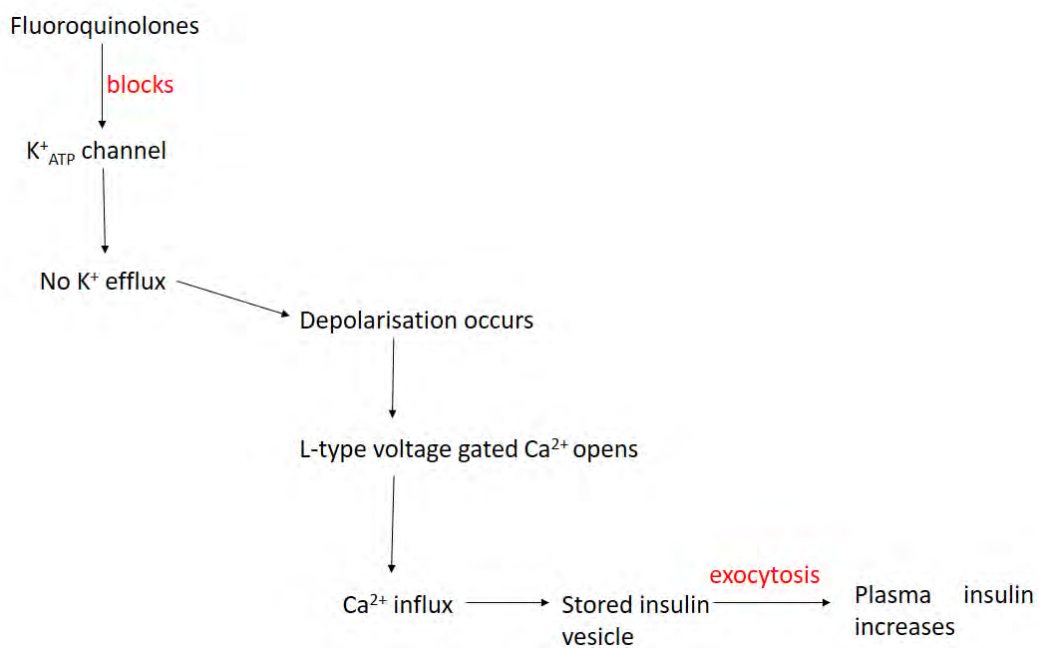


Figure 1.4: An illustration of fluoroquinolone's mechanism of action in the pancreatic beta-cell. Fluoroquinolones have been demonstrated to block the ATP-sensitive potassium channel. The closure of ATP-sensitive channels results in a subsequent L-type voltage-gated calcium channel opening, resulting in the influx of calcium ions in the islet cells. Subsequent events lead to an increase in insulin secretion (156).

1.6.1.3 Effect of quinolones on glucose uptake by target cells

To date, no reports have demonstrated the direct effect of fluoroquinolones in stimulating glucose uptake by the target cells. Although the focus is on how to explore fluoroquinolone's effect on

glucose uptake, however, a related compound, chloroquine, will be briefly explored. As mentioned previously, the synthesis of chloroquine led to the development of fluoroquinolones (143, 145). Chloroquine, an antimalarial agent structurally related to fluoroquinolones, is well known for its hypoglycaemic effects. This antimalarial agent has been shown to induce hypoglycaemia in malaria animal models, which was associated with increased plasma insulin concentration (159). Recent studies have reported that the hypoglycaemic effect of chloroquine is due to an increase in glucose uptake and glycogen synthesis in the skeletal muscle (160). At a molecular level, chloroquine has been shown to activate ataxia telangiectasia mutated (ATM), a protein that stimulates protein kinase B (AKT), thus increasing glucose disposal. Additionally, it has been demonstrated that chloroquine can reverse insulin resistance in *in vitro* using the L3 skeletal muscle cell line (160). For these reasons, chloroquine has the potential for the management of DM. A recent clinical trial found that chloroquine had a modest effect on mitigating diabetes-associated parameters (161). Therefore, this shows that fluoroquinolones and related compounds affect glucose homeostasis, which could be directly or indirectly.

1.6.1.4 Insulinotropic effects of quinolones

Gatifloxacin has shown a higher risk of severe hypoglycaemia and hyperglycaemia than the other quinolones, which may explain its withdrawal from the market. A few laboratories reported mechanistic insights on how gatifloxacin induces dysglycaemia. A recent study by Yabe *et al.* demonstrated that gatifloxacin induces greater glycaemic aberrations than lomefloxacin and levofloxacin (162). In this study, 5 to 6-week-old male rats were administered 300 mg/kg of the quinolones mentioned above daily for 14 days. The observed data demonstrated a significant decline in plasma insulin concentration, accompanied by increases in glycosylated albumin in animals treated with gatifloxacin after one day. As mentioned earlier, gatifloxacin has a high affinity for pancreatic cells. Indeed, higher gatifloxacin concentrations were found to be almost double that of either levofloxacin or lomefloxacin in the pancreas. Upon further investigations, beta-cell vacuolation was observed due to the dilation of the endoplasmic reticulum (162). The dilation of the cisternae is associated with insulin production disturbances. *In vitro* studies by Yamada *et al.* demonstrated a decrease in insulin contents together with insulin messenger mRNA expression in cultured mouse islets treated with gatifloxacin (163).

In a study done by Tomita *et al.*, it was reported that pretreatment of cultured HIT-T15 cells with fluoroquinolone decreases insulin production upon sulphonylureas stimulation (164). Studies conducted by Ghaly *et al.* extensively reported on the insulinotropic effect of fluoroquinolones using a multi-approach *in vitro* (165). In these studies, it was apparent that ciprofloxacin, lomefloxacin and gatifloxacin stimulate insulin secretion, and it was also demonstrated that fluoroquinolone-induced insulin secretion involved the blockage of the K^+ _{ATP} channel (Figure 1.4). However, the introduction of diazoxide abolished the fluoroquinolone induced insulin secretion. Diazoxide is a well-known K^+ _{ATP} channel activator. To further confirm this phenomenon, insulin secretion was blunted when authors used SUR1 KO mice islets, which lack the K^+ _{ATP} channel. Interestingly, in this study, it was apparent that fluoroquinolones did not instigate insulin secretion; instead, they enhanced or improved insulin secretion. To demonstrate this, separate preparations of islets cells were incubated with glucose at different concentrations (5 and 10 mM). Fluoroquinolone-induced insulin secretion was only observed in the preparations incubated with 10 mM of glucose. In this scenario, 5 mM represented basal glucose concentration. Therefore, these observations may suggest that fluoroquinolones do not induce inappropriate insulin secretion. Although these observations are controversial, they could mean that fluoroquinolones possess desirable property as antidiabetic agents, which only enhances insulin secretion when blood glucose rises beyond the basal level. These observations agreed with those reported earlier by Maeda *et al.*, where they showed no insulin secretion induced by quinolones at a glucose concentration of 3 mM using mouse islets (166).

A conventional secretagogue (sulphonylureas) is also known to exert a potent enhancing effect in glucose concentrations higher than basal concentrations. However, at higher doses, sulphonylureas stimulate insulin secretion even in the absence of glucose. On the contrary, Saraya *et al.* found an increase in insulin secretion at a glucose concentration of 5.5 mM, which suggested an increase in insulin secretion stimulated by fluoroquinolones (300 μ M) at basal glucose concentrations (167). These observations could also explain the hypoglycaemia observed in patients on quinolone therapy. Mechanistically, fluoroquinolones have been found to bind to the Kirb subunits, thus inhibiting the potassium channel. Although a decline in insulin as a long-term effect of quinolone treatment, studies have revealed that it precedes an increase in insulin production. Physiologically, the consensus is that insulin is produced as pro-insulin in the rough endoplasmic reticulum. Pro-

insulin is then sent to the Golgi apparatus for further processing, which includes insulin cleavage. In clinical settings, patients on quinolone therapy are likely to experience hypoglycaemia within the first three days of therapy, whereas hyperglycaemia is likely to develop later (168, 169). It is not surprising that the effect of quinolones on animals described above only reported hyperglycaemia since they only focused on day 14 and not the early days of therapy initiation. Although *in vitro* studies are critical in supporting clinical observations, these concentrations used *in vitro* are multiple folds than those found in plasma during fluoroquinolone therapy. A study conducted by Yoshimatsu and colleagues revealed that administering a high dose of gatifloxacin intravenously induced acute transient hypoglycaemia followed by hyperglycaemia in monkeys (170). Despite conflicting evidence noted, however, it has been proven that gatifloxacin induces dysglycaemia on numerous occurrences. The effect induced by quinolones, whether hypoglycaemia or hyperglycaemia, depends on several factors, including the dose, mode of administration and duration of treatment (162).

1.6.1.5 Quinolone interaction with other anti-hyperglycaemic agents

Another mechanism by which quinolones cause hypoglycaemia is through the cytochrome P450 (CYP450) system. Quinolones are inhibitors of the CYP450 system. The CYP450 are responsible for the metabolism of some of the antidiabetic agents, which include glipizide – metabolised by CYP2C9, glimepiride – metabolised by CYP2C9, glyburide – metabolised by CYP2C9, nateglinide – metabolised by CYP2C9, pioglitazone – metabolised by CYP2C8 and CYP3A4, rosiglitazone – metabolised by CYP2C8 and CYP2C9 and repaglinide – metabolised by CYP2C8 (171). Therefore, concomitant use of these antidiabetic agents with quinolones will increase their serum concentration, enhancing their hypoglycaemic effect. When levofloxacin, ciprofloxacin, gatifloxacin, and moxifloxacin were used concomitantly with glyburide, it was reported that the serum concentration of glyburide was increased (157, 171).

1.6.1.6 Clinical studies

Glycaemic dysregulation has long been recognised in clinical settings, clinical trials and patients on fluoroquinolones. These outcomes prompted experimental studies to understand the mechanistic insights of fluoroquinolones in both *in vitro* and *in vivo* settings. Prior clinical trials

did not show apparent glycaemic aberrations in participants, perhaps alluding to the fact that these were young, healthy volunteers (172, 173). Although the risk of hypoglycaemia was observed in a few subjects, it was not significant to be listed as a safety concern in the packaging. Biggs was among the first to report on glycaemic abnormalities in hospitalised patients. The four cases reported included old diabetic patients on either sulphonylureas, insulin or metformin (174). Upon admission due to bacterial infections, these patients were given gatifloxacin 200-400 mg together with the regular antidiabetics they were receiving. However, three out of four patients presented with symptoms of hypoglycaemia. After that, gatifloxacin was discontinued. Although these observations might have indicated a potential interaction between fluoroquinolone and antidiabetics, hypoglycaemia was observed even when gatifloxacin was used without an antidiabetic agent. This, therefore, represented a direct hypoglycaemic effect elicited by fluoroquinolone. However, in these reported cases, it should be mentioned that the patients had renal insufficiency.

Fluoroquinolones, including gatifloxacin, are eliminated through the kidneys; therefore, renal insufficiency may impair their clearance, thus resulting in the exacerbation of adverse effects and glycaemic disturbance in this regard. Thomas *et al.*, conducted a retrospective cohort study intended to compare the effect of gatifloxacin and levofloxacin on the rates of hypoglycaemia and hyperglycaemia in patients over 65 years (175). In this study, 3.2% and 12.6% of the population experienced hypoglycaemia and hyperglycaemia, respectively. Hypoglycaemia was observed at the early stages of the treatment, which agrees with animal studies reporting hypersecretion of insulin during the initiation stage of fluoroquinolone. The late onset of hyperglycaemia observed in this study was also in line with animal studies. Long-term use of gatifloxacin has been shown to inhibit insulin biosynthesis. Although both fluoroquinolones demonstrated glycaemic dysregulations, gatifloxacin's effects were more pronounced than levofloxacin. Similarly, a retrospective study by Mohr *et al.* reported similar observations, although there were clear discrepancies' between gatifloxacin and levofloxacin (176). On the contrary, a multi-centre randomised trial that aimed to compare the efficacy of gatifloxacin and ciprofloxacin to treat shigellosis in Vietnamese children showed no significant glycaemic dysregulation (177). These observations suggest that glycaemic irregularities associated with fluoroquinolones are mainly limited to elderly patients, perhaps with additional co-morbidities. With more studies reporting on

glycaemic disturbances, gatifloxacin in all forms was withdrawn from the market in 2008. As of 2018, the food and drug administration (FDA) made a call to make it a requirement for additional labelling on fluoroquinolones which warns providers and patients about the risks of developing hypoglycaemia. A recent comparison investigated the association between antibiotics therapy and hypoglycaemia and the influence of glucose-lowering medications using the FDA adverse reporting system. In this study, it was noted that levofloxacin and moxifloxacin had been associated with hypoglycaemia. However, none of the fluoroquinolones was associated with hypoglycaemia (178). Few studies have reported on the effect of glycaemic abnormalities associated with ciprofloxacin in non-diabetic patients. A recent study by Berhe *et al.* has provided evidence of hypoglycaemia associated with ciprofloxacin (179). This study reported on 35 cases where ciprofloxacin administration was associated with hypoglycaemia in 17 countries. In 10 cases, withdrawal of ciprofloxacin resulted in normoglycaemia. However, in 20 cases, severe hypoglycaemia was observed, which was associated with two fatalities. Ciprofloxacin was the sole drug in almost half of the patients, suggesting a strong association with hypoglycaemia. Ciprofloxacin has been demonstrated to inhibit CYP1A4 isoenzymes that result in drug interactions, particularly with diabetic drugs such as glyburide (180). However, none of the study participants was receiving an antidiabetic drug. Considering the hypoglycaemic effects that authors have reported on, this may present an opportunity to use quinolones as a scaffold to develop potential antidiabetic agent.

1.6.1.7 Emergence of quinolone derivatives as an antidiabetic agent

There is extensive research into DM, where authors report on several potential antihyperglycaemic agents. Quinolones are drugs that have been reported to possess hypoglycaemic side effects, hence this may represent an opportunity to repurpose some of the quinolones for managing DM through the modification of their structural features. The ability of fluoroquinolones to enhance insulin secretion could be advantageous in managing DM. At present, sulphonylureas are one of the existing class of drugs available in the market that lowers blood glucose concentration through this mechanism. Fluoroquinolones may provide an opportunity to develop another class with a similar mechanism of action. Therefore, there is a need to embark on and pursue studies seeking to fully understand the mechanism of quinolones on insulin secretion, including exploration of the structure-activity relationship to identify new pharmacophoric units required in treating DM.

Although there is an understanding of the effect of quinolones on insulin secretion and its associated mechanisms, there is limited knowledge to provide the required understanding of key structural features responsible for this effect.

Although fluoroquinolones possess hypoglycaemic properties, very few studies have reported on novel quinolones derivatives synthesised solely for antidiabetic activity. In a study conducted by Edmont *et al.*, quinolinoylguanidines were synthesized and tested for their potential hypoglycaemic activity *in vivo* (181). The experiment envisaged that having a carbonylguanidine group at position 2 rather than position 3 could enhance the hypoglycaemic effect. One of the compounds synthesised (Figure 1.5) has a hypoglycaemic effect greater than that of metformin. The hypoglycaemic effect of the compound was enhanced by possibly adding a carbonylguanidine group at position 2, an ethoxy group at position 4, and a fluorine atom at position 6.

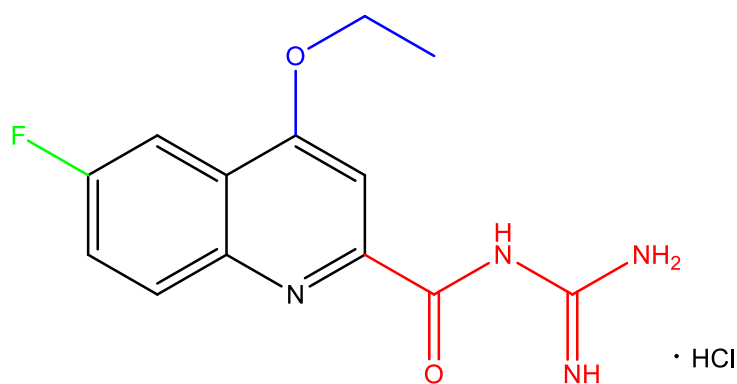


Figure 1.5: A fluoroquinolone derivative known as quinolinoylguanidine. This compound has a carbonylguanidine group at position 2 (red), an ethoxy group at position 4 (blue), and a fluorine atom at position 6 (green).

Muluk *et al.* also investigated novel quinolone derivatives for their antidiabetic properties. The compounds investigated were substituted benzimidazole quinolone, which was synthesised by modifying quinolone structure through the reaction of *o*-phenylenediamine with the carboxylic group of ciprofloxacin and levofloxacin (182). The resulting intermediates were transformed through the Mannich reaction to produce substituted benzimidazole quinolones. The resulting derivatives were screened *in vitro* for their antidiabetic activity using alpha-glucosidase inhibitory assay at concentrations of 150 and 200 $\mu\text{g/mL}$. From the synthesised compounds, some

compounds (Figure 1.6) showed promising antidiabetic activities at a concentration of 200 $\mu\text{g/mL}$ when compared to a standard drug (acarbose).

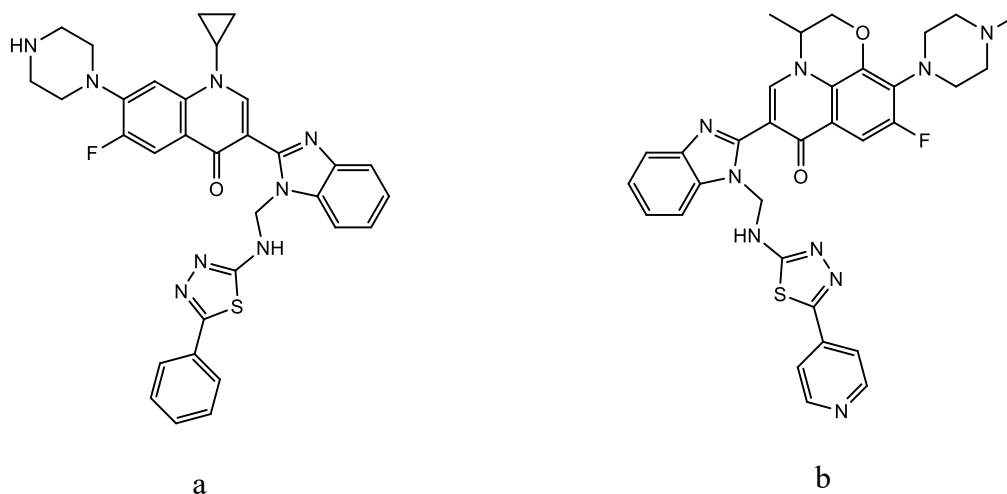


Figure 1.6: Substituted benzimidazole quinolone derivatives synthesised from ciprofloxacin (a) and levofloxacin (b) by reacting *o*-phenylenediamine with the carboxylic group of ciprofloxacin and levofloxacin. The resulting intermediates were transformed through the Mannich reaction to produce substituted benzimidazole quinolones. These compounds exhibited inhibitory activity against alpha-glucosidase at 200 $\mu\text{g/mL}$.

1.7 Quinolone compounds of interest in this study

From the above literature, there is evidence that quinolone-based compounds elicit hypoglycaemic properties. Extending further from this literature, four novel quinolone derivatives were examined on selected key DM therapeutic targets. The four compounds are quinolinyl-chalcone hybrids, and their names are:

- Compound 1: (*E*)-ethyl 6-(3-(5-chloro-2-nitrophenyl)acryloyl)-1-ethyl-4-oxo-1,4-dihydroquinoline-3-carboxylate.

- Compound 2: (*E*)-ethyl 1-ethyl-6-(3-(4-nitrophenyl)acryloyl)-4-oxo-1,4-dihydroquinoline-3-carboxylate.
- Compound 3: (*E*)-ethyl 6-(3-(3,5-dichlorophenyl)acryloyl)-1-ethyl-4-oxo-1,4-dihydroquinoline-3-carboxylate.
- Compound 4: (*E*)-ethyl 6-(3-(4-(dimethylamino)phenyl)acryloyl)-1-ethyl-4-oxo-1,4-dihydroquinoline-3-carboxylate.

In this study, compound 1 will be referred to as quinolone derivative 1 (QD1), compound 2 as quinolone derivative 2 (QD2), compound 3 as quinolone derivative 3 (QD3) and compound 4 as quinolone derivative 4 (QD4). The quinolone scaffold for the four compounds is substituted with an ethyl group at position 1, an ethyl ester group at position 3 and a substituted chalcone moiety at position 6 (Figure 1.7). The chalcone moiety is substituted with chloride and a nitro group at position 3 and 6, respectively, for QD1, a nitro group at position 4 for QD2, a chloride atom at position 3 and 5 for QD3 and a dimethylamino group at position 4, for QD4.

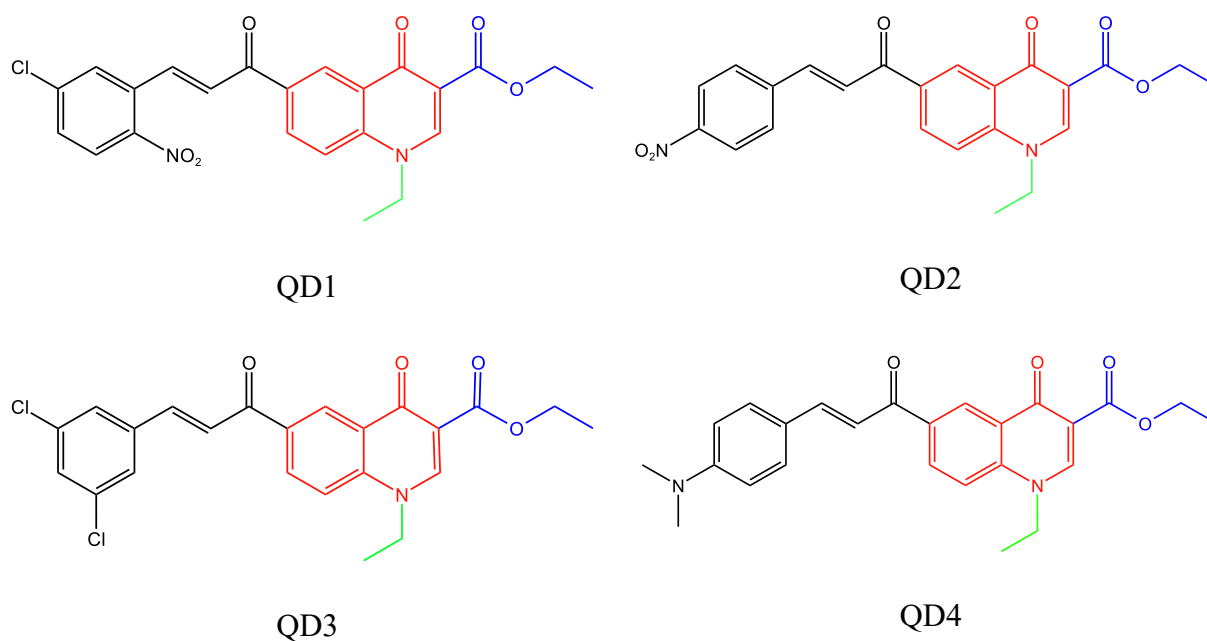


Figure 1.7: Structure of the quinolone derivatives investigated for their antidiabetic and cardio-protective properties. The quinolone scaffold is drawn in red, and it is substituted with an ethyl

group at position 1 (green), an ethyl ester group at position 3 (blue) and a substituted chalcone moiety at position 6 (black).

1.8 Justification of the study

Diabetes mellitus is one of the major disorders found in every population and region of the world, and over the years, there has been a steady increase in the number of diabetic cases. DM often result in complications, including CVD, which is the leading cause of death in diabetic patients. DM and CVD were the diseases of interest in this study due to their pathological link and increased prevalence. Furthermore, the devastating effects of these diseases on patients and the dire need for effective pharmacological therapies as made them an area of interest. Although there are available antidiabetic agents, they present with undesirable effects, and they provide little to no protection against the development of CVD. Also, over time, they become less effective, thus making treatment therapy challenging. Therefore, the need for newer antidiabetic agents with minimal side effects, prolonged efficacy and possible cardio-protective effect has become an issue of importance. Hence, this study will focus on screening novel quinolone derivatives on selected diabetic therapeutic targets and cardio-protective activities. Quinolones were the compounds of interest because they have been reported to exhibit a hypoglycaemic effect through the stimulation of insulin release. Therefore, investigating novel quinolone derivatives may provide an avenue for the development of newer antidiabetic agents with lesser side effects and enhanced activity.

1.9 Aim

This study is aimed at determining the effect of novel quinolone derivatives on pharmacological targets of hyperglycaemia, lipidaemia and hypercoagulation.

1.10 Objectives

1.10.1 Cell-free assays

1. Predicting the drug-likeness and gastrointestinal tract absorption of novel quinolone derivatives.

2. *In vitro* screening of novel quinolone derivatives to determine their antidiabetic activity on selected therapeutic targets using the following assays:
 - a) Alpha-amylase inhibition assay.
 - b) Alpha-glucosidase inhibition assay.
 - c) DPP4 inhibition assay.
 - d) PTP1B inhibition assay.
 - e) Aldose reductase inhibition assay.
3. *In vitro* screening of novel quinolone derivatives to determine their effect on selected therapeutic targets for cardiovascular diseases using the following assays:
 - a) Factor Xa inhibition assay.
 - b) HMG-CoA reductase inhibition assay.
4. *In vitro* screening of novel quinolone derivatives to determine their antioxidant activity by using the following assays:
 - a) 2,2-diphenyl-1-picrylhydrazyl (DPPH) radical scavenging assay.
 - b) Ferric reducing antioxidant power (FRAP) assay.

1.10.2 Cell-based assays

5. *In vitro* screening of novel quinolone derivatives for their effect on glucose uptake in:
 - a) Skeletal muscle (C2C12) cell lines.
 - b) Hepatic (HepG2) cell lines.
6. *In vitro* screening of novel quinolone derivatives to determine their effect on cell viability in:
 - a) Skeletal muscle cell lines.
 - b) Hepatic cell lines.

CHAPTER 2: MATERIALS AND METHODOLOGY

2.1 Chemicals

Sodium carbonate, sodium chloride, hydrochloric acid (HCl), sodium hydroxide, dimethyl sulfoxide (DMSO), sodium phosphate monobasic, sodium phosphate dibasic, sodium acetate, methanol, alpha-amylase from porcine pancreas, alpha-glucosidase from *Saccharomyces cerevisiae*, aldose reductase human recombinant, protein tyrosine phosphatase-1B (PTP1B) full length active human, acarbose, ascorbic acid, sodium orthovanadate, quercetin, starch, maltose, sodium azide, 3,5-dinitrosalicylic acid (DNSA), sodium potassium tartrate tetrahydrate, *p*-nitrophenyl- α -D-glucopyranoside (*p*NPG), *p*-nitrophenol, *p*-nitrophenyl phosphate (*p*NPP), DPPH, 2,4,6-tris(2-pyridyl)-*s*-triazine (TPTZ), iron (III) chloride hexahydrate (FeCl₃.6H₂O), iron (II) chloride, NADPH, DL-glyceraldehyde, TRIS hydrochloride (TRIS HCl), ethylenediaminetetraacetic acid (EDTA), dithiothreitol (DTT), β -mercaptoethanol, DPP4 inhibitor screening kit, factor Xa inhibitor screening kit, HMG-CoA reductase assay kit, Dulbecco's modified eagle's medium (DMEM), minimum essential medium eagle (MEM) fetal bovine serum (FBS), and penicillin-streptomycin, were purchased from Sigma-Aldrich (Johannesburg, South Africa). C2C12 and HepG2 cell lines were sourced from Dr Ngcobo at the University of KwaZulu-Natal (Durban, South Africa). All other chemicals and reagents were of analytical grade.

2.2 Equipment

SpectraMax M3 multi-mode microplate reader (100 – 240V~3.5A 50 – 60Hz; manufactured in China, designed in California, USA), UV-VIS Spectrophotometer (UVmini-1240)(AC 220 – 240~50/60Hz 160VA; SHIMADZU CORPORATION, made in China, Incubator (FSOH4)(220/240V 50Hz, 0.5kW; Labcon (pty) ltd 15 Aschenberg street Chamdor Krugersdorp Transvaal), BV1000 vortex mixer (230VAC 50Hz, 0.75amps; Benchmark Scientific Inc. PO BOX 709, Edison, NJ 08818, USA; made in Taiwan), hotplate stirrer (H3760-HSE)(230V, 60Hz; (Lasec Laboratories) Benchmark Scientific Inc. PO BOX 709, Edison, NJ 08818, USA), Accu-Check Performa glucometer and contour plus test stripes.

2.3 Synthesis and characterisation of quinolone derivative compounds

The synthesis and characterisation of the four quinolone derivatives were performed by the Drug Discovery and Pharmaceutical Chemistry Group (Division of Pharmaceutical Chemistry, Rhodes University) under the supervision of Prof. S.D. Khanye. The synthesis process is summarized below.

2.3.1 Synthesis of ethyl 6-acetyl-4-oxo-1,4-dihydroquinoline-3-carboxylate

In a round bottom flask, 4-aminoacetophenone was mixed with diethyl-ethoxymethylenemalonate, and the reaction mixture was heated to 150 °C for 12 hours without a solvent. After the disappearance of the starting material, which was checked using thin layer chromatography (TLC), diphenyl ether was added, and the reaction mixture was refluxed further at 265 °C for 1 hour. Thereafter, the crude mixture was transferred into a beaker and hexane was added. A beige solid precipitate formed, and it was filtered using vacuum filtration and washed with acetone to remove unreacted material. The structure of the synthesised compound was established by a combination of spectroscopic methods, which includes IR, ¹H and ¹³C NMR.

2.3.2 Synthesis of ethyl 6-acetyl-1-ethyl-4-oxo-1,4-dihydroquinoline-3-carboxylate

In a round bottom flask containing dry dimethylformamide (DMF), ethyl 6-acetyl-4-oxo-1,4-dihydroquinoline-3-carboxylate, ethyl group and K₂CO₃ were added. The reaction mixture was left to stir at room temperature overnight. After the completion of the reaction, the crude was poured into ice-cold water, and the pH was adjusted to 5, using acetic acid to form a precipitate, which was filtered and washed several times with water to give a beige solid. The structure of the synthesized compound was established by a combination of spectroscopic methods, which includes IR, ¹H and ¹³C NMR.

2.3.3 Synthesis of quinolinyl-chalcone hybrids

An appropriate acetyl-quinolone and benzaldehydes in ethanol were added into a round bottom flask. SOCl₂ was added dropwise to this reaction mixture, and the reaction mixture was left stirring

at room temperature for 12 hours. The reaction progress was monitored by TLC. After completion, the reaction product was poured into a beaker of ice-cold water, neutralized with NaHCO₃ and extracted with ethyl acetate. The organic layers were combined and dried over anhydrous MgSO₄ and concentrated under reduced pressure to give crude products, which were further purified using preparative plates (dichloromethane (DCM): methanol (MeOH)). The structures of all the synthesized hybrid compounds were established by a combination of spectroscopic methods, which includes IR, ¹H and ¹³C NMR and high-resolution electrospray ionization mass spectrometry (ESI-HRMS).

2.4 Predicting the drug-likeness and gastrointestinal absorption of the quinolone derivatives

The predicted drug-likeness and bioavailability of the quinolone derivatives were done using the SwissADME web tool (183). The SwissADME is able to compute the physicochemical descriptors and also predict the absorption, distribution, metabolism and excretion (ADME) parameters of a molecule. These parameters are essential in drug discovery because they can predict the druggability of a molecule. To generate these parameters, the canonical SMILES for each compound were incorporated into this tool for computational simulation, after which the Lipinski parameters and BOILED-Egg model were generated. Lipinski's parameters evaluate the drug-likeness or chemical and physical properties of a chemical compound to predict if it will be orally active. The BOILED-Egg model (*Brain Or IntestinaL EstimateD permeation predictive model*) is a rapid, easily reproducible and robust method for predicting the passive GIT absorption and blood-brain barrier (BBB) permeability of small molecules intended for drug discovery and development.

2.5 Cell-free assay

2.5.1 Preparation of compounds for *in vitro* testing

A stock solution for QD1, QD2, QD3 and QD4 with a concentration of 1000 µg/mL was prepared by weighing out 0.01g of each compound and dissolved in 1ml DMSO. It was then made up to 10 mL with distilled water. These stock solutions were diluted further to make the desired

concentrations (15, 30, 60, 120 and 240 $\mu\text{g}/\text{mL}$) using the $C_1V_1 = C_2V_2$ formula. A reference drug was used for each assay, and each reference drug was prepared into the desired concentrations. For each assay, the desired concentrations were freshly prepared using distilled water or the required buffer.

2.5.2 Antidiabetic assays

2.5.2.1 Alpha-amylase inhibition assay

Principle

This assay was performed using the 3,5-dinitrosalicylic acid (DNSA) method. The alpha-amylase activity is measured using a colorimetric method with DNSA reagent. In this method, the substrate (starch) is converted into maltose by alpha-amylase, and the amount of maltose released is measured by the reduction of DNSA. Maltose reduces the pale-yellow alkaline DNSA to an orange-red colour. This intensity change in colour is proportional to the concentration of maltose present in the sample, and the absorbance is measured with a spectrophotometer at a wavelength of 540 nm. The presence of an alpha-amylase inhibitor such as acarbose decreases the liberation of maltose, hence leading to a decrease in the reduction of DNSA and absorbance detected.

Protocol

The alpha-amylase inhibition assay was performed using the DNSA method with slight modifications (184). In a test tube, 1 mL of alpha-amylase (1 U/mL) in phosphate buffer solution (0.02 M with 0.006 M NaCl at pH 6.9) was mixed with 1 mL quinolone derivative at different concentrations (15, 30, 60, 120 and 240 $\mu\text{g}/\text{mL}$) and preincubated at 37 °C for 10 minutes. Thereafter, 1 mL of starch solution (1% w/v) was added to each test tube and incubated for 10 minutes. The reaction was terminated by adding 1 mL DNSA reagent (12 g of sodium potassium tartrate tetrahydrate in 8.0 mL of 2 M NaOH and 20 mL of 96 mM of DNSA solution) and boiled for 5 minutes in a water bath at 85 °C. The mixture was cooled to room temperature and diluted with 5 mL distilled water, after which the absorbance was measured with a spectrophotometer at a wavelength of 540 nm. Acarbose was used as the standard drug at concentrations of 15, 30, 60, 120 and 240 $\mu\text{g}/\text{mL}$. At the same time, the absolute control with 100% enzyme activity was prepared following the same procedure replacing the quinolone derivatives with buffer. The assay

was performed in triplicates, and the alpha-amylase inhibitory activity was calculated as percentage inhibition using the equation below:

$$\text{Percentage inhibition (\%)} = \left(\frac{\text{absorbance of control} - \text{absorbance of sample}}{\text{absorbance of control}} \right) * 100$$

The percentage inhibition (%) was plotted against the concentrations used, and the concentrations needed to inhibit 50 % of enzyme activity (IC₅₀) were determined from the plot using GraphPad Prism version 8.0.2 (GraphPad Software, San Diego, California USA, www.graphpad.com) in built method which uses non-linear regression (curve fit) to determine IC₅₀.

2.5.2.1.1 Enzyme kinetics and mode of alpha-amylase inhibition

An enzyme's mode of inhibition describes an inhibitor's binding to a targeted enzyme. Enzyme inhibitors are molecules that interact with enzymes to reduce the rate of an enzyme-catalyzed reaction or prevent enzyme activity (185). The different types of enzyme inhibition are classified according to the effect of V_{\max} (maximum reaction rate catalysed by the enzyme) and K_m (Michaelis constant, which is the concentration of substrate resulting in half maximal enzyme activity) as the concentration of the enzyme's substrate is varied (186). The different types of inhibition include: (i) competitive inhibition: inhibitor binds to the enzyme's active site, preventing the substrate from binding. In this type of inhibition, K_m increases while V_{\max} is more or less the same (187), (ii) uncompetitive inhibition: the inhibitor binds only to the enzyme-substrate complex, and in this type of inhibition, both K_m and V_{\max} decreases (188), (iii) non-competitive inhibition: the inhibitor binds to an allosteric site resulting in decreased efficacy of the enzyme. The K_m remains unchanged while V_{\max} decreases in this type of inhibition (189) and (iv) mixed inhibition: this type of inhibition is a combination of competitive and noncompetitive inhibition. In this type of inhibition, the inhibitor binds to the enzyme whether or not the substrate has already bound. The inhibitor is also capable of binding to the enzyme binding site and an allosteric site. The V_{\max} decreases while K_m can either decrease or increase, depending on whether the inhibitor has more affinity for either the active site or the enzyme substrate complex (190-192).

The mode of inhibition of the alpha-amylase enzyme by the quinolone derivatives was determined using QD4 because it had the lowest IC₅₀, indicating that it is the most potent for inhibiting alpha-amylase activity among the quinolone derivatives investigated. To determine the kinetics, in a set

of test tubes, 1 mL of alpha-amylase (1 U/mL) in phosphate buffer solution (0.02 M with 0.006 M NaCl at pH 6.9) was mixed with 1 mL QD4 at a fixed concentration (120 µg/mL) and preincubated at 37 °C for 10 minutes. In another set of test tubes, alpha-amylase was incubated with 1 ml of phosphate buffer (0.02 M with 0.006 M NaCl at pH 6.9). After that, 1mL of starch solution at increasing concentrations (0.25, 0.50, 1.0, 2.0 and 4.0 mM) was added to each set of test-tube and incubated for 10 minutes. The reaction was terminated by adding 1mL DNSA reagent and boiled for 5 minutes in a water bath at 85 °C. The mixture was cooled to room temperature and diluted with 5 mL distilled water, after which the absorbance was measured at 540 nm. The concentration of reducing sugars released was determined using a maltose standard curve (concentrations ranging from 1 to 7 mM) generated using the DNSA method (Appendix 1). Afterwards, the generated concentrations were converted to reaction velocities. A double reciprocal plot (1/V versus 1/S) where V is reaction velocity and S is substrate concentration was plotted. The mode of inhibition of QD4 on alpha-amylase activity was determined by using the V_{max} and K_m generated from the Michaelis-Menten plot, and the data set intersection point on the double reciprocal (Lineweaver-Burk) plot generated from the Michaelis-Menten plot.

2.5.2.2 Alpha-glucosidase inhibition assay

Principle

Alpha-glucosidase acts on the substrate *p*-nitrophenyl- α -D-glucopyranoside (pNPG) to form *p*-nitrophenol and α -D-glucopyranoside. The absorbance of *p*-nitrophenol liberated is measured with a spectrophotometer at 405 nm. A potent inhibitor such as acarbose inhibits alpha-glucosidase activity on the substrate, resulting in a reduction in the absorbance, which is a measure of the *p*-nitrophenol formed.

Protocol

The effect of quinolone derivatives on alpha-glucosidase activity was determined according to the literature method with minor modifications (193). In a white 96-well plate, a reaction mixture containing 100 µL of phosphate buffer (0.1 M, pH = 6.8), 40 µL of alpha-glucosidase (0.1 U/mL), and 80 µL quinolone derivative at different concentrations (15, 30, 60, 120, and 240 µg/mL) were preincubated at 37°C for 10 min. The reaction was then initiated by the addition of 20 µL of pNPG (2 mM), and the mixture was then incubated for 10 min at 37°C. The reaction was stopped by

adding 100 μL of Na_2CO_3 (0.1 M), after which the absorbance of the yellow-coloured *p*-nitrophenol released from *p*NPG was measured with a spectrophotometer at a wavelength of 405 nm. Acarbose was used as the standard drug at concentrations of 15, 30, 60, 120 and 240 $\mu\text{g}/\text{mL}$, while the absolute control with 100% enzyme activity was prepared following the same procedure replacing the quinolone derivatives with buffer. The assay was performed in triplicates, and the alpha-glucosidase inhibitory activity was calculated as percentage inhibition using the equation below:

$$\text{Percentage inhibition (\%)} = \left(\frac{\text{absorbance of control} - \text{absorbance of sample}}{\text{absorbance of control}} \right) * 100$$

The percentage inhibition (%) was plotted against the concentrations used, and the concentrations of the IC_{50} were determined from the plot using Graphpad Prism version 8.0.2 in-built method, which uses non-linear regression (curve fit) to determine IC_{50} .

2.5.2.2.1 Enzyme kinetics and mode of inhibition of alpha-glucosidase

The mode of inhibition of the alpha-glucosidase enzyme by the quinolone derivatives was determined using QD1 because it had the lowest IC_{50} , indicating that it is the most potent for inhibiting alpha-glucosidase activity among the quinolone derivatives investigated. Briefly, in a white 96-well plate, a reaction mixture containing 100 μL of phosphate buffer (0.1 M, $\text{pH} = 6.8$), 40 μL of alpha-glucosidase (0.1 U/mL), and 80 μL of QD1 at a fixed concentration (120 $\mu\text{g}/\text{mL}$) was preincubated at 37°C for 10 minutes. Control was also prepared by replacing the quinolone derivative with phosphate buffer (0.1 M, $\text{pH} = 6.8$). The reaction was then initiated by the addition of 20 μL of *p*NPG at increasing concentrations (0.125, 0.25, 0.5, 1.0, 2.0 and 4.0 mM), and the mixture was then incubated for 10 minutes at 37°C . The reaction was stopped by adding 100 μL of Na_2CO_3 (0.1 M), and the absorbance was measured at 405 nm. The amount of *p*-nitrophenol released was determined using a *p*-nitrophenol standard curve at concentrations ranging from 10 to 100 μM (Appendix 2) and converted to reaction velocities. A double reciprocal plot ($1/V$ versus $1/S$) where V is reaction velocity and S is substrate concentration was plotted. The mode of inhibition of QD1 on alpha-glucosidase activity was determined by using the V_{max} and K_m generated from the Michaelis-Menten plot, and the data set intersection point on the double reciprocal (Lineweaver-Burk) plot generated from the Michaelis-Menten plot.

2.5.2.3 DPP4 inhibition assay

Principle

This assay was performed using a DPP4 inhibitor screening kit purchased from Sigma Aldrich (Johannesburg, South Africa). The assay uses the fluorogenic substrate, Gly-Pro-Aminomethylcoumarin to measure DPP4 activity. Cleavage of the peptide bond by DPP4 releases the aminomethylcoumarin group, resulting in fluorescence that can be measured at an excitation wavelength of 360 nm and emission wavelength of 460 nm. The introduction of a potent inhibitor such as sitagliptin reduces the formation of the aminomethylcoumarin fluorogenic substrate and, therefore, reduces fluorescence detection.

Protocol

The assay was conducted using the manufacturer's instructions. Briefly, in a black 96-well plate, a reaction mixture containing 49 μL of DPP4 buffer, 1 μL of the DPP4 enzyme and 100 μL of quinolone derivatives at different concentrations (15, 30, 60, 120 and 240 $\mu\text{g}/\text{mL}$) were incubated at 37°C for 10 minutes. After incubation, 23 μL of DPP4 buffer and 2 μL of DPP4 substrate was added. Fluorescence was then measured at an excitation and emission wavelength of 360 nm and 460 nm, respectively, in kinetic mode every minute for 30 minutes at 37°C. Sitagliptin at IC_{50} was provided by the manufacturer as the standard drug. At the same time, the absolute control with 100% enzyme activity was prepared following the same procedure replacing the quinolone derivatives with DPP4 kit buffer. The assay was performed in triplicates, and the DPP4 inhibitory activity was calculated as percentage inhibition using the equation below:

$$\text{Percentage inhibition (\%)} = \left(\frac{\Delta\text{fluorescence of control} - \Delta\text{fluorescence of sample}}{\Delta\text{fluorescence of control}} \right) * 100$$

The percentage inhibition (%) was plotted against the concentrations used, and the concentrations of the IC_{50} were determined from the plot using Graphpad Prism version 8.0.2 in-built method, which uses non-linear regression (curve fit) to determine IC_{50} .

2.5.2.4 Protein tyrosine phosphatase 1B inhibition assay

Principle

The protein tyrosine phosphatase 1B (PTP1B) enzyme dephosphorylates the substrate *p*-nitrophenyl phosphate (*p*NPP), generating *p*-nitrophenol, which produces an intense yellow colour that can be measured spectrophotometrically at a wavelength of 405 nm. Therefore, potent inhibitors of PTP1B, such as sodium orthovanadate, inhibit the enzymatic activity, preventing the release of *p*-nitrophenol, resulting in a decrease in absorbance.

Protocol

The effect of quinolone derivatives on PTP1B activity was determined according to literature reported method with slight modification (194). In a white 96-well plate, a reaction mixture containing 100 μ L of TRIS-HCl buffer (25 mM, pH 7.5 containing 1 mM EDTA, 1 mM dithiothreitol, 2 mM β -mercaptoethanol), 50 μ L of alpha-glucosidase (1 μ g/mL), and 100 μ L quinolone derivatives at different concentrations (15, 30, 60, 120, and 240 μ g/mL) were preincubated at 37°C for 10 minutes. The reaction was then initiated by the addition of 50 μ L of *p*NPP (4 mM), and the mixture was then incubated for 10 minutes at 37°C. The absorbance of the yellow-coloured *p*-nitrophenol released from *p*NPP was measured with a spectrophotometer at a wavelength of 405 nm. Sodium orthovanadate was used as the standard drug at concentrations of 15, 30, 60, 120 and 240 μ g/mL. At the same time, the absolute control with 100% enzyme activity was prepared following the same procedure replacing the quinolone derivatives with buffer. The assay was performed in triplicates, and the PTP1B inhibitory activity was calculated as percentage inhibition using the equation below:

$$\text{Percentage inhibition (\%)} = \left(\frac{\text{absorbance of control} - \text{absorbance of sample}}{\text{absorbance of control}} \right) * 100$$

The percentage inhibition (%) was plotted against the concentrations used, and the concentrations of the IC₅₀ were determined from the plot using Graphpad Prism version 8.0.2 in-built method, which uses non-linear regression (curve fit) to determine IC₅₀.

2.5.2.5 Aldose reductase inhibition assay

Principle

The enzymatic activity of the aldose reductase enzyme results in a decrease in NADPH absorption. Using DL-glyceraldehyde as a substrate, the enzyme uses up NADPH leading to its reduction, which can be detected spectrophotometrically at 340 nm. Hence, potent inhibitors such as quercetin inhibit the activity of the enzyme on NADPH.

Protocol

The effect of quinolone derivatives on aldose reductase activity was determined with minor modifications to the reported literature method (195). In a white 96-well plate, a reaction mixture containing 100 μL of phosphate buffer (0.1 M, pH = 6.2), 30 μL of aldose reductase (2 $\mu\text{g}/\text{mL}$), 60 μL quinolone derivatives at different concentrations (15, 30, 60, 120, and 240 $\mu\text{g}/\text{mL}$), and 60 μL NADPH (0.15 mM) were incubated at 37°C for 10 minutes. The reaction was initiated by adding 30 μL DL-glyceraldehyde (10 mM). Absorbance was measured kinetically every minute for 30 minutes with a spectrophotometer at a wavelength of 340 nm. Quercetin was used as the standard drug at concentrations of 15, 30, 60, 120 and 240 $\mu\text{g}/\text{mL}$, while the absolute control with 100% enzyme activity was prepared following the same procedure replacing the quinolone derivatives with a buffer. The assay was performed in triplicates, and the aldose reductase inhibitory activity was calculated as percentage inhibition using the equation below:

$$\text{Percentage inhibition (\%)} = \left(\frac{\Delta\text{Absorbance of control} - \Delta\text{Absorbance of sample}}{\Delta\text{Absorbance of control}} \right) * 100$$

The percentage inhibition (%) was plotted against the concentrations used, and the concentrations of the IC_{50} were determined from the plot using Graphpad Prism version 8.0.2 in-built method, which uses non-linear regression (curve fit) to determine IC_{50} .

2.5.3 Cardio-protective activity assay

2.5.3.1 Factor Xa inhibition assay

Principle

This assay was performed using a clotting factor Xa (FXa) inhibitor screening kit purchased from Sigma Aldrich (Johannesburg, South Africa). The assay utilizes the ability of FXa to cleave a synthetic substrate, thereby releasing a fluorophore, 7-amino-4-methylcoumarin (AMC), which a fluorescence reader can quantify at an excitation wavelength of 350 nm and emission wavelength of 450 nm. In the presence of an inhibitor such 1,5-dansyl-Glu-Gly-Arg chloromethyl ketone (GGACK) dihydrochloride, the extent of the cleavage reaction is reduced or completely abolished.

Protocol

The assay was conducted using the manufacturer's instructions. Briefly, in a white 96-well plate, a reaction mixture containing 49 μL of FXa buffer, 1 μL of FXa enzyme and 10 μL of quinolone derivatives at different concentrations (15, 30, 60, 120 and 240 $\mu\text{g}/\text{mL}$) were incubated at 25°C for 10 minutes. After incubation, 38 μL of FXa buffer and 2 μL of FXa substrate was added. Fluorescence was then measured at an excitation and emission wavelength of 350 nm and 450 nm, respectively, in kinetic mode every minute for 30 minutes at 37°C. GGACK dihydrochloride was provided by the manufacturer as the standard drug. At the same time, the absolute control with 100% enzyme activity was prepared following the same procedure replacing the quinolone derivative with FXa buffer. The assay was performed in triplicates, and the FXa inhibitory activity was calculated as percentage inhibition using the equation below:

$$\text{Percentage inhibition (\%)} = \left(\frac{\Delta\text{fluorescence of control} - \Delta\text{fluorescence of sample}}{\Delta\text{fluorescence of control}} \right) * 100$$

The percentage inhibition (%) was plotted against the concentrations used, and the concentrations of the IC_{50} were determined from the plot using Graphpad Prism version 8.0.2 in-built method, which uses non-linear regression (curve fit) to determine IC_{50} .

2.5.3.2 HMG-CoA reductase assay

Principle

This assay was performed using a 3-hydroxy-3-methylglutaryl coenzyme A reductase (HMGR) assay kit purchased from Sigma Aldrich (Johannesburg, South Africa). The assay is based on the spectrophotometric measurement of the decrease in absorbance at 340 nm, which represents the oxidation of NADPH by the catalytic subunit of HMGR in the presence of the substrate 3-hydroxy-3-methylglutaryl coenzyme A (HMG-CoA).

Protocol

The assay was conducted using the manufacturer's instructions. Briefly, in a white 96-well plate, a reaction mixture containing 181 μL of assay buffer, 1 μL of quinolone derivatives at different concentrations (15, 30, 60, 120 and 240 $\mu\text{g}/\text{mL}$), 4 μL NADPH, 12 μL HMG-CoA and 2 μL HMGR. Absorbance was then measured at a wavelength of 340 nm in kinetic mode every minute for 10 minutes at 37°C. Pravastatin was provided by the manufacturer as the standard drug, while the absolute control with 100% enzyme activity was prepared following the same procedure replacing the quinolone derivative with assay buffer. The assay was performed in triplicates, and the HMG-CoA reductase inhibitory activity was calculated as percentage inhibition using the equation below:

$$\text{Percentage inhibition (\%)} = \left(\frac{\Delta\text{Absorbance of control} - \Delta\text{Absorbance of sample}}{\Delta\text{Absorbance of control}} \right) * 100$$

The percentage inhibition (%) was plotted against the concentrations used, and the concentrations of the IC_{50} were determined from the plot using Graphpad Prism version 8.0.2 in-built method, which uses non-linear regression (curve fit) to determine IC_{50} .

2.5.4 Antioxidant activity assay

2.5.4.1 DPPH radical scavenging activity assay

Principle

DPPH free radical, which is purple in colour, accepts a hydrogen atom in a one-electron reaction to form 2,2-diphenyl-1-picrylhydrazine (DPPH-H), which is pale yellow in colour, and this colour

change is associated with a decrease in absorbance at 517 nm. Therefore, the reduction in absorbance is proportional to the antioxidant capacity of the inhibitor sample.

The scavenging reaction can be written as $\text{DPPH} + (\text{H-D}) \longrightarrow \text{DPPH-H} + \text{D}$

Purple

Yellow

Protocol

The DPPH radical scavenging activity was determined according to Kwon *et al.* with slight modification (196). In a white 96-well plate, 100 μL of DPPH (0.01 mM) in methanol was added to 200 μL of quinolone derivatives at different concentrations (15, 30, 60, 120, and 240 $\mu\text{g}/\text{mL}$), after which it was allowed to stand in the dark at room temperature for 30 minutes. Absorbance was then measured at a wavelength of 517 nm. Ascorbic acid was used as the standard drug at concentrations of 15, 30, 60, 120 and 240 $\mu\text{g}/\text{mL}$. At the same time, the absolute control with 100% enzyme activity was prepared following the same procedure replacing the quinolone derivatives with methanol. The assay was performed in triplicates, and the percentage DPPH radical scavenging activity was expressed as:

$$\text{DPPH radical scavenging activity (\%)} = \left(\frac{\text{absorbance of control} - \text{absorbance of sample}}{\text{absorbance of control}} \right) * 100$$

The DPPH radical scavenging activity (%) was plotted against the concentrations used, and the concentrations of the IC_{50} were determined from the plot using Graphpad Prism version 8.0.2 in built method, which uses non-linear regression (curve fit) to determine IC_{50} .

2.5.4.2 Ferric reducing antioxidant power (FRAP) assay

Principle

The FRAP assay principle is based on electron transfer due to the reduction of ferric-tripyridyltriazine (Fe^{3+} -TPTZ) to ferrous-tripyridyltriazine (Fe^{2+} -TPTZ). When the reduction of Fe^{3+} to Fe^{2+} occurs in the presence of 2,4,6-tris(2-pyridyl)-s-triazine, the reaction is accompanied by the formation of a violet-blue complex of Fe^{2+} and these changes are evaluated spectrophotometrically at a wavelength of 593 nm. Therefore, an increase in the antioxidant activity will result in an increase in the absorbance detected at 593 nm.

Protocol

The FRAP assay was carried out as described by Benzie and Strain with minor modifications (197). In a white 96-well plate, a reaction mixture containing 50 μL of quinolone derivatives at different concentrations (15, 30, 60, 120 and 240 $\mu\text{g}/\text{mL}$) and 250 μL of FRAP reagent (0.25 M sodium acetate buffer (pH 3.6), 10 mM TPTZ solution and 20 mM of $\text{FeCl}_3 \cdot 6\text{H}_2\text{O}$ solution in a ratio of 10:1:1 in volume) was incubated at 37 °C for 15 minutes in the dark. The increase in absorbance at the wavelength of 593 nm was then measured. Ascorbic acid (15, 30, 60, 120 and 240 $\mu\text{g}/\text{mL}$) was used as the standard drug, while the absolute control contained all the assay reagents except the investigated compounds. The assay was done in 3 replicates. The absorbance values were used to determine the mass of Iron (II) formed (μM) per gram of dry mass by extrapolating from the standard curve (Appendix 3) generated by plotting the absorbance of iron (II) against an increasing concentration (100, 200, 300, 400, 500, 600, 700, 800, 900 and 1000 μM).

2.6 Cell-based assay

2.6.1 Preparations of compounds

A stock solution of QD1, QD2, QD3 and QD4 with a concentration of 1000 $\mu\text{g}/\text{mL}$ was prepared by weighing out 0.01 g of each compound and dissolved in 1 mL DMSO, and it was then made up to 10 mL with the required media (DMEM or MEM). These stock solutions were diluted further to make the desired concentrations (15, 30 and 60 $\mu\text{g}/\text{mL}$) using the $C_1V_1 = C_2V_2$ formula. For each assay, the desired concentrations were freshly prepared using the relevant tissue culture media.

2.6.2 Cell culture and differentiation

In a cell culture flask, C2C12 myoblasts were maintained in Dulbecco's modified eagle's medium (DMEM), and HepG2 cell lines were maintained in minimum essential medium eagle (MEM) supplemented with 10% fetal bovine serum (FBS) and 1% penicillin-streptomycin in a 5% CO_2 environment at 37°C. After the cells had grown to confluence, they were trypsinised (detaching cells from the bottom of the flask) and seeded into a 24-well plate. For the C2C12 myoblast,

differentiation into myotubes was induced by switching the medium to DMEM supplemented with 2% FBS and 1% penicillin-streptomycin for four days. The media was changed every day, and the extent of differentiation was established by using a microscope to observe for multinucleated myotubes.

2.6.3 Glucose uptake assay

The glucose uptake was determined by measuring the concentration of glucose present in the medium after 24 hours according to the method described by Cruz-Bermúdez *et al.* (198). To achieve this, the HepG2 cells and the differentiated C2C12 myoblasts that have fused into multinucleate myotubes in a 24-well plate were used. The old cultured medium was removed, and the cells were washed three times with 200 μ L of phosphate buffer solution (PBS), after which the cells in wells were exposed to 200 μ L of quinolone derivatives (15, 30 and 60 μ g/mL) in medium supplemented with 10% FBS and 1% penicillin-streptomycin. Afterwards, the cells were incubated in a 5% CO₂ environment at 37°C for 24 hours. Following the same procedure, 200 μ L of the medium was added to the cells as a control. After incubating for 24 hours, the concentration of glucose in the medium was measured using an Accu-Check Performa glucometer (198). The assay was performed in triplicates.

2.6.4 Cell viability assay

Principle

Acid phosphatase is a ubiquitous lysosomal enzyme that hydrolyses organic phosphates at an acid pH and is found in cellular components of tissues (199). The cytosolic acid phosphatase in viable cells is able to hydrolyse *p*NPP to *p*-nitrophenol, which absorbs light at 405 nm when read spectrophotometrically. Therefore, the higher the absorbance, the higher the activity of acid phosphatase, which in turn is a measure of cell number.

Protocol

Cell viability was measured using the acid phosphatase method (200). Briefly, C2C12 and HepG2 cells seeded in a 24-well plate were exposed to 200 μ L of quinolone derivatives (15, 30 and 60 μ g/mL) in a medium and incubated in a 5% CO₂ environment at 37°C for 24 hours. After 24 hours,

the culture medium was removed, and each well was washed three times with 200 μL PBS. To each well, 200 μL of buffer containing 0.1 M sodium acetate (pH 5.0), 0.1% Triton X-100 and 5 mM *p*NPP was added. The plate was incubated at 37°C for 2 hours, and after incubation, the reaction was stopped by adding 20 μL of 1 N NaOH. The absorbance of the yellow-coloured *p*-nitrophenol released from *p*NPP was measured with a spectrophotometer at a wavelength of 405 nm. Control with 100% cell viability was prepared by replacing the compounds with a medium. The assay was performed in triplicates, and the percentage of cells still viable was calculated using the equation below:

$$\text{Percentage viability (\%)} = \left(\frac{\text{absorbance of sample}}{\text{absorbance of control}} \right) * 100$$

2.7 Data and statistical analysis

Each experiment was carried out in triplicates, and all data were expressed as mean \pm standard deviation (SD) represented by an error bar ($n = 3$) on a column graph. Statistical analysis on the absorbance/fluorescence readings before normalisation obtained for each experiment was determined using Graphpad Prism version 8.0.2. The statistical analysis of data includes a one-way analysis of variances (ANOVA) followed by Dunnett's multiple comparisons test for significance between the test compounds and the control at $p < 0.05$. The result of the one-way ANOVA followed by Dunnett's multiple comparison test for statistical significance at $p < 0.05$ was indicated on the graph with an asterisk (*). The asterisks represent the significant statistical difference between the inhibitor compound and the control.

CHAPTER 3: RESULTS

3.1 Drug-likeness and gastrointestinal absorption of the quinolone derivatives

Drug-likeness is a qualitative assessment of a molecule to determine whether it is druggable, and this assessment is often estimated from its molecular structure. Lipinski's rule of 5, which Christopher Lipinski proposed, is a fast and simple approach to evaluating the drug-likeness or chemical and physical properties of a chemical compound to predict if it will be orally active. The components of Lipinski's rule of 5 are (i) molecular weight ≤ 500 daltons, (ii) octanol-water partition coefficient ($\text{Log } P$) ≤ 5 , (iii) hydrogen bond donors ≤ 5 , and (iv) hydrogen bond acceptors ≤ 10 .

Lipinski's rule of 5 parameters was generated for the quinolone derivatives using the SwissADME web tool, and the results are presented in Table 3.1. From the results, the quinolone derivatives did not violate any of Lipinski's rules of 5. Hence, we can predict that the quinolone derivatives will be orally bioavailable due to their acceptable drug-like characteristics.

Table 3.1: Predicted Lipinski's rule of 5 parameters for the quinolone derivatives.

Compounds	Molecular formula	Lipinski's rule of 5				Lipinski rule of 5 violation
		Molecular weight (g/mol)	Hydrogen bond donors	Hydrogen bond acceptors	Log <i>P</i>	
QD1	C ₂₃ H ₁₉ O ₆ ClN ₂	454.86	0	6	3.61	0
QD2	C ₂₃ H ₂₀ N ₂ O ₆	420.41	0	6	3.10	0
QD3	C ₂₃ H ₁₉ O ₄ Cl ₂ N	444.31	0	4	4.86	0
QD4	C ₂₅ H ₂₆ N ₂ O ₄	418.48	0	4	3.86	0

The BOILED-Egg model is a rapid, robust method for predicting the gastrointestinal absorption and the blood-brain barrier (BBB) penetration of small molecules intended for drug development. The model has a yellow and white region representing BBB penetration and GIT absorption, respectively. The BOILED-Egg model generated for the quinolone derivatives using SwissADME is presented in Figure 3.1. From the generated model, the four quinolone derivatives fall within the white region, but only QD4 falls within the yellow region. Hence, we can predict that the quinolone derivatives will have good GIT absorption and only QD4 will penetrate the BBB.

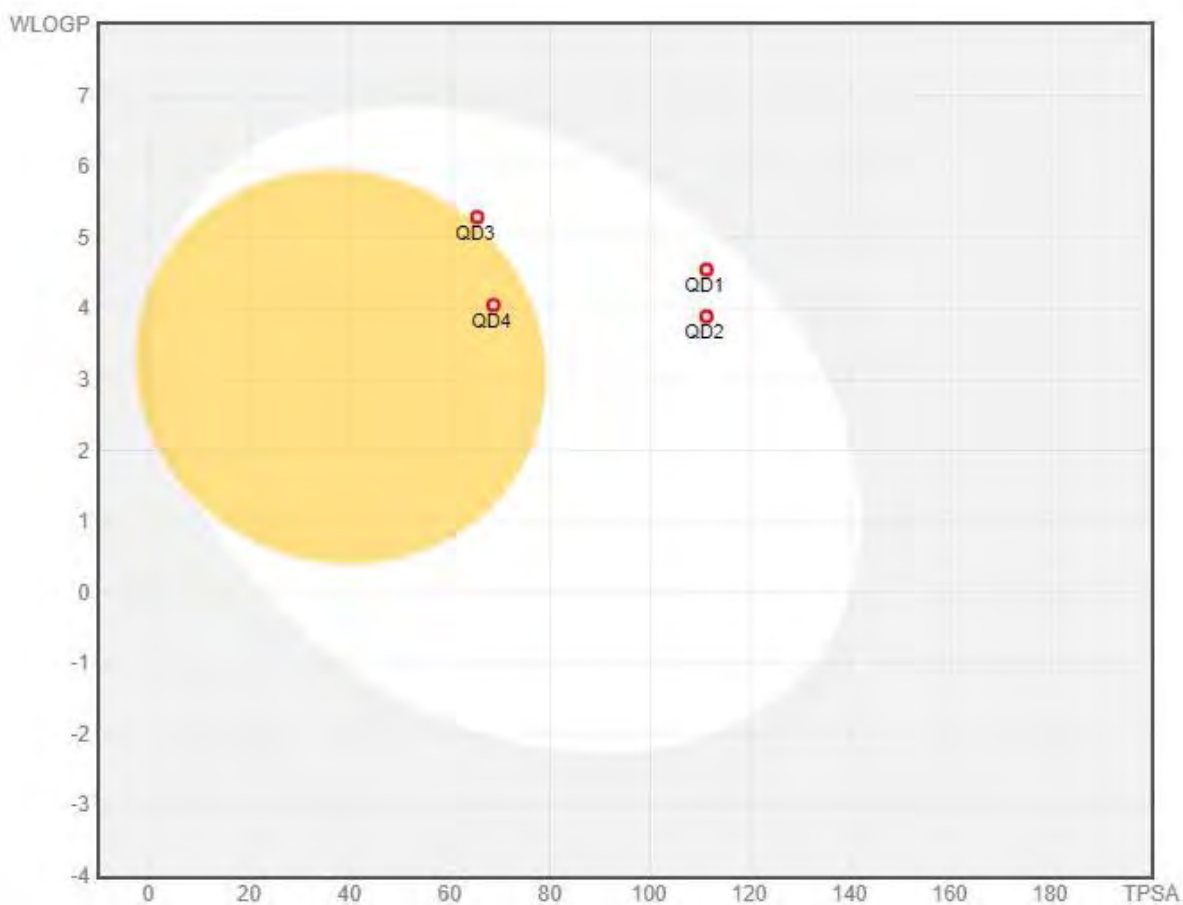


Figure 3.1: The BOILED-Egg model showing the location of the quinolone derivatives on the model. The yellow region represents BBB penetration, while the white region represents GIT absorption.

3.2 Cell-free assay

3.2.1 Antidiabetic assays

3.2.1.1 Alpha-amylase inhibition assay

The percentage of alpha-amylase inhibited by the quinolone derivatives and acarbose (standard reference drug) at concentrations of 15, 30, 60, 120 and 240 $\mu\text{g/mL}$ are presented in Figure 3.2. All four quinolone derivatives and acarbose at the different concentrations showed a significant statistical difference from the control at $p < 0.05$. The percentage inhibition for the four quinolone derivatives across all concentrations was greater than 50%. The control is considered to have zero percentage inhibition. The IC_{50} concentrations determined for all four quinolone derivatives and acarbose are presented in Table 3.2. QD4 has the smallest IC_{50} compared to the other quinolone derivatives. Therefore, QD4 is the most potent for inhibiting alpha-amylase among the four quinolone derivatives.

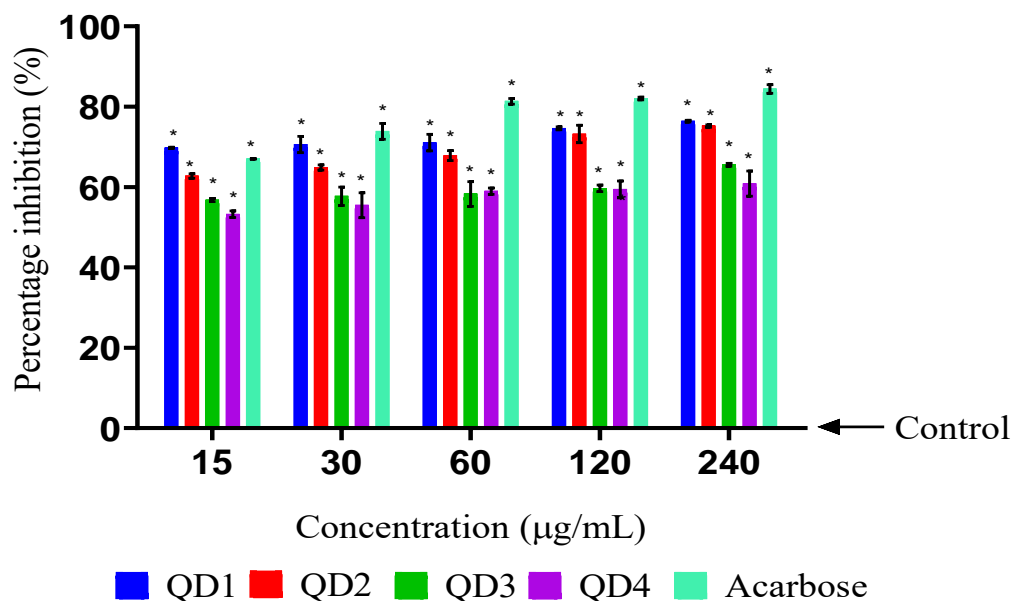


Figure 3.2: The inhibition of alpha-amylase activity by quinolone derivatives and acarbose at different concentrations. The data are presented as mean \pm SD represented with error bars, ($n = 3$), and the asterisk (*) represents the statistical difference between the test compounds and the control at $p < 0.05$.

Table 3.2: The IC₅₀ concentrations for the quinolone derivatives and acarbose obtained from the alpha-amylase inhibitory assay.

Compounds	IC ₅₀ (µg/mL)
QD1	88.01
QD2	65.70
QD3	135.4
QD4	42.76
Acarbose	36.14

3.2.1.1.1 Alpha-amylase kinetics study

From Table 3.2, QD4 had the smallest IC₅₀. Therefore, QD4 was investigated further for its mode of inhibition on alpha-amylase. A Michaelis-Menten curve was generated (Figure 3.3) by plotting maltose concentration (generated from the maltose standard curve) against substrate concentrations (0.25, 0.50, 1.0, 2.0 and 4.0 mM). V_{max} and K_m were obtained from the curve. Afterwards, the reciprocal of the reaction velocity versus the reciprocal of the substrate concentrations were used to generate a Lineweaver-Burk plot (Figure 3.4). From Figure 3.3, K_m increases (control K_m = 0.1604 and QD4 K_m = 0.3155) while V_{max} decreases (control V_{max} = 0.4340 and QD4 V_{max} = 0.3739), and from Figure 3.4, the data set line intersect but not on the x-axis or y-axis of the Lineweaver-Burk plot. Therefore, the mode of inhibition of alpha-amylase by QD4 is mixed type inhibition - inhibitor is capable of binding to the enzyme binding site as well as an allosteric site (190-192).

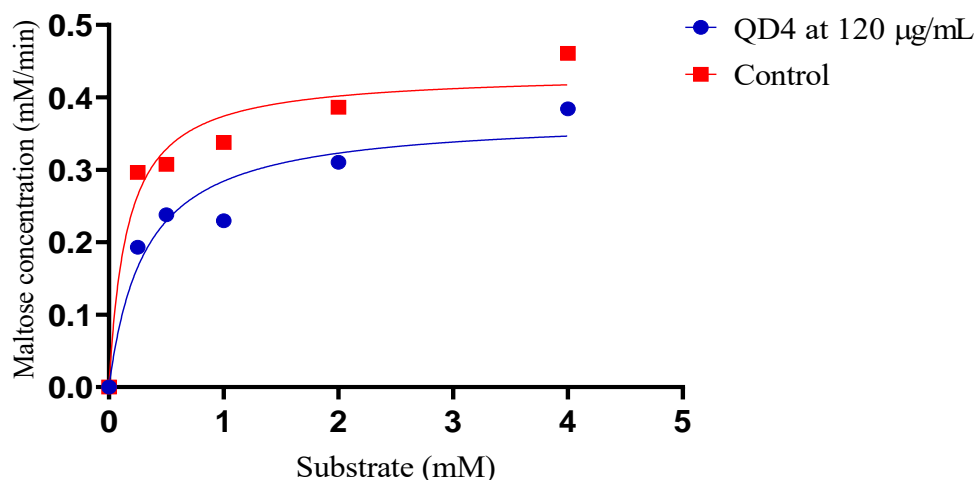


Figure 3.3: Michaelis-Menten curve showing the mode of inhibition of alpha-amylase in the presence (blue) and absence (red) of an inhibitor. The curve was generated by plotting maltose concentration against substrate concentration ranging from 0.25 to 4.0 mM. From the curve, V_{\max} and K_m were generated – QD4 at 120 $\mu\text{g}/\text{mL}$ $V_{\max} = 0.3739$ and $K_m = 0.3155$ while control's $V_{\max} = 0.4340$ and $K_m = 0.1604$.

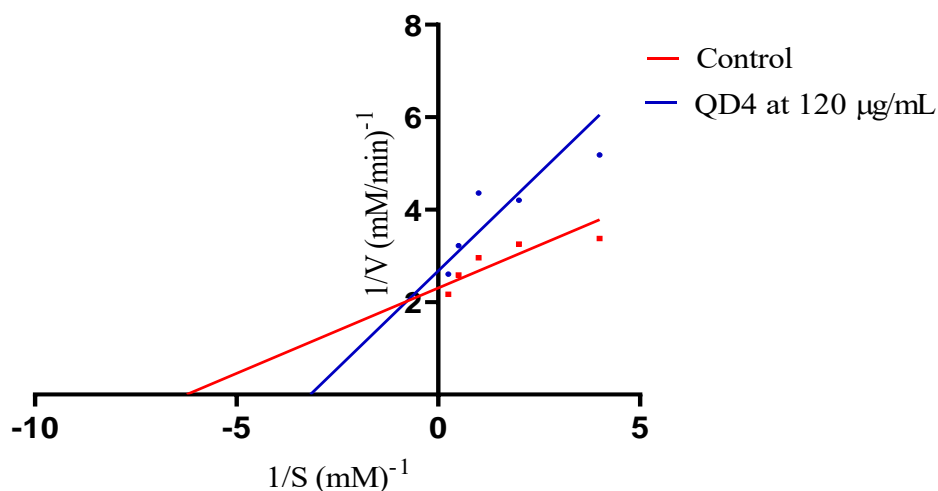


Figure 3.4: Lineweaver-Burk plot of the reaction of alpha-amylase in the presence (blue) and absence (red) of an inhibitor. The plot was generated by plotting the reciprocal of the reaction velocity ($1/V$) against the reciprocal of the substrate concentrations ($1/S$). From the plot, a mixed-type inhibition of alpha-amylase by QD4 can be deduced because as K_m increases, V_{\max} decreases, and the data set lines intersect, but not on the x-axis or y-axis.

3.2.1.2 Alpha-glucosidase inhibition assay

The inhibitory effect of quinolone derivatives and acarbose (standard reference drug) on alpha-glucosidase enzyme was evaluated using *in vitro* assay at different concentrations of 15, 30, 60, 120 and 240 $\mu\text{g/mL}$. The results are presented in Figure 3.5. All four quinolone derivatives and acarbose at the different concentrations showed a significant statistical difference from the control at $p < 0.05$. The percentage inhibition for QD1 and QD2 was less than 50% at concentrations of 15 and 30 $\mu\text{g/mL}$ but greater than 50% at concentrations of 60, 120 and 240 $\mu\text{g/mL}$. The percentage inhibition for QD3 and QD4 across all concentrations was less than 50%. The control is considered to have zero percentage inhibition. The IC_{50} concentrations determined for all four quinolone derivatives and acarbose are presented in Table 3.3. QD1 has the smallest IC_{50} compared to the other quinolone derivatives. Therefore, QD1 is the most potent for inhibiting alpha-glucosidase activity among the four quinolone derivatives.

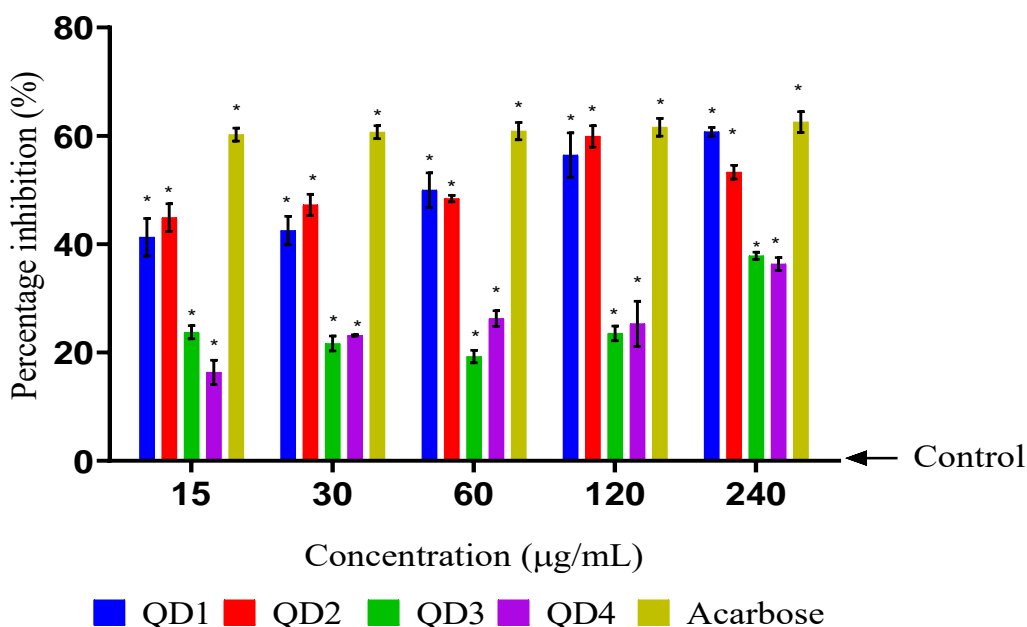


Figure 3.5: The inhibition of alpha-glucosidase activity by quinolone derivatives and acarbose at different concentrations. The data are presented as mean \pm SD represented with error bars, ($n = 3$), and the asterisk (*) represents the statistical difference between the test compounds and the control at $p < 0.05$.

Table 3.3: The IC₅₀ concentrations for the quinolone derivatives and acarbose obtained from the alpha-glucosidase inhibitory assay.

Compounds	IC ₅₀ (µg/mL)
QD1	68.38
QD2	76.69
QD3	124.30
QD4	72.91
Acarbose	89.85

3.2.1.2.1 Alpha-glucosidase kinetics study

From Table 3.4, QD1 had the smallest IC₅₀. Therefore, QD1 was investigated further for its mode of inhibition on alpha-glucosidase. A Michaelis-Menten curve was generated (Figure 3.6) by plotting *p*-nitrophenyl concentration (generated from the *p*-nitrophenyl standard curve) against substrate concentrations (0.125, 0.25, 0.5, 1.0, 2.0 and 4.0 mM). V_{max} and K_m were obtained from the curve. Afterwards, the reciprocal of the reaction velocity versus the reciprocal of the substrate concentrations were used to generate a Lineweaver-Burk plot (Figure 3.7). From Figure 3.6, K_m increases (control K_m = 1.505 and QD1 K_m = 2.158) while V_{max} is constant (control V_{max} = 8.268 and QD1 V_{max} = 8.244) and from Figure 3.7, the data set line intersects on the y-axis of the Lineweaver-Burk plot. Therefore, the mode of inhibition of alpha-glucosidase by QD1 is competitive inhibition - competitive inhibitor binds to the active site of the enzyme, preventing the substrate from binding (187).

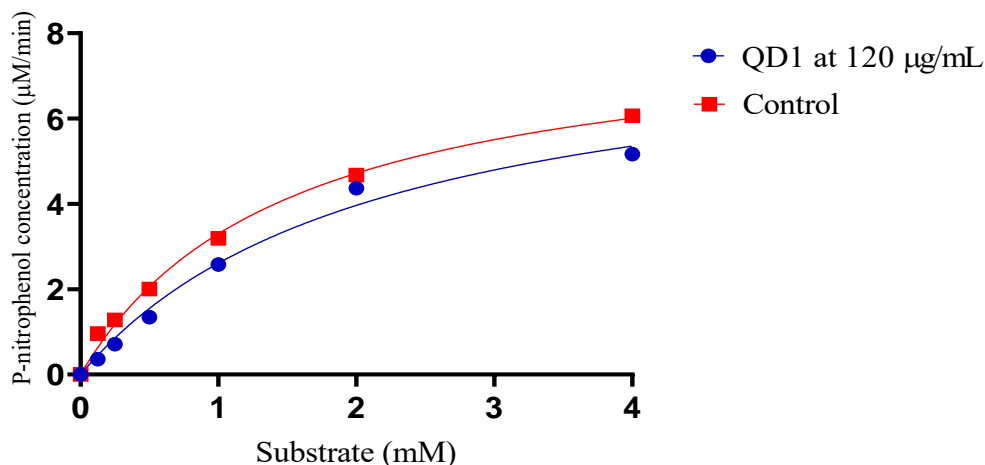


Figure 3.6: Michaelis-Menten curve showing the mode of inhibition of alpha-glucosidase in the presence (blue) and absence (red) of an inhibitor. The curve was generated by plotting *p*-nitrophenyl concentration against substrate concentration ranging from 0.125 to 4.0 mM. From the curve, V_{\max} and K_m were generated – QD1 at 120 $\mu\text{g}/\text{mL}$ $V_{\max} = 8.244$ and $K_m = 2.158$ while control's $V_{\max} = 8.268$ and $K_m = 1.505$.

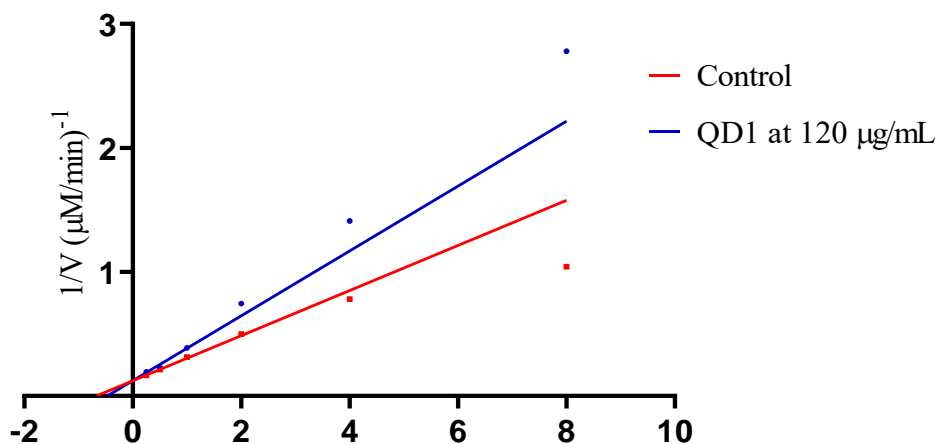


Figure 3.7: Lineweaver-Burk plot of the reaction of alpha-glucosidase in the presence (blue) and absence (red) of an inhibitor. The plot was generated by plotting the reciprocal of the reaction velocity ($1/V$) against the reciprocal of the substrate concentrations ($1/S$). From the plot, competitive inhibition of alpha-glucosidase by QD1 can be deduced because as K_m increases, V_{\max} remains constant, and the data set line intersect on the y-axis.

3.2.1.3 DPP4 inhibition assay

The percentage of DPP4 activity inhibited by quinolone derivatives at concentrations of 15, 30, 60, 120 and 240 $\mu\text{g/mL}$ and sitagliptin (standard reference drug) at IC_{50} concentration are presented in Figure 3.8. QD2 at the different concentrations and sitagliptin at IC_{50} concentration showed a significant statistical difference from the control at $p < 0.05$. While QD1 showed a significant statistical difference to the control at $p < 0.05$ at concentrations of 120 and 240 $\mu\text{g/mL}$ and QD3 and QD4 had no significant statistical difference to the control at $p < 0.05$ at concentrations of 30, 60, 120 and 240 $\mu\text{g/mL}$. The percentage inhibition for the four quinolone derivatives across all concentrations was less than 50%. The control is considered to have zero percentage inhibition. The IC_{50} concentrations determined for all four quinolone derivatives are presented in Table 3.4. QD1 has the smallest IC_{50} compared to the other quinolone derivatives. Therefore, QD1 is the most potent for inhibiting DPP4 among the four quinolone derivatives.

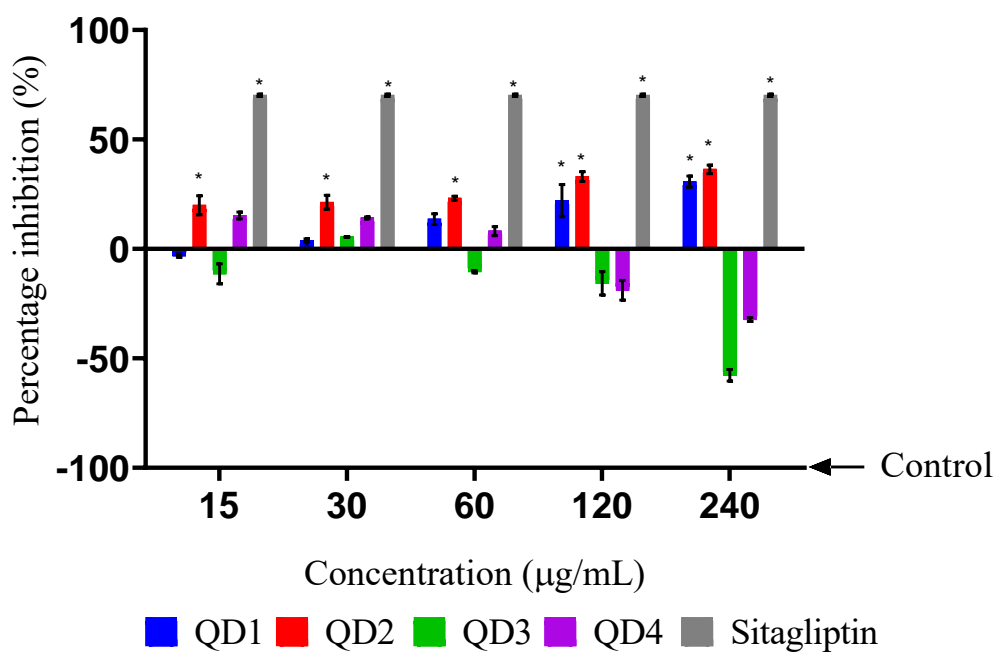


Figure 3.8: The inhibition of DPP4 by quinolone derivatives at different concentrations and sitagliptin at IC_{50} concentration. The data are presented as mean \pm SD represented with error bars, ($n = 3$), and the asterisk (*) represents the statistical difference between the test compounds and the control at $p < 0.05$.

Table 3.4: The IC₅₀ concentrations for the quinolone derivatives obtained from the DPP4 inhibitory assay.

Compounds	IC ₅₀ (µg/mL)
QD1	62.40
QD2	84.45
QD3	129.0
QD4	93.90

3.2.1.4 Protein tyrosine phosphatase inhibition assay

The inhibitory effect of quinolone derivatives and sodium orthovanadate (standard reference compound) on PTP1B enzyme was evaluated using *in vitro* assay at different concentrations of 15, 30, 60, 120 and 240 µg/mL. The results are presented in Figure 3.9. All four quinolone derivatives at the different concentrations showed no significant statistical difference to the control at $p < 0.05$. While sodium orthovanadate at 60 and 120 µg/mL showed a significant statistical difference from the control at $p < 0.05$. The percentage inhibition for the four quinolone derivatives across all concentrations was less than 0%. The control is considered to have zero percentage inhibition. IC₅₀ was not calculated for the quinolone derivatives because they showed no inhibitory activity against the PTP1B enzyme.

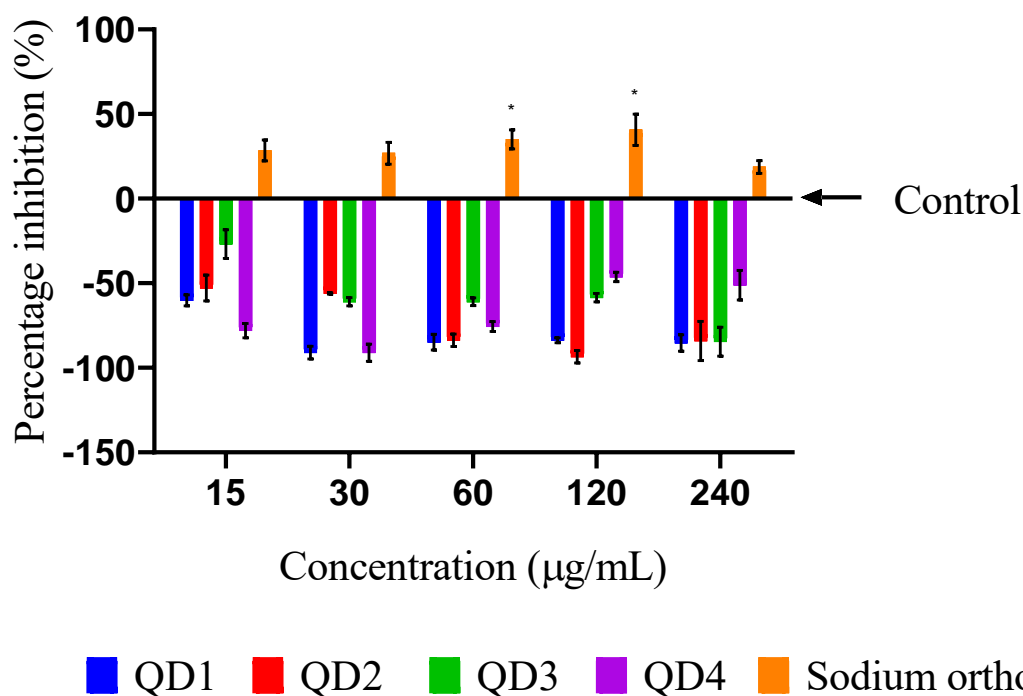


Figure 3.9: The inhibition of PTP1B by quinolone derivatives and sodium orthovanadate at different concentrations. The data are presented as mean \pm SD represented with error bars, ($n = 3$), and the asterisk (*) represents the statistical difference between the test compounds and the control at $p < 0.05$.

3.2.1.5 Aldose reductase inhibition assay

The inhibitory effect of quinolone derivatives and quercetin (standard reference compound) on aldose reductase enzyme was evaluated using *in vitro* assay at different concentrations of 15, 30, 60, 120 and 240 $\mu\text{g/mL}$. The results are presented in Figure 3.10. QD1, QD4 and quercetin at the different concentrations showed significant statistical differences from the control at $p < 0.05$. QD2 showed a significant statistical difference from the control at $p < 0.05$ at concentrations of 15, 30, 60 and 120 $\mu\text{g/mL}$, and QD3 showed a significant statistical difference from the control at $p < 0.05$ at concentrations of 15, 30 and 60 $\mu\text{g/mL}$. The percentage inhibition for the four quinolone derivatives across all concentrations was less than 50%. The control is considered to have zero percentage inhibition. The IC_{50} concentrations determined for all four quinolone derivatives and quercetin are presented in Table 3.5. QD1 has the smallest IC_{50} compared to the other quinolone

derivatives. Therefore, QD1 is the most potent for inhibiting aldose reductase among the four quinolone derivatives.

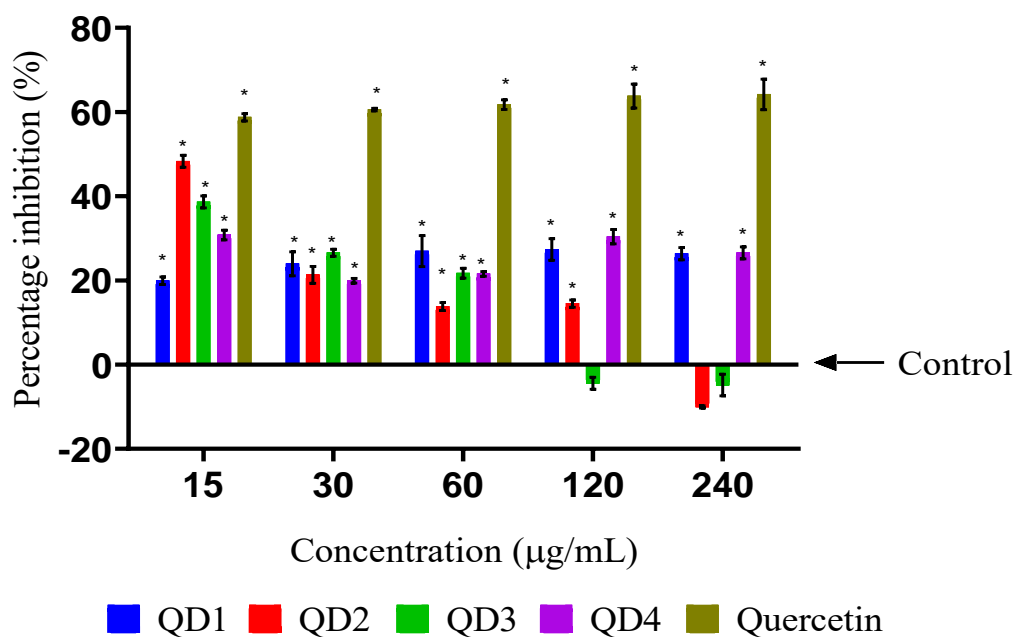


Figure 3.10: The inhibition of aldose reductase activity by quinolone derivatives and quercetin at different concentrations. The data are presented as mean \pm SD represented with error bars, ($n = 3$), and the asterisk (*) represents the statistical difference between the test compounds and the control at $p < 0.05$.

Table 3.5: The IC_{50} concentrations for the quinolone derivatives and quercetin obtained from aldose reductase inhibitory assay.

Compounds	IC_{50} ($\mu\text{g/mL}$)
QD1	29.42
QD2	52.71
QD3	70.80
QD4	90.40
Quercetin	37.01

3.2.2 Cardio-protective activity assay

3.2.2.1 Factor Xa inhibition assay

The inhibitory effect of quinolone derivatives and GGACK dihydrochloride (standard reference compound) on factor Xa (FXa) was evaluated using *in vitro* assay at different concentrations of 15, 30, 60, 120 and 240 $\mu\text{g}/\text{mL}$. The results are presented in Figure 3.11. QD3 and GGACK dihydrochloride at the different concentrations showed a significant statistical difference from the control at $p < 0.05$. While QD1 showed a significant statistical difference to the control at $p < 0.05$ at concentrations of 120 and 240 $\mu\text{g}/\text{mL}$, QD2 showed a significant statistical difference to the control at $p < 0.05$ at concentrations of 30, 60, 120 and 240 $\mu\text{g}/\text{mL}$ and QD4 showed a significant statistical difference to the control at $p < 0.05$ at concentrations of 15 and 30 $\mu\text{g}/\text{mL}$. The percentage inhibition for the four quinolone derivatives across all concentrations was less than 50%. The control is considered to have zero percentage inhibition. The IC_{50} concentrations determined for all four quinolone derivatives and GGACK dihydrochloride are presented in Table 3.6. QD2 has the smallest IC_{50} compared to the other quinolone derivatives. Therefore, QD2 is the most potent for inhibiting FXa among the four quinolone derivatives.

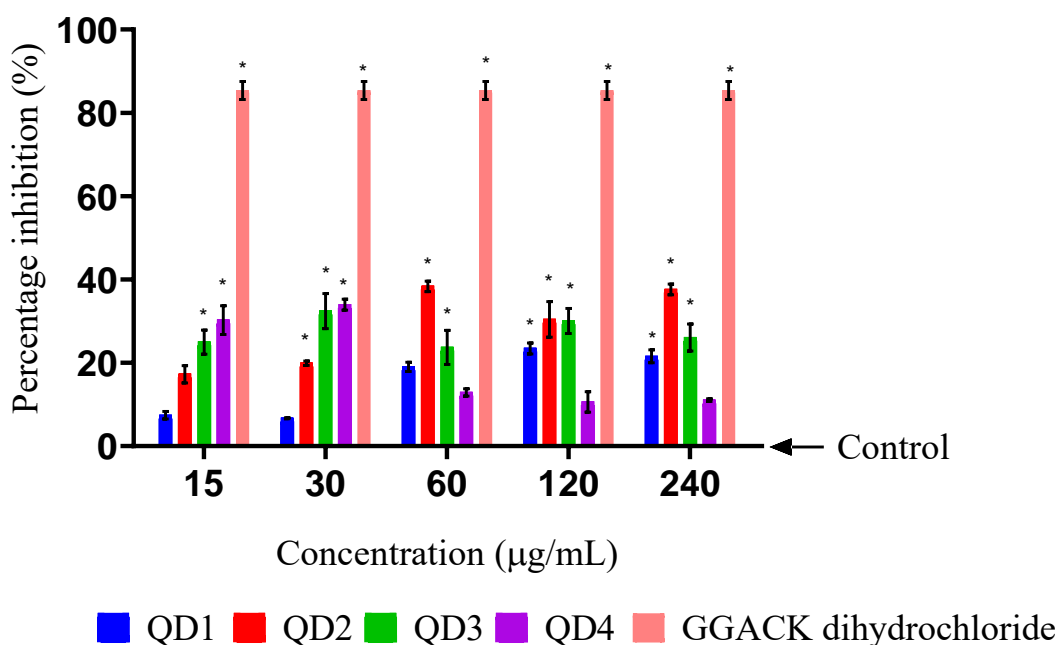


Figure 3.11: The inhibition of FXa by quinolone derivatives at different concentrations and GGACK dihydrochloride. The data are presented as mean \pm SD represented with error bars, (n = 3), and the asterisk (*) represents the statistical difference between the test compounds and the control at $p < 0.05$.

Table 3.6: The IC₅₀ concentrations for the quinolone derivatives obtained from FXa inhibitory assay.

Compounds	IC ₅₀ (µg/mL)
QD1	56.63
QD2	32.60
QD3	1211
QD4	54.85

3.2.2.2 HMG-CoA reductase inhibition assay

The inhibitory effect of quinolone derivatives and pravastatin (standard reference drug) on HMGR was evaluated using *in vitro* assay at different concentrations of 15, 30, 60, 120 and 240 $\mu\text{g/mL}$. The results are presented in Figure 3.12. All four quinolone derivatives and pravastatin at the different concentrations showed significant statistical differences from the control at $p < 0.05$. The percentage inhibition for the four quinolone derivatives across all concentrations was less than 50%. The control is considered to have zero percentage inhibition. The IC_{50} concentrations determined for all four quinolone derivatives and pravastatin are presented in Table 3.7. QD2 has the smallest IC_{50} compared to the other quinolone derivatives. Therefore, QD2 is the most potent for inhibiting HMGR among the four quinolone derivatives.

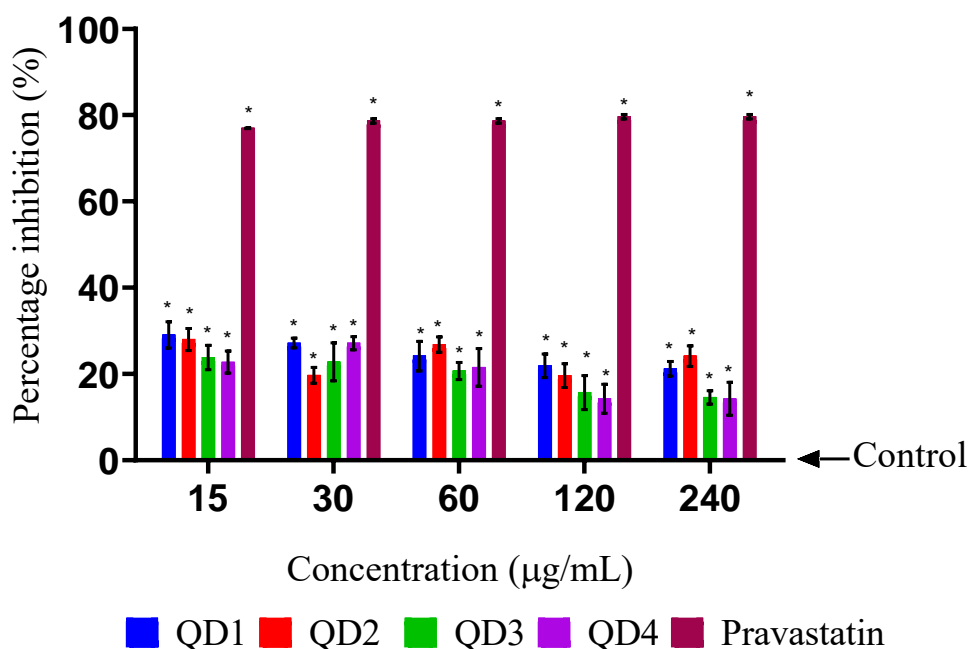


Figure 3.12: The inhibition of HMG-CoA reductase by quinolone derivatives and pravastatin at different concentrations. The data are presented as mean \pm SD represented with error bars, ($n = 3$), and the asterisk (*) represents the statistical difference between the test compounds and the control at $p < 0.05$.

Table 3.7: The IC₅₀ concentrations for the quinolone derivatives and pravastatin obtained from HMG-CoA reductase inhibitory assay.

Compounds	IC ₅₀ (µg/mL)
QD1	49.02
QD2	48.71
QD3	70.73
QD4	60.94
Pravastatin	33.01

3.2.3 Antioxidant assays

3.2.3.1 DPPH inhibition assay

The percentage of DPPH radical scavenging activity of quinolone derivatives and ascorbic acid (standard reference compound) at concentrations of 15, 30, 60, 120 and 240 µg/mL are presented in Figure 3.13. QD1, QD2, QD3 and ascorbic acid at the different concentrations showed a significant statistical difference to the control at $p < 0.05$. While QD4 showed a significant statistical difference at a concentration of 15 µg/mL only. The percentage of DPPH radical scavenging activity for QD1 and QD2 at 15, 30, and 60 µg/mL was less than 50%, while at 120 and 240 µg/mL, the percentage scavenging activity was greater than 50%. The percentage DPPH radical scavenging activity for QD3 and QD4 across all concentrations was less than 50%. The control is considered to have zero percentage DPPH radical scavenging activity. The IC₅₀ concentrations determined for all four quinolone derivatives and ascorbic acid are presented in Table 3.8. From the result obtained, QD2 has the smallest IC₅₀ compared to the other quinolone derivatives. Therefore, QD2 is the most potent among the four quinolone derivatives.

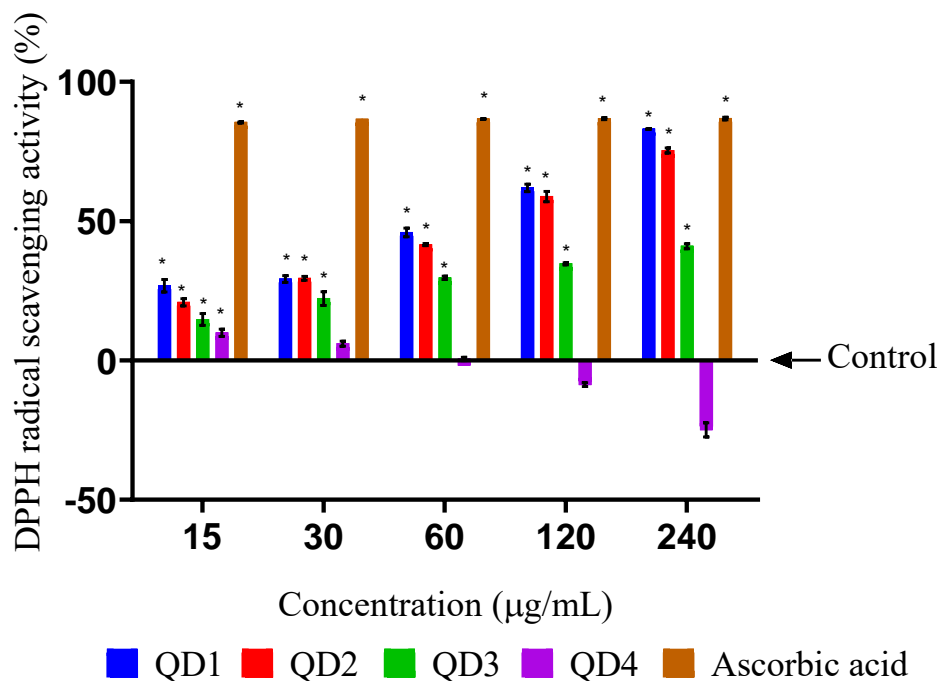


Figure 3.13: DPPH radical scavenging activity by quinolone derivatives and ascorbic acid at different concentrations. The data are presented as mean \pm SD represented with error bars, ($n = 3$), and the asterisk (*) represents the statistical difference between the test compounds and the control at $p < 0.05$.

Table 3.8: The IC_{50} concentrations for the quinolone derivatives and ascorbic acid obtained from DPPH radical scavenging assay

Compounds	IC_{50} ($\mu\text{g/mL}$)
QD1	86.53
QD2	53.93
QD3	74.88
QD4	98.19
Ascorbic acid	25.56

3.2.3.2 Ferric reducing antioxidant power (FRAP) assay

The ferric reducing antioxidant power of quinolone derivatives and ascorbic acid (standard reference compound) at concentrations of 15, 30, 60, 120 and 240 $\mu\text{g/mL}$ are presented in Figure 3.14 as FRAP value ($\mu\text{M/g}$ dry mass). QD2 and ascorbic acid at the different concentrations showed significant statistical differences from the control at $p < 0.05$. QD1 showed a significant statistical difference from the control at all concentrations except at 30 $\mu\text{g/mL}$. QD3 showed a significant statistical difference from the control at all concentrations except at 15 $\mu\text{g/mL}$, while QD4 showed a significant statistical difference from the control at concentrations of 120 and 240 $\mu\text{g/mL}$. From the results, QD2 has the highest FRAP activity compared to the other quinolone derivatives since it shows the highest FRAP value.

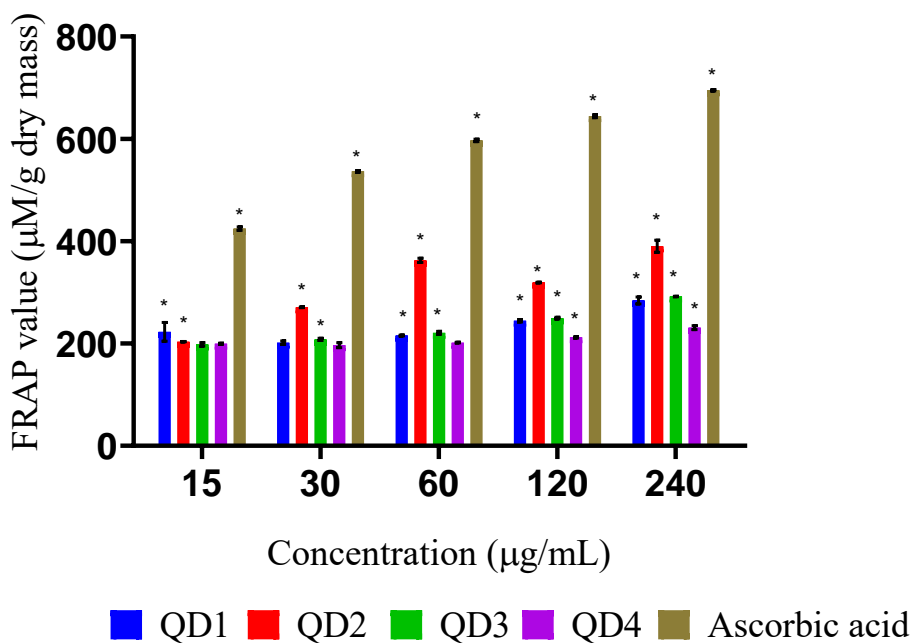


Figure 3.14: Ferric reducing antioxidant power of quinolone derivatives and ascorbic acid at different concentrations. The data are presented as mean \pm SD represented with error bars, ($n = 3$), and the asterisk (*) represents the statistical difference between the test compounds and the control at $p < 0.05$.

3.3 Cell-based assay

3.3.1 Glucose uptake assay

The media glucose concentrations after exposing C2C12 and HepG2 cell lines to quinolone derivatives at concentrations of 15, 30 and 60 $\mu\text{g}/\text{mL}$ for 24 hours are presented in Figures 3.15 and 3.16, respectively. For the C2C12 cells, there was no significant statistical difference between the quinolone derivatives and the control at $p < 0.05$, while for the HepG2 cells, there was a significant statistical difference between the quinolone derivatives and the control at $p < 0.05$. In the HepG2 cells, there was a higher glucose uptake in the control group than in the test compound group.

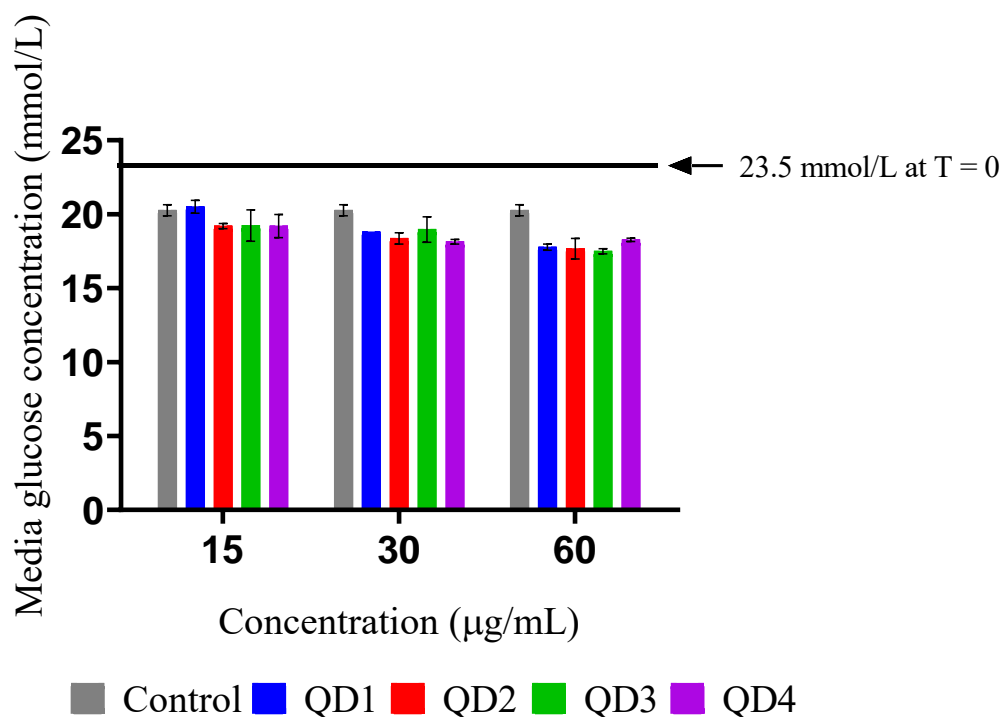


Figure 3.15: Media glucose concentration after exposing C2C12 cells to quinolone derivatives at 15, 30 and 60 $\mu\text{g}/\text{mL}$ for 24 hours. The data are presented as mean \pm SD represented with error bars, ($n = 3$). The horizontal line at 23.5 mmol/L represents the media glucose concentration at time = 0 hours.

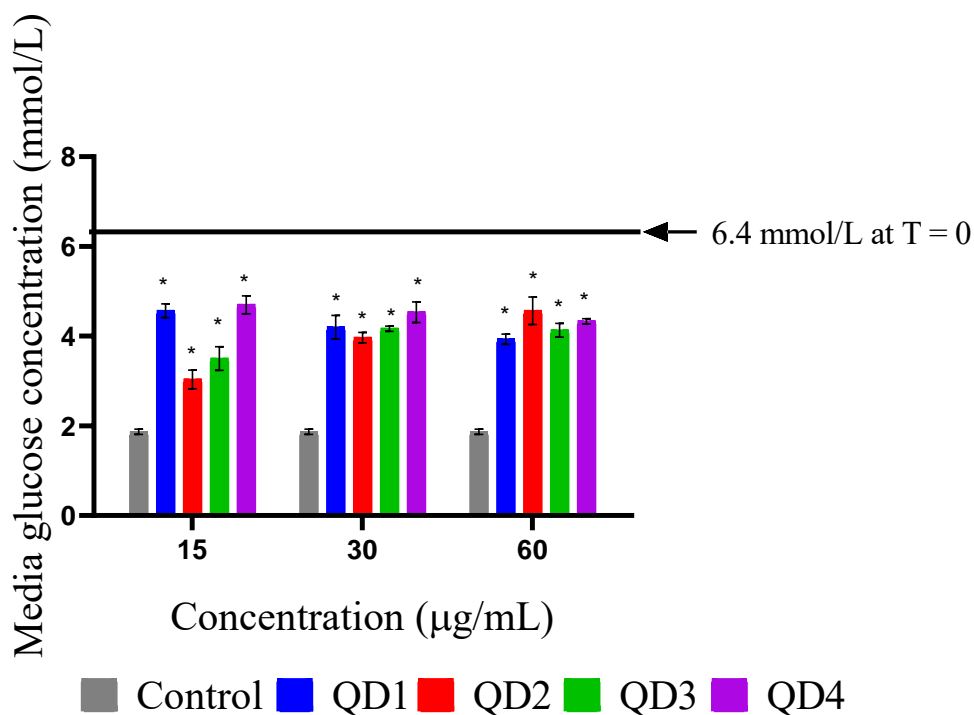


Figure 3.16: Media glucose concentration after exposing HepG2 cells to quinolone derivatives at 15, 30 and 60 µg/mL for 24 hours. The data are presented as mean ± SD represented with error bars, (n = 3), and the asterisk (*) represents the statistical difference between the test compounds and the control at $p < 0.05$. The horizontal line at 6.4 mmol/L represents the media glucose concentration at time = 0 hours.

3.3.2 Cell viability assay

The effect of quinolone derivatives on C2C12 and HepG2 cell viability at concentrations of 15, 30 and 60 µg/mL are presented in Figures 3.17 and 3.18. Cell viability refers to the number of live, healthy cells in a sample. The control was considered to have 100% cell viability. Therefore, percentage viability below 80% is considered cytotoxic. The percentage cell viability for the four quinolone derivatives across all the concentrations used is greater than 80%. Therefore, the quinolone derivatives are non-cytotoxic. There was no significant statistical difference between the quinolone derivatives and the control at $p < 0.05$ in both cell lines.

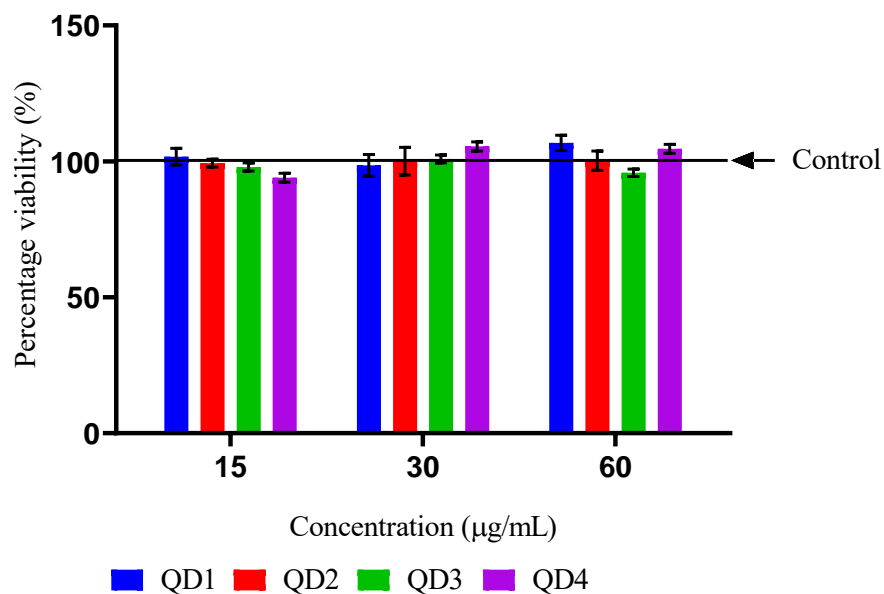


Figure 3.17: Percentage cell viability for C2C12 cell lines after 24 hours of exposure to quinolone derivatives at 15, 30 and 60 µg/mL. The horizontal line at 100% represents the control. The data are presented as mean ± SD represented with error bars, (n = 3).

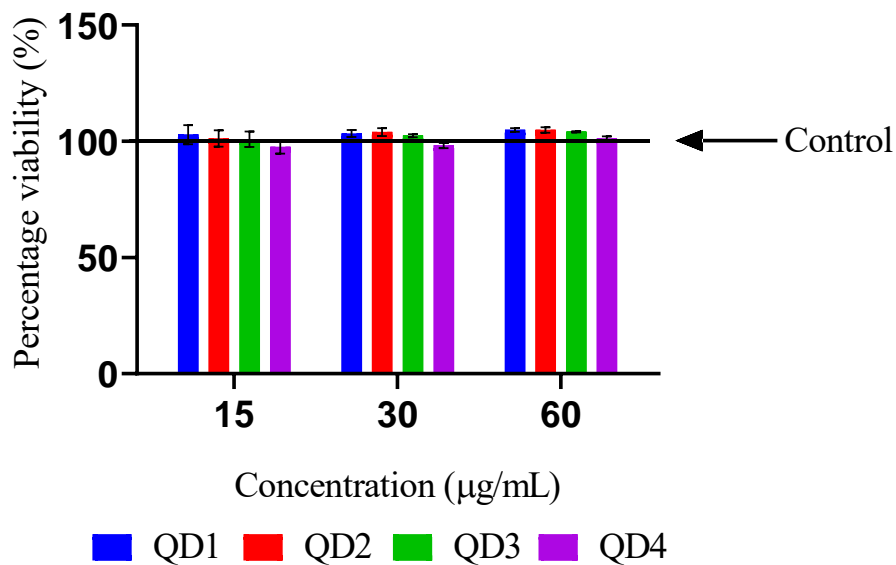


Figure 3.18: Percentage cell viability for HepG2 cell lines after 24 hours of exposure to quinolone derivatives at 15, 30 and 60 µg/mL. The horizontal line at 100% represents the control. The data are presented as mean ± SD represented with error bars, (n = 3).

CHAPTER 4: DISCUSSION

The increase in diabetic cases and its associated complications, along with conventional drugs presenting with adverse effects and less efficacy over time, has prompted research into investigating novel compounds with long-term efficacy and minimal side effects. We investigated quinolone because they have been reported to present with adverse effects, which include hypoglycaemia (8). Due to this hypoglycaemic effect, few studies have investigated the role of quinolones on the enzymes implicated in the pathology of DM (181, 182). In this study, the quinolone derivatives that were investigated are novel compounds with their quinolone scaffold substituted with an ethyl group at position 1, an ethyl ester group at position 3 and a substituted chalcone moiety at position 6.

Predicting the druggability and absorption profile for novel compounds is essential to avoid intractable targets and to focus drug discovery efforts on compounds offering better prospects (201). In this regard, we predicted the drug-likeness and absorption profile of the novel quinolone derivatives. From Table 3.1, the four quinolone derivatives did not violate Lipinski's rule of five – a fast and simple approach to evaluating the drug-likeness or chemical and physical properties of a chemical compound to predict if it will be orally active (202). These rules' properties are important because compounds with smaller molecular weights are easily absorbed and distributed into cells, directly impacting bioavailability (203-205). Secondly, lipophilicity ($\log P$) has an effect on transport processes, including intestinal absorption, membrane permeability, protein binding, and distribution to different tissues and organs (204, 206). Highly lipophilic compounds may result in low aqueous solubility, poor oral absorption and undesired affinity towards hydrophobic targets other than the desired target, hence increasing the risk of toxicity (207, 208). On the other hand, low lipophilicity can negatively impact permeability and potency, resulting in low bioavailability and efficacy. Lastly, the formation of hydrogen bonds through hydrogen bond donors and acceptors can increase solubility and the ability to establish important interactions with enzymes' active binding sites (209, 210). Although this rule is still relevant in drug discovery, it disregards the role of transporters and assumes that passive diffusion is the only important mechanism for drug entry into cells (211, 212). Novel compounds do not have to conform to Lipinski's rule of 5 before they are clinically approved, nor compounds that do not violate any of

the rules of five criteria necessarily orally bioavailable (205, 206, 212). Furthermore, a BOILED-Egg model was generated for the quinolone derivatives to predict their GIT and BBB permeability. Since the brain is not involved in the aetiology and pathology of DM and CVD, antidiabetic and cardio-protective drugs are not required to cross the BBB to exert their activity. Therefore, our focus is on the GIT absorption and not the BBB permeability. From Figure 3.1, the quinolone derivatives lie within the BOILED-Egg white, a region occupied by compounds that are predicted to be passively absorbed in the GIT. Therefore, this predicts that the quinolone derivatives will be highly absorbed in the GIT. Hence, we can predict that the quinolone derivatives can be formulated for oral use.

Glucose homeostasis is important in maintaining blood glucose concentration within a narrow limit to achieve a steady-state level to prevent hypoglycaemia or hyperglycaemia. Achieving and maintaining a steady-state level of blood glucose concentration involves a balance between several factors, including the rate of consumption and intestinal absorption of carbohydrates, pancreatic hormone secretion, hepatic glucose production and glucose utilisation by peripheral tissues (10, 11). The digestion of carbohydrates is carried out by alpha-amylase, an enzyme that breaks down α -1,4 bonds of starch to maltose and alpha-glucosidase, a brush border enzyme which further hydrolyses maltose to glucose which is absorbed (12-15). The absorption of glucose after a meal from the GIT results in postprandial hyperglycaemia, which is more pronounced in diabetic patients. Targeting alpha-amylase and alpha-glucosidase by inhibiting their activity reduces glucose absorption resulting in a decrease in blood glucose concentration. This, therefore, enhances the control of postprandial hyperglycaemia, which will be beneficial in managing DM.

This study investigated quinolone derivatives for their effect on alpha-amylase and alpha-glucosidase activity. From the alpha-amylase inhibition result (Figure 3.2), all four quinolone derivatives showed a good percentage inhibition profile with percentage inhibition greater than 50% across the different concentrations used. From Table 3.2, QD4 has the smallest IC_{50} , making it the most potent compound against the inhibition of alpha-amylase, and also, its IC_{50} was close to that of acarbose. Acarbose was used as a reference drug because it is a known alpha-amylase and alpha-glucosidase inhibitor which is structurally similar to natural oligosaccharides. Studies have reported that the primary mode of alpha-amylase inhibition by compounds is through hydrogen bond and hydrophobic interaction between the lipophilic amino acid residues Leu162,

Leu165 and Ile235 in the alpha-amylase active site and the hydrophobic groups of the inhibitor compound (213, 214). Furthermore, functional groups, which include methoxy group, carboxylate group and aliphatic chains, may also be crucial for binding (214-216). The inhibitory effect against alpha-amylase observed for the four quinolone derivatives may be attributed to the ketone group present on the compounds, which may be used to form hydrogen bonds, and the presence of carboxylate group and aliphatic chains, which is crucial for binding.

To further understand the effect of QD4 on alpha-amylase, its mode of inhibition was investigated. From Figures 3.3 and 3.4, QD4 mode of inhibition is mixed. Mixed inhibition occurs when an inhibitor is capable of binding to an enzyme binding site as well as an allosteric site, and it is a combination of both competitive and non-competitive inhibition (190, 191). Due to the multi-binding ability of mixed inhibitors, they are more potent than competitive and non-competitive inhibitors (191). Therefore, a smaller concentration will be required to produce an effect resulting in lesser side effects. The inhibitory activity shown by the quinolone derivatives against alpha-amylase would be envisaged to reduce glucose absorption from the GIT, resulting in a decrease in blood glucose concentration.

One of the reasons why these novel quinolone derivatives are being investigated against alpha-amylase is because conventional alpha-amylase inhibitors have side effects, which include gastrointestinal disturbances (19). Although the quinolone derivatives showed good activity against alpha-amylase, however, compounds that mildly inhibit alpha-amylase are recommended over compounds that strongly inhibit alpha-amylase. Excessive inhibition of alpha-amylase has been shown to result in excessive bacterial fermentation of undigested carbohydrates in the colon, hence resulting in gastrointestinal disturbances (217, 218).

Another enzyme of interest was alpha-glucosidase because, as with alpha-amylase, it is also involved in the breakdown of carbohydrates to glucose which is implicated in DM. From the alpha-glucosidase inhibition result (Figure 3.5), only QD1 and QD2 at 120 and 240 µg/mL showed a good percentage inhibition profile with a percentage inhibition greater than 50%. QD1 exhibits a dose-dependent inhibitory activity, and it is the most potent because it has the smallest IC₅₀ (Table 3.3). Interestingly its IC₅₀ was smaller than that of acarbose - a known alpha-glucosidase and alpha-amylase inhibitor with 10⁴ to 10⁵ higher affinity for alpha-glucosidase. Inhibitors such as acarbose interact with the protein side chains on alpha-glucosidase through the presence of hydrogen bond

donors and acceptors. These include the side chain hydroxyl group of Ser244 on the enzyme acting as the hydrogen bond donor while the amino acid Thr 215 on the enzyme acts as the hydrogen bond acceptor (219). From Table 3.1, QD1 and QD2 have six hydrogen bond acceptors, while QD3 and QD4 have four hydrogen bond acceptors. Due to QD1 and QD2 having the highest number of hydrogen bond acceptors, this suggests that they were able to interact with the protein side chains of alpha-glucosidase, thus exhibiting a good inhibition profile against alpha-glucosidase at concentrations 120 and 240 $\mu\text{g/mL}$ as compared to QD3 and QD4 with a lower number of hydrogen bond acceptors. Furthermore, the hydrophobic interaction between the aromatic ring of a ligand and the residues of alpha-glucosidase may contribute to the inhibition observed. In a study conducted by Chen *et al.*, π - π stack interaction between the aromatic ring A of cyanidin and residue Phe311 of alpha-glucosidase may have played a crucial role in the binding of the inhibitor to the enzyme (220). Therefore, the presence of aromatic rings in the quinolone derivatives and their ability to form hydrogen bonds with the enzyme might have been the reason for the observed inhibition.

Further investigation was conducted on QD1 to determine its mode of inhibition. From the result in Figures 3.6 and 3.7, QD1 mode of inhibition is competitive. Competitive inhibition occurs when an inhibitor binds to the active site of the enzyme, preventing the substrate from binding (190). Competitive inhibition is advantageous because the inhibitor binds specifically to the actual binding site of the enzyme, thus preventing unwanted side effects which may occur if it binds to other binding sites (221). However, suppose the substrate has a higher concentration or a stronger affinity for the binding site, a higher concentration of the inhibitor will be required to displace the substrate from the binding site to produce an effect, and this might result in increased side effects or toxicity (190, 222). The inhibitory activity shown by the quinolone derivatives against alpha-glucosidase would lead to a reduction in glucose absorption from the GIT, resulting in a decrease in blood glucose concentration, while the competitive inhibition exhibited will enhance high potency and reduced toxicity.

Insulin plays a vital role in the maintenance of glucose homeostasis. Insulin release is stimulated by the pancreatic beta-cells and the gut-derived peptide hormones known as incretins - GIP and GLP-1. Incretins are nutrient-dependent and responsible for approximately 70% of glucose-dependent insulin secretion (25-27). Incretin effect, the stimulation of insulin release is short-lived

due to the degradation of incretins by DPP4 - a glycoprotein that cleaves X-proline or X-alanine dipeptides from the N-terminus of polypeptides (223-225). Over the years, DPP4 inhibitors known as gliptins have been used as add-on therapy in uncontrollable DM because they enhance and inhibit insulin and glucagon secretion, respectively. Also, DPP4 inhibition decreases gastric emptying, resulting in decreased blood glucose concentration. The beneficial effect of DPP4 inhibition has led to exploring the quinolone derivatives for their effect on DPP4 activity.

In this study, quinolone derivatives were investigated for their effect on DPP4 activity. The result (Figure 3.8) from the DPP4 inhibition showed that QD1 and QD2 had weak activity against DPP4 inhibition. Less than 50% inhibition of DPP4 activity is considered weak because the available DPP4 inhibitors demonstrate a high efficacy in inhibiting DPP4 activity by at least 70–90% (26, 226, 227). The DPP4 active site has a common binding region that includes an S₁ (hydrophobic) and S₂ (hydrophilic) pocket. The S₁ and S₂ pockets have a favourable affinity to polar molecules with hydrogen bond donors and acceptors, as well as hydrophobic and aromatic groups (228). Studies have reported that the presence of a trifluoromethyl (CF₃) group on the structure of DPP4 inhibitors (Figure 4.1) plays a key role in their inhibitory activity (229, 230). The CF₃ group interacts with the enzyme side chain residues Ser209 and Arg358 in the S₂ extensive subsite. DPP4 inhibitors reside inside the hydrophobic cavity of the enzyme made up of Arg125, Glu205, Glu206, Phe357, Tyr547, Ser630, Tyr662, and Tyr666, and inhibitors such as sitagliptin (Figure 4.1) form a strong salt bridge with Glu205 and Glu206 through its amine group (230, 231). It also forms a strong π - π interaction with Phe357 through its triazolopyrazine group and a reaction between CF₃ and Arg358. QD1 and QD2 possess hydrogen bond acceptors and aromatic rings, which enhances their hydrophobicity. Hence, we may deduce that this is the reason for the weak inhibitory activity exhibited. The inhibitory effect of the quinolone derivatives can be enhanced by modifying their structures to contain substituents such as CF₃ and amines.

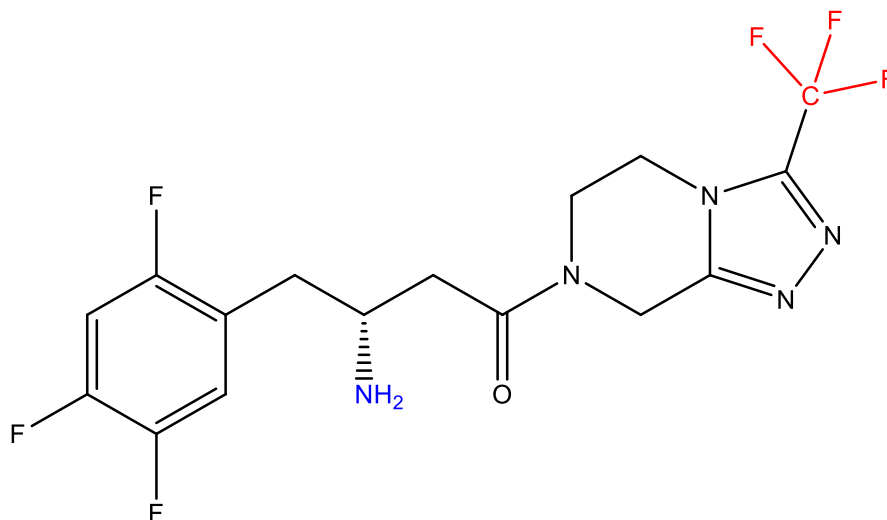


Figure 4.1: Structure of sitagliptin, a known DPP4 inhibitor. The trifluoromethyl (CF₃) group on the structure is essential for binding to DPP4 side chain residue Ser209 and Arg358 in the S₂ extensive subsite, while the amine group (NH₂) forms a strong salt bridge with Glu205 and Glu206 on the binding site.

After insulin secretion, insulin signalling takes place. Insulin signalling involves the formation of an insulin-receptor complex with tyrosine kinase receptor resulting in the activation of PI3K, which facilitates insulin-stimulated glucose uptake via GLUT4 translocation (33-38). The insulin signalling pathway can be switched off by PTP, an enzyme that inactivates insulin receptors – PTP1B is a major negative regulator of the insulin signalling pathway. Reports have stated that there is an increased activity of PTP in insulin-resistant diabetic patients (39). Therefore, inhibiting this enzyme could attenuate insulin resistance. For this reason, the quinolone derivatives were investigated for their effect on PTP1B activity.

From the result in Figure 3.9, the four quinolone derivatives showed no inhibitory activity against PTP1B across the different concentrations used. In contrast, sodium orthovanadate, used as a reference compound, exhibited inhibitory activity. Due to quinolone derivatives' lack of inhibitory activity, we can predict that the compounds might be enhancing PTP1B activity. Enhancing PTP1B activity leads to the inactivation of insulin receptors resulting in a decrease in insulin-stimulated glucose uptake. PTP1B has an active catalytic site A which consists of His214, Cys215, Ser216, Ala217, Gly218, Ile219, Gly220 and Arg221 and an aryl phosphate-binding site which is adjacent to site A (232, 233). Furthermore, the enzyme has a noncatalytic binding site B which

consists of Arg24, Arg254, Met258, and Gly259 and site C, which contains Arg47 and Asp48. Binding sites B and C are important for PTP1B inhibitor selectivity. Vanadium compounds, such as sodium orthovanadate, can form an intermediate transition state that allows them to oxidize the amide group of the active site amino acid residues (234).

To date, only a few PTP1B inhibitors, including ertiprotafib and trodusquemine have been tested in clinical trials. Unfortunately, most of them were discontinued due to their insufficient efficiency, poor selectivity and specificity, poor oral bioavailability and notable side effects (235, 236). Currently, no PTP1B inhibitor has been approved for use clinically. Therefore, new compounds are needed to be developed to address these challenges.

Insulin stimulates glucose uptake in skeletal muscle, adipose tissue and hepatic cells by increasing glucose transport through the activation of PI3K resulting in the translocation of insulin-sensitive GLUT4 (237, 238). The skeletal muscle accounts for about 75-80% of glucose uptake, whereas the proportion of glucose uptake into adipose tissue and the hepatic cell is substantially smaller (238, 239). Insulin-stimulated glucose uptake is essential to prevent high blood glucose concentration. However, glucose uptake is impaired in DM due to insulin resistance. In this study, the effect of quinolone derivatives on glucose uptake in skeletal and hepatic cells was investigated. From the results (Figure 3.15 and 3.16.), there was no substantial increase in glucose uptake as compared to the control group. The poor glucose uptake demonstrated can also be explained by the inability of the quinolone derivatives to inhibit PTP1B. Taking these observations together, we can therefore suggest that these compounds cannot work as insulin mimetics. Moreover, the quinolone derivatives investigated demonstrated no cytotoxicity in both cell lines used in this study. Compounds are considered non-cytotoxic if the percentage cell viability is greater than 80% (240). Therefore, the lack of a substantial effect on glucose uptake cannot be attributed to a cytotoxic effect.

DM often presents with complications, and this could be due to sustained uncontrolled hyperglycaemia. The development of DM complications such as CVD can often be linked to factors which include the activation of polyol pathways, oxidative stress, enhancement of the coagulation cascade and comorbidities.

In uncontrolled DM, there is an increase in sorbitol production from glucose due to an increase in aldose reductase activity (60, 61). The accumulation of sorbitol causes peripheral tissue damage,

including retinopathy, neuropathy and nephropathy. Furthermore, the accumulation of sorbitol contributes to oxidative stress and AGEs formation, which are implicated in DM complications. Therefore, inhibiting aldose reductase activity in the polyol pathway will reduce the accumulation of intracellular sorbitol, which is beneficial in managing DM complications.

The quinolone derivatives were investigated for their effect on aldose reductase - a rate-limiting enzyme in the polyol pathway. From Figure 3.10, all four compounds showed poor inhibitory activity against aldose reductase, with percentage inhibition less than 50% for each compound across the different concentrations. The aldose reductase binding site consists of a catalytic region (anion binding pocket) which is formed by the nicotinamide ring of the cofactor (NADP⁺) and the enzyme side chains Trp20, Val47, Tyr48, His110 and Trp111, while a second hydrophobic pocket (specificity pocket) is flanked by Trp moiety and the C-terminal loop region of the enzyme which consist of Thr113, Phe115, Phe122, Ala299, Leu300, Leu301, Ser302, Cys303 and Tyr309 (241, 242). Aldose reductase inhibitors have a polar and non-polar moiety that can interact with the enzyme's anion binding pocket and the non-polar region, respectively. Most aldose reductase inhibitors are grouped into three main classes (Figure 4.2): cyclic imides such as fidarestat, a polyphenolic compound such as quercetin and carboxylic acid derivatives such as epalrestat (243). The presence of these functional groups/structures is crucial for binding to the active site of the aldose reductase enzyme. In this study, quercetin was used as a reference compound and from the result in Figure 3.10, it exhibited good inhibitory activity against aldose reductase. This was expected because quercetin possesses a polyphenolic structure. Therefore, we may suggest that the quinolone derivatives exhibited poor inhibitory effect on aldose reductase because they lack the required functional groups/structure required for binding to the enzymes active site. To enhance the activity of the quinolone derivatives, their structure has to be modified to contain substituents that are able to bind to the aldose reductase binding site.

of a denser fibrin network that is more resistant to fibrinolysis (98). Eventually, this leads to the formation of a thrombus or an embolus which is implicated in the development of CVD, such as cerebrovascular accidents, pulmonary embolism and peripheral artery diseases. The quinolone derivatives were investigated for their effect on clotting FXa because FXa is involved in platelet activation and clot formation. Developing new clotting FXa inhibitors is essential because the conventional clotting FXa inhibitors such as rivaroxaban, fondaparinux, apixaban and edoxaban present with limitations, including a high risk of bleeding and dose benefit-to-risk profile – the maximum dose depend on the amount that can be administered safely rather than the dose providing the best efficacy (244, 245). Before novel compounds can be considered ideal inhibitors of clotting FXa, it has to have a good inhibition profile against FXa, rapid onset of action, high safety and a predictable pharmacokinetics profile that will allow for fixed oral dosing without routine monitoring and great efficacy with minimal risk of bleeding.

The result of FXa inhibition in Figure 3.11 showed that the quinolone derivatives had poor inhibitory activity against FXa (percentage inhibitions is less than 50% across the concentrations used) compared to GGACK dihydrochloride which was used as a reference drug. FXa is a trypsin-like serine protease with a catalytic domain with two similar antiparallel β -barrel folds forming the catalytic triad and binding site (246). For inhibitors to bind to the FXa binding site, they must have an amide moiety that bonds to the S₁ deep large hydrophobic cleft, which contains Asp189 and Tyr228 side chains (246). The S₁ subsite is the main binding site. They can also bind to the S₄ strong hydrophobic pocket, which contains Tyr99, Phe174 and Trp215, the catalytic triad, which consists of His57, Asp102 and Ser195 and the β -strand region. Most of the serine protease inhibitors bind in the S₁ and one or more subsites. The quinolone derivatives' poor inhibitory activity can be explained by the lack of an amide moiety which is required for binding to the S₁ subunit of the FXa active site. While the good inhibitory profile of GGACK dihydrochloride might be due to its amide group (Figure 4.3), which can bind to the S₁ subsite of FXa. The activity of the quinolone derivatives may be enhanced through the modification of their structure by substituting the benzene ring with an amide moiety.

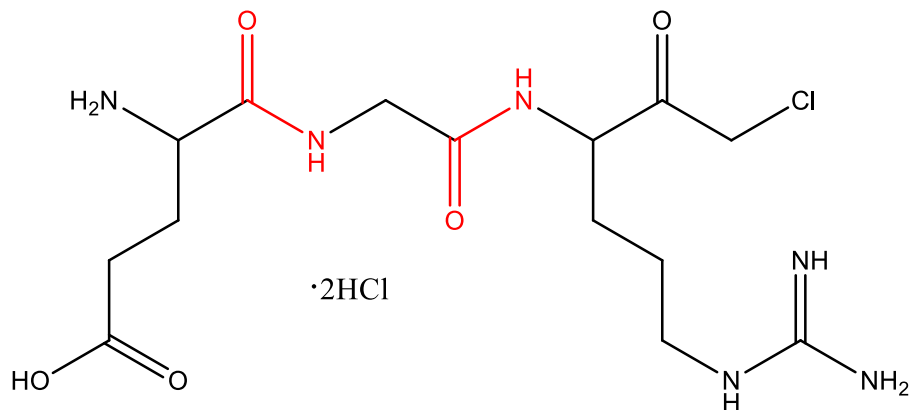


Figure 4.3: The structure of GGACK dihydrochloride, a potent FXa inhibitor. The amide moiety of the inhibitor is required for bonding with the S₁ subsite of clotting FXa.

Dyslipidaemia is one of the comorbidities often associated with DM and is known to aggravate CVDs. This is because there is an increase in the release of free fatty acid in insulin-resistant fat cells, resulting in increased triglyceride secretion (89). Subsequently, the secretion of Apo B and VLDL cholesterol is enhanced, and the catabolism of HDL-C is increased. Also, hyperglycaemia enhances the glycosylation and oxidation of LDL and VLDL, resulting in the development of aggressive atherosclerosis (91). The decrease in the concentration of HDL-C and an increase in the concentration of LDL, VLDL and Apo B are risk factors for developing CVD. HMG-CoA reductase (HMGR) is a rate-controlling enzyme in the mevalonate pathway that produces cholesterol. Therefore, inhibiting this enzyme decreases cholesterol synthesis, which upregulates the expression of LDL receptors in the liver; hence, more LDL-C is cleared, reducing the risk of CVD. Statins are HMGR inhibitors used clinically for managing dyslipidaemia, but they present side effects such as myalgia due to the depletion of ubiquinone (coenzyme Q10) (138, 247). Therefore, novel compounds developed should have higher efficacy and fewer side effects.

The quinolone derivatives were investigated against HMGR activity. The result in Figure 3.12 shows that the quinolone derivatives had poor inhibitory activity against HMGR, with percentage inhibition less than 50% across the concentrations used. Pravastatin, used as the reference drug, exhibited a good inhibitory profile. This was expected because pravastatin is a statin which is known to inhibit HMGR. Statins have a structural component (HMG-moiety) that is essential for binding to the active site of HMGR (Figure 4.4). This essential structure includes a dihydroxy heptanoic acid unit, a ring system with different substituents and maintaining a 3R,5R

stereochemistry because HMGR is stereoselective (248). This HMG-moiety forms a polar interaction with the enzyme amino acid residue Asp690, Lys691, Lys692 and Ser684, while the terminal carboxylate group of the HMG-moiety forms a salt-bridge with Lys735. The O5 hydroxyl group of the hydroxyglutartic acid component of statins also forms a hydrogen bond with Glu559, Asp767 and Lys691 and van der Waals interaction with the enzymes hydrophobic side chain, which consists of Ala856, Leu562, Leu853, Leu857 and Val683 (249). Furthermore, statins are grouped into type 1 (simvastatin and pravastatin) and type 2 (atorvastatin and rosuvastatin), with type 1 statins having a butyryl group while type 2 statins have a fluorophenyl group on the ring component (249). The fluorine atom on the fluorophenyl group of type 2 statins allows for the additional formation of polar interaction with the Arg590 residue of the enzyme. Since the quinolone derivatives lack the HMG-moiety, we can conclude that the lack of the HMG-moiety accounts for the poor inhibitory activity against HMGR. The activity of the quinolone derivatives may be enhanced by modifying their structure to contain the statin pharmacophore.

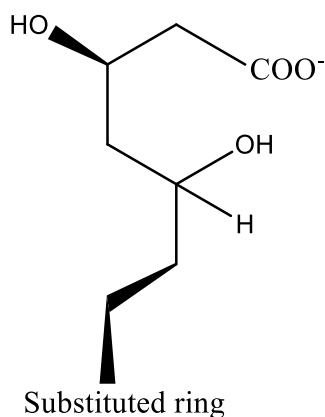


Figure 4.4: Statin pharmacophore essential for binding to the active site of HMGR.

Oxidative stress contributes to the aetiology and progression of DM and its complications, including CVD, resulting from prolonged hyperglycaemia and a myriad of pathological processes, including accumulation of sorbitol in the polyol pathway and overpowering of the cellular antioxidant defence system by reactive free radicals. Therefore, investigating the quinolone derivatives for their antioxidant properties was of paramount importance.

The antioxidant properties of the quinolone derivatives were investigated using DPPH and FRAP assay. From Figures 3.13 and 3.14, QD1, QD2 and QD3 exhibited some antioxidant activity, with

QD2 having the highest radical scavenging activity and FRAP value. The quinolone derivatives possess electron-withdrawing groups (EWG) attached to a benzene ring, and this has been reported to enhance the antioxidant activity of quinolones (250). The EWGs on the quinolone derivatives include nitro, ketone, ester and chloride substituent. Therefore, we can attribute the antioxidant activity of the quinolone derivatives to the presence of the EWGs. The antioxidant activity of these compounds can help enhance the body's antioxidant defence system, thus slowing down the progression of DM and the development of DM complications.

Overall, the inhibitory activity of the investigated quinolone derivatives against the selected therapeutic targets was moderate. This could be attributed to the presence of ketone groups, aromatic rings, aliphatic chains, carboxylate groups and hydrogen bond acceptors in the structure of the compounds (Figure 4.5). The quinolone derivatives could be ideal for managing DM and its associated complications due to their multimodal function, as they could address multiple factors implicated in DM, resulting in controlled hyperglycaemia in an *in vivo* setting. Although the overall inhibition profile is moderate, this would be preferred to having a stronger inhibition against all therapeutic targets because a stronger inhibition could pose the risk of severe hypoglycaemia. The limited inhibitory activity against some of the selected therapeutic targets could be due to the lack of necessary structural features that enables the binding of quinolones derivatives to the active site of the enzymes implicated in DM and its associated complications. Therefore, modifying the structure of these quinolone derivatives to contain moieties specific to binding and inhibiting enzymes implicated in DM might enhance their antidiabetic effect. Furthermore, the proposed mechanism by which quinolone causes hypoglycaemia is through stimulation of insulin secretion from the pancreatic beta-cell (156, 167). Therefore, investigating these quinolone derivatives on pancreatic cells could give us more insight into their antidiabetic effect.

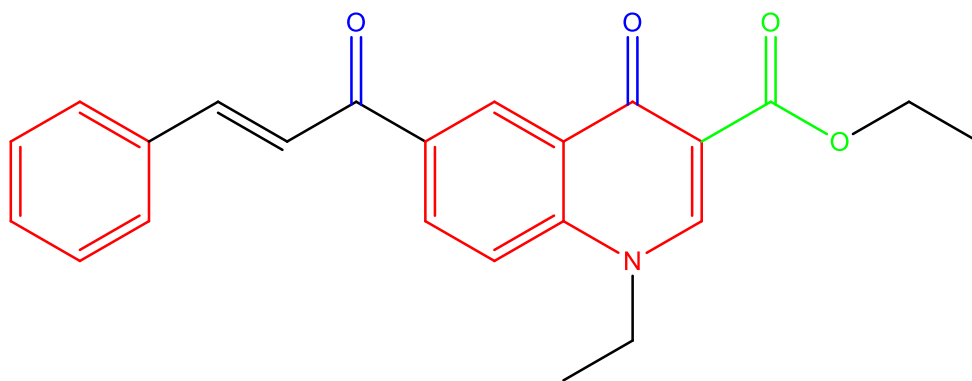


Figure 4.5: The basic structure common to the four quinolone derivatives. On this structure are ketone groups (blue), aromatic rings (red), carboxylate group (green), aliphatic chains and hydrogen bond acceptors that aided the moderate inhibitory effect exhibited by the quinolone derivatives.

CHAPTER 5: CONCLUSIONS, LIMITATIONS AND FUTURE STUDIES

CONCLUSIONS

Diabetes mellitus (DM) and its associated complications are a global concern due to the increased prevalence of DM and increased mortality rate resulting from cardiovascular complications. This has led researchers to investigate novel compounds for potential antidiabetic effects and protection against DM complications. We investigated quinolone-containing compounds because studies have reported that the adverse effect of quinolones includes hypoglycaemia. Therefore, this has made them an area of interest, but only a few studies have been conducted on their antidiabetic effect. From the investigation of the drug-likeness and the GIT absorption properties of the quinolone derivatives, we can envisage that these compounds are druggable and can be absorbed in the GIT. Therefore, these quinolone derivatives can be formulated for oral use.

From investigating the quinolone derivatives against selected therapeutic targets for their antidiabetic and cardio-protective activity, the compounds exhibited a strong inhibitory activity against alpha-amylase and a moderate inhibitory activity against the other targets except for PTP1B enzyme where there was no inhibition observed. Also, moderate antioxidant activity was observed for the quinolone derivatives. Therefore, the overall inhibitory profile and antioxidant activity for the quinolone derivatives is moderate, and these could be attributed to the presence of ketone groups, aromatic rings, aliphatic chains, carboxylate groups and hydrogen bond acceptors present in the structure of the compounds. However, a moderate inhibitory profile would be preferred to having a stronger inhibition against all therapeutic targets because a stronger inhibition could pose the risk of severe hypoglycaemia.

From the cell-based assay, there was no substantial increase in glucose uptake as compared to the control group. The poor glucose uptake demonstrated can also be explained by the inability of the quinolone derivatives to inhibit PTB1B. Taking these observations together, we can therefore suggest that these compounds cannot work as insulin mimetics.

Furthermore, the ability of the quinolone derivatives to inhibit various pharmacological enzyme targets can be harnessed in favour of the management of DM and its associated complications. For

these reasons, further investigations and developments towards improving the quinolone derivatives as potential antidiabetic agents are warranted.

LIMITATIONS AND FUTURE STUDIES

In vitro studies involving enzymes often presents with difficulties in assay standardization and enzymes instability due to storage conditions resulting in misleading results. While *in vitro* cell-based assays are prone to infections. Also, *in vitro* studies should be done in replicates and repeated over time to ascertain if a specific trend is observed, which increases the accuracy and confidence in the result obtained. However, in this study, assays, especially those involving the use of kits, could not be repeated due to cost and limited resources. In future studies, multiple experiments need to be carried out in replicates maintaining the same conditions as much as possible. Furthermore, to improve the clinical relevance of this study, insulin secretion studies should be conducted. Also, *in vivo* studies and the use of docking tools to quantify specific interactions, as well as the required conformations essential for the activity of these compounds against therapeutic targets, should be conducted.

REFERENCES

1. American Diabetes Association. Diagnosis and classification of diabetes mellitus: *Diabetes Care*. 2014 Jan 1;37(suppl_1):S81-90.
2. World Health Organization. *World health statistics 2021: monitoring health for the SDGs, sustainable development goals*. Switzerland: World Health Organization; 2021. 121 p.
3. International Diabetes Federation. *Diabetes facts & figures* [Internet]. Brussels, Belgium: International Diabetes Federation; 2021 [updated 2021 Dec 9; cited 2022 Jan 10]. Available from: <https://idf.org/aboutdiabetes/what-is-diabetes.html>.
4. Mphasha MH, Skaal L, Mothiba TM. Prevalence of overweight and obesity amongst patients with diabetes and their non-diabetic family members in Senwabarwana, Limpopo province, South Africa. *S Afr Fam Pract*. 2022 May 25;64(1):e1-7
5. World Health Organization. *Classification of diabetes mellitus*. Geneva: World Health Organization; 2019 April. 36 p.
6. American Diabetes Association. Diagnosis and classification of diabetes mellitus: *Diabetes Care*. 2009 Jan;32(suppl_1):S62-7.
7. Silver B, Ramaiya K, Andrew SB, Fredrick O, Bajaj S, Kalra S, et al. EADSG guidelines: insulin therapy in diabetes. *Diabetes Ther*. 2018 Mar 5;9(2):449-92.
8. Park-Wyllie LY, Juurlink DN, Kopp A, Shah BR, Stukel TA, Stumpo C, et al. Outpatient gatifloxacin therapy and dysglycemia in older adults. *N Engl J Med*. 2006 Mar 3;354(13):1352-61.
9. Tirone TA, Brunicardi FC. Overview of glucose regulation. *World J Surg*. 2001 Apr 11;25(4):461-7.
10. Szablewski L. Glucose homeostasis—mechanism and defects. *Diabetes Dam Treat*. 2011:227-56.
11. Röder PV, Wu B, Liu Y, Han W. Pancreatic regulation of glucose homeostasis. *Exp Mol Med*. 2016 Mar 11;48(3):e219.

12. Holmes R. Carbohydrate digestion and absorption. *J Clin Pathol Suppl (R Coll Pathol)*. 1971;5:10-3.
13. Sitrin MD. Digestion and absorption of carbohydrates and proteins. *Gastrointest Syst*. 2014 Mar 24;137-58.
14. Levin RJ. Digestion and absorption of carbohydrates—from molecules and membranes to humans. *Am J Clin Nutr*. 1994 Mar 1;59(3):690-8.
15. Hinsberger A, Sandhu B. Digestion and absorption. *Curr Paediatr*. 2004 Dec;14(7):605-11.
16. Ferraris RP. Dietary and developmental regulation of intestinal sugar transport. *Biochem J*. 2001 Nov 26;360(2):265-76.
17. Wood IS, Trayhurn P. Glucose transporters (GLUT and SGLT): expanded families of sugar transport proteins. *Br J Nutr*. 2003;89(1):3-9.
18. Brown G. Glucose transporters: structure, function and consequences of deficiency. *J Inherit Metab Dis*. 2000 May 1;23(3):237-46.
19. Standl E, Schnell O. Alpha-glucosidase inhibitors 2012—cardiovascular considerations and trial evaluation. *Diab Vasc Dis Res*. 2012 Apr 16;9(3):163-9.
20. Gonzalez A, Merino B, Marroquí L, Neco P, Alonso-Magdalena P, Caballero-Garrido E, et al. Insulin hypersecretion in islets from diet-induced hyperinsulinemic obese female mice is associated with several functional adaptations in individual β -cells. *Endocrinol*. 2013 Oct 1;154(10):3515-24.
21. Fridlyand LE, Philipson LH. Glucose sensing in the pancreatic beta cell: a computational systems analysis. *Theor Biol Med Model*. 2010 May 24;7(1):1-44.
22. Hiriart M, Aguilar-Bryan L. Channel regulation of glucose sensing in the pancreatic β -cell. *Am J Physiol Endocrinol Metab*. 2008 Dec 1;295(6):1298-306.
23. Govindappa M. A review on role of plant (s) extracts and its phytochemicals for the management of diabetes. *J Diabetes Metab*. 2015;6(7):1-38.
24. Jamaludina UK, Dochertyb P, Preiserc JC. Incretin effects and enteral feed transitions. *Diet Nutr Crit Care*. 2016 Dec 10:1269-81.

25. Holst JJ, Gromada J. Role of incretin hormones in the regulation of insulin secretion in diabetic and nondiabetic humans. *Am J Physiol Endocrinol Metab.* 2004 Aug 1;287(2):199-206.
26. Gallwitz B. Clinical use of DPP-4 inhibitors. *Front Endocrinol.* 2019 Jun 19;10:389.
27. Vilsbøll T, Holst J. Incretins, insulin secretion and type 2 diabetes mellitus. *Diabetologia.* 2004 Feb 13;47(3):357-66.
28. Omar B, Ahrén B. Pleiotropic mechanisms for the glucose-lowering action of DPP-4 inhibitors. *Diabetes.* 2014 Jun 14;63(7):2196-202.
29. Röhrborn D, Wronkowitz N, Eckel J. DPP4 in diabetes. *Front Immunol.* 2015 Jul 27;6:386.
30. Mentlein R. Dipeptidyl-peptidase IV (CD26)-role in the inactivation of regulatory peptides. *Regul Pept.* 1999 Nov 30;85(1):9-24.
31. Kasina SVSK, Baradhi KM. Dipeptidyl peptidase IV (DPP IV) inhibitors [Internet]. Treasure Island (FL): StatPearls Publishing; 2022 Jan [cited 2022 Feb 17]. Available from: <https://www.ncbi.nlm.nih.gov/books/NBK542331/>.
32. Capuano A, Sportiello L, Maiorino MI, Rossi F, Giugliano D, Esposito K. Dipeptidyl peptidase-4 inhibitors in type 2 diabetes therapy—focus on alogliptin. *Drug Des Devel Ther.* 2013 Sep 17;7:989-1001.
33. Nolte MS. Pancreatic hormones and antidiabetic drugs. *Basic Clin Pharmacol.* 2004;693-715.
34. Lizcano JM, Alessi DR. The insulin signalling pathway. *Curr Biol.* 2002 Apr 2;12(7):R236-8.
35. Pessin JE, Saltiel AR. Signaling pathways in insulin action: molecular targets of insulin resistance. *J Clin Invest.* 2000 Jan 15;106(2):165-9.
36. Chang L, Chiang SH, Saltiel AR. Insulin signaling and the regulation of glucose transport. *Mol Med.* 2004 Jul;10(7):65-71.
37. Saltiel AR, Pessin JE. Insulin signaling in microdomains of the plasma membrane. *Traffic.* 2003 Oct 10;4(11):711-6.

38. Okada T, Kawano Y, Sakakibara T, Hazeki O, Ui M. Essential role of phosphatidylinositol 3-kinase in insulin-induced glucose transport and antilipolysis in rat adipocytes. Studies with a selective inhibitor wortmannin. *J Biol Chem*. 1994 Feb 4;269(5):3568-73.
39. Goldstein BJ, Ahmad F, Ding W, Li P-M, Zhang W-R. Regulation of the insulin signalling pathway by cellular protein-tyrosine phosphatases. *Mol Cell Biochem*. 1998 May;182(1):91-9.
40. Sun J, Qu C, Wang Y, Huang H, Zhang M, Zou W. Type 2 diabetes mellitus and protein-tyrosine phosphatase 1b. *J Diabetes Metab Disord Control*. 2016 Dec 30;3(8):180-3.
41. Crans DC, Smee JJ, Gaidamauskas E, Yang L. The chemistry and biochemistry of vanadium and the biological activities exerted by vanadium compounds. *Chem Rev*. 2004 Jan 29;104(2):849-902.
42. Liu G. Protein tyrosine phosphatase 1B inhibition: opportunities and challenges. *Curr Med Chem*. 2003 Aug 1;10(15):1407-21.
43. Hatting M, Tavares CD, Sharabi K, Rines AK, Puigserver P. Insulin regulation of gluconeogenesis. *Ann N Y Acad Sci*. 2017 Sep 3;1411(1):21-35.
44. Gastaldelli A, Toschi E, Pettiti M, Frascerra S, Quinones-Galvan A, Sironi AM, et al. Effect of physiological hyperinsulinemia on gluconeogenesis in nondiabetic subjects and in type 2 diabetic patients. *Diabetes*. 2001 Aug 1;50(8):1807-12.
45. Kjos SL, Buchanan TA. Gestational diabetes mellitus. *N Engl J Med*. 1999 Dec 2;341(23):1749-56.
46. Ozougwu J, Obimba K, Belonwu C, Unakalamba C. The pathogenesis and pathophysiology of type 1 and type 2 diabetes mellitus. *J Physiol Pathophysiol*. 2013 Sep 30;4(4):46-57.
47. Pino SC, Kruger AJ, Bortell R. The role of innate immune pathways in type 1 diabetes pathogenesis. *Curr Opin Endocrinol Diabetes Obes*. 2010 Apr;17(2):126-30.
48. Virally M, Blicklé JF, Girard J, Halimi S, Simon D, Guillausseau PJ. Type 2 diabetes mellitus: epidemiology, pathophysiology, unmet needs and therapeutical perspectives. *Diabetes Metab*. 2007 Sep 1;33(4):231-44.

49. Barker JM, Barriga KJ, Yu L, Miao D, Erlich HA, Norris JM, et al. Prediction of autoantibody positivity and progression to type 1 diabetes: Diabetes Autoimmunity Study in the Young (DAISY). *J Clin Endocrinol Metab.* 2004 Aug 1;89(8):3896-902.
50. Tuomi T, Groop LC, Zimmet PZ, Rowley MJ, Knowles W, Mackay IR. Antibodies to glutamic acid decarboxylase reveal latent autoimmune diabetes mellitus in adults with a non—insulin-dependent onset of disease. *Diabetes.* 1993 Feb 1;42(2):359-62.
51. Giorgino F, Laviola L, Leonardini A. Pathophysiology of type 2 diabetes: rationale for different oral antidiabetic treatment strategies. *Diabetes Res Clin Pract.* 2005 Jun 1;68:S22-9.
52. Baynes HW. Classification, pathophysiology, diagnosis and management of diabetes mellitus. *J Diabetes Metab.* 2015 May 1;6(5):1-9.
53. Padberg I, Peter E, Gonzalez-Maldonado S, Witt H, Mueller M, Weis T, et al. A new metabolomic signature in type-2 diabetes mellitus and its pathophysiology. *PLoS One.* 2014 Jan 17;9(1):e85082.
54. Triplitt CL, Repas T, Alvarez C. Diabetes Mellitus. In: DiPiro JT, Talbert RL, Yee GC, Matzke GR, Wells BG, Posey L, editors. *Pharmacotherapy: A pathophysiologic approach, 10e* [Internet]. McGraw Hill; 2017 [cited 2022 Jan 12]. Available from: <https://accesspharmacy.mhmedical.com/content.aspx?bookid=1861§ionid=14606589> 1.
55. Bogardus C, Lillioja S, Mott D, Hollenbeck C, Reaven G. Relationship between degree of obesity and in vivo insulin action in man. *Am J Physiol Endocrinol Metab.* 1985 Mar 1;248(3):E286-91.
56. Stumvoll M, Goldstein BJ, Van Haefen TW. Type 2 diabetes: principles of pathogenesis and therapy. *Lancet.* 2005 Apr 9;365(9467):1333-46.
57. Wu Y, Ding Y, Tanaka Y, Zhang W. Risk factors contributing to type 2 diabetes and recent advances in the treatment and prevention. *Int J Med Sci.* 2014 Sep 6;11(11):1185-200.

58. Yamagishi SI, Imaizumi T. Diabetic vascular complications: pathophysiology, biochemical basis and potential therapeutic strategy. *Curr Pharm Des* 2005;11(18):2279-99.
59. Rhee SY, Kim YS. The role of advanced glycation end products in diabetic vascular complications. *Diabetes Metab J*. 2018 May 31;42(3):188-95.
60. Garcia Soriano F, Virag L, Jagtap P, Szabo E, Mabley JG, Liaudet L, et al. Diabetic endothelial dysfunction: the role of poly (ADP-ribose) polymerase activation. *Nat Med*. 2001 Jan;7(1):108-13.
61. Brownlee M. The pathobiology of diabetic complications: a unifying mechanism. *Diabetes*. 2005 Jun 1;54(6):1615-25.
62. Gerald P, King GL. Activation of protein kinase C isoforms and its impact on diabetic complications. *Circ Res*. 2010 Apr 30;106(8):1319-31.
63. Ohiagu FO, Chikezie PC, Chikezie CM. Pathophysiology of diabetes mellitus complications: Metabolic events and control. *Biomed Res Ther*. 2021 Mar 31;8(3):4243-57.
64. Ojo O. An overview of diabetes and its complications. *Diabetes Res Open J*. 2016 Sep 12;2(2):e4-6.
65. Cade WT. Diabetes-related microvascular and macrovascular diseases in the physical therapy setting. *Phys Ther*. 2008 Nov 1;88(11):1322-35.
66. Solomon SD, Chew E, Duh EJ, Sobrin L, Sun JK, VanderBeek BL, et al. Diabetic retinopathy: a position statement by the American Diabetes Association. *Diabetes Care*. 2017 Mar 1;40(3):412-8.
67. Forbes JM, Cooper ME. Mechanisms of diabetic complications. *Physiol Rev*. 2013 Jan 1;93(1):137-88.
68. Frank RN. Diabetic retinopathy. *N Engl J Med*. 2004 Jan 1;350(1):48-58.
69. Shankar U, Gunasundari R. A review on electrophysiology based detection of diabetic retinopathy. *Procedia Comput Sci*. 2015 Jan 1;48:630-7.

70. Peters V, Yard B, Schmitt CP. Carnosine and diabetic nephropathy. *Curr Med Chem*. 2020 Apr 1;27(11):1801-12.
71. Donate-Correa J, Luis-Rodríguez D, Martín-Núñez E, Tagua VG, Hernández-Carballo C, Ferri C, et al. Inflammatory targets in diabetic nephropathy. *J Clin Med*. 2020 Feb 7;9(2):458.
72. Vinod P. Pathophysiology of diabetic nephropathy. *Clin Queries: Nephrol*. 2012 Apr;1(2):121-6.
73. CE ML, San Martín Ojeda CA, JJ RP, CJ FZ. Pathophysiology of diabetic nephropathy: a literature review. *Medwave*. 2017 Jan 12;17(1):e6839.
74. Pálsson R, Patel UD. Cardiovascular complications of diabetic kidney disease. *Adv Chronic Kidney Dis*. 2014 May 1;21(3):273-80.
75. Selvarajah D, Wilkinson ID, Emery CJ, Harris ND, Shaw PJ, Witte DR, et al. Early involvement of the spinal cord in diabetic peripheral neuropathy. *Diabetes Care*. 2006 Dec 1;29(12):2664-9.
76. Saberzadeh-Ardestani B, Karamzadeh R, Basiri M, Hajizadeh-Saffar E, Farhadi A, Shapiro AJ, et al. Type 1 diabetes mellitus: cellular and molecular pathophysiology at a glance. *Cell J*. 2018 May 28;20(3):294-301.
77. Kaur S, Pandhi P, Dutta P. Painful diabetic neuropathy: an update. *Ann Neurosci*. 2011 Oct;18(4):168-75.
78. Vinik AI, Maser RE, Mitchell BD, Freeman R. Diabetic autonomic neuropathy. *Diabetes Care*. 2003 May 1;26(5):1553-79.
79. Volmer-Thole M, Lobmann R. Neuropathy and diabetic foot syndrome. *Int J Mol Sci*. 2016 Jun 10;17(6):917.
80. Laing S, Swerdlow A, Slater S, Burden A, Morris A, Waugh NR, et al. Mortality from heart disease in a cohort of 23,000 patients with insulin-treated diabetes. *Diabetologia*. 2003 May 28;46(6):760-5.
81. Matheus AS, Tannus LR, Cobas RA, Palma CC, Negrato CA, Gomes MD. Impact of diabetes on cardiovascular disease: an update. *Int J Hypertens*. 2013 Mar 4;2013.

82. Schering D, Kasten S. The link between diabetes and cardiovascular disease. *J Pharm Pract.* 2004 Feb;17(1):61-5.
83. Petrie JR, Guzik TJ, Touyz RM. Diabetes, hypertension, and cardiovascular disease: clinical insights and vascular mechanisms. *Can J Cardiol.* 2018 May 1;34(5):575-84.
84. Leon BM, Maddox TM. Diabetes and cardiovascular disease: epidemiology, biological mechanisms, treatment recommendations and future research. *World J Diabetes.* 2015 Oct 10;6(13):1246-58.
85. Schena FP, Gesualdo L. Pathogenetic mechanisms of diabetic nephropathy. *J Am Soc Nephrol.* 2005 Mar 1;16:S30-3.
86. Lastra G, Syed S, Kurukulasuriya LR, Manrique C, Sowers JR. Type 2 diabetes mellitus and hypertension: an update. *Endocrinol Metab Clin.* 2014 Mar 1;43(1):103-22.
87. de Kloet AD, Krause EG, Woods SC. The renin angiotensin system and the metabolic syndrome. *Physiol Behav.* 2010 Jul 14;100(5):525-34.
88. Ribeiro-Oliveira Jr A, Nogueira AI, Pereira RM, Boas WW, Dos Santos RA, Simões AC. The renin–angiotensin system and diabetes: an update. *Vasc Health Risk Manag.* 2008 Aug;4(4):787-803.
89. Wu L, Parhofer KG. Diabetic dyslipidemia. *Metabolism.* 2014 Dec 1;63(12):1469-79.
90. Parhofer KG. Interaction between glucose and lipid metabolism: more than diabetic dyslipidemia. *Diabetes Metab J* 2015 Oct 22;39(5):353-62.
91. Behbodikhah J, Ahmed S, Elyasi A, Kasselmann LJ, De Leon J, Glass AD, et al. Apolipoprotein B and Cardiovascular Disease: Biomarker and Potential Therapeutic Target. *Metabolites.* 2021 Oct 8;11(10):690.
92. King R, Grant P. Diabetes and cardiovascular disease: pathophysiology of a life-threatening epidemic. *Herz.* 2016 Mar 30;41(3):184-92.
93. Rucker D, Dhamoon AS. Physiology, Thromboxane A2 [Internet]. Treasure Island (FL): StatPearls Publishing; 2022 Jan [cited 2022 Feb 18]. Available from: <https://www.ncbi.nlm.nih.gov/books/NBK539817/>.

94. Wang B, Wu L, Chen J, Dong L, Chen C, Wen Z, et al. Metabolism pathways of arachidonic acids: Mechanisms and potential therapeutic targets. *Signal Transduct Target Ther.* 2021 Feb 26;6(1):1-30.
95. Parker WA, Storey RF, Ajjan RA. Platelets, coagulation, and antithrombotic therapy in diabetes. *Endotext.* South Dartmouth (MA): MDText.com, Inc; 2022.
96. Hess K, Grant PJ. Inflammation and thrombosis in diabetes. *Thromb Haemost.* 2011 Apr 11;105(supp_1):S43-54.
97. Grant PJ. Diabetes mellitus as a prothrombotic condition. *J Intern Med.* 2007 Jun 26;262(2):157-72.
98. Seljeflot I, Larsen J, DAHL-JØRGENSEN K, Hanssen K, Arnesen H. Fibrinolytic activity is highly influenced by long-term glycemic control in Type 1 diabetic patients. *J Thromb Haemost.* 2006 Feb 6;4(3):686-8.
99. Mansfield MW, Stickland MH, Grant PJ. PAI-1 concentrations in first-degree relatives of patients with non-insulin-dependent diabetes: metabolic and genetic associations. *Thromb Haemost.* 1997;77(02):357-61.
100. Kohler HP, Grant PJ. Plasminogen-activator inhibitor type 1 and coronary artery disease. *N Engl J Med.* 2000 Jun 15;342(24):1792-801.
101. Bohl KS, West JL. Nitric oxide-generating polymers reduce platelet adhesion and smooth muscle cell proliferation. *Biomaterials.* 2000 Nov 15;21(22):2273-8.
102. Naseem KM. The role of nitric oxide in cardiovascular diseases. *Mol Aspects Med.* 2005 Feb-Apr;26(1-2):33-65.
103. Singh U, Jialal I. Oxidative stress and atherosclerosis. *Pathophysiology.* 2006 Aug 1;13(3):129-42.
104. Vogiatzi G, Tousoulis D, Stefanadis C. The role of oxidative stress in atherosclerosis. *Hellenic J cardiol.* 2009 Sep 1;50(5):402-9.
105. Erdmann E, Charbonnel B, Wilcox R. Thiazolidinediones and cardiovascular risk—a question of balance. *Curr Cardiol Rev.* 2009 Aug 1;5(3):155-65.

106. Steck AK, Rewers MJ. Epidemiology and risk factors for type 1 diabetes mellitus. *Int Text Diabetes Mellit*. 2015 Mar 6:17-28.
107. McCall AL. Insulin therapy and hypoglycemia. *Endocrinol Metab Clin North Am*. 2012 Mar 1;41(1):57.
108. Herman ME, O'Keefe JH, Bell DS, Schwartz SS. Insulin therapy increases cardiovascular risk in type 2 diabetes. *Prog Cardiovasc Dis*. 2017 Nov 1;60(3):422-34.
109. DeFronzo RA. Pharmacologic therapy for type 2 diabetes mellitus. *Ann Intern Med*. 1999 Aug 17;131(4):281-303.
110. Proks P, Reimann F, Green N, Gribble F, Ashcroft F. Sulfonylurea stimulation of insulin secretion. *Diabetes*. 2002 Dec 1;51(suppl_3):S368-76.
111. Bell DS. Do sulfonylurea drugs increase the risk of cardiac events?. *Can Med Assoc J*. 2006 Jan 17;174(2):185-6.
112. Murad MH, Coto-Yglesias F, Wang AT, Sheidaee N, Mullan RJ, Elamin MB, et al. Drug-induced hypoglycemia: a systematic review. *J Clin Endocrinol Metab*. 2009 Mar 1;94(3):741-5.
113. Chaudhury A, Duvoor C, Reddy Dendi VS, Kraleti S, Chada A, Ravilla R, et al. Clinical review of antidiabetic drugs: implications for type 2 diabetes mellitus management. *Front Endocrinol*. 2017 Jan 24;8:6.
114. Bodmer M, Meier C, KRahenbuhl S, Jick SS, Meier CR. Metformin, sulfonylureas, or other antidiabetes drugs and the risk of lactic acidosis or hypoglycemia: a nested case-control analysis. *Diabetes Care*. 2008 Nov 1;31(11):2086-91.
115. Fowler MJ. Diabetes treatment: oral agents. *Clin Diabetes*. 2010;28(3):132-6.
116. Dominguez LJ, Davidoff AJ, Srinivas PR, Standley PR, Walsh MF, Sowers JR. Effects of metformin on tyrosine kinase activity, glucose transport, and intracellular calcium in rat vascular smooth muscle. *Endocrinol*. 1996 Jan 1;137(1):113-21.
117. Pawlyk AC, Giacomini KM, McKeon C, Shuldiner AR, Florez JC. Metformin pharmacogenomics: current status and future directions. *Diabetes*. 2014 Aug 1;63(8):2590-9.

118. Zhang Q, Li S, Li L, Li Q, Ren K, Sun X, et al. Metformin treatment and homocysteine: a systematic review and meta-analysis of randomized controlled trials. *Nutrients*. 2016 Dec 9;8(12):798.
119. Kim J, Ahn CW, Fang S, Lee HS, Park JS. Association between metformin dose and vitamin B12 deficiency in patients with type 2 diabetes. *Medicine*. 2019 Nov 15;98(46):e17918.
120. Pu R, Shi D, Gan T, Ren X, Ba Y, Huo Y, et al. Effects of metformin in obesity treatment in different populations: a meta-analysis. *Ther Adv Endocrinol Metab*. 2020 May 21;11.
121. Yki-Järvinen H. Thiazolidinediones. *N Engl J Med*. 2004 Sep 9;351(11):1106-18.
122. Lebovitz HE. Thiazolidinediones: the forgotten diabetes medications. *Curr Diab Rep*. 2019 Nov 27;19(12):1-13.
123. Hanefeld M, Schaper F. Acarbose: oral antidiabetes drug with additional cardiovascular benefits. *Expert Rev Cardiovasc Ther*. 2008 Feb 1;6(2):153-63.
124. Poudel RR. Renal glucose handling in diabetes and sodium glucose cotransporter 2 inhibition. *Indian J Endocrinol Metab*. 2013 Jul-Aug;17(4):588-93.
125. Peters AL, Buschur EO, Buse JB, Cohan P, Diner JC, Hirsch IB. Euglycemic diabetic ketoacidosis: a potential complication of treatment with sodium–glucose cotransporter 2 inhibition. *Diabetes Care*. 2015 Sep 1;38(9):1687-93.
126. Halimi S, Vergès B. Adverse effects and safety of SGLT-2 inhibitors. *Diabetes Metab*. 2014 Dec 1;40(6):S28-34.
127. Barnett A. DPP-4 inhibitors and their potential role in the management of type 2 diabetes. *Int J Clin Pract*. 2006 Oct 11;60(11):1454-70.
128. Trujillo JM, Nuffer W, Ellis SL. GLP-1 receptor agonists: a review of head-to-head clinical studies. *Ther Adv Endocrinol Metab*. 2015;6(1):19-28.
129. del Olmo-Garcia MI, Merino-Torres JF. GLP-1 receptor agonists and cardiovascular disease in patients with type 2 diabetes. *J Diabetes Res*. 2018 Apr 2;2018.

130. Filippatos TD, Panagiotopoulou TV, Elisaf MS. Adverse effects of GLP-1 receptor agonists. *Rev Diabet Stud.* 2015 Feb 10;11(3):202-30.
131. Nauck M. Incretin therapies: highlighting common features and differences in the modes of action of glucagon-like peptide-1 receptor agonists and dipeptidyl peptidase-4 inhibitors. *Diabetes Obes Metab.* 2015 Oct 22;18(3):203-16.
132. Boschmann M, Engeli S, Dobberstein K, Budziarek P, Strauss A, Boehnke J, et al. Dipeptidyl-peptidase-IV inhibition augments postprandial lipid mobilization and oxidation in type 2 diabetic patients. *Journal Clin Endocrinol Metab.* 2009 Mar 1;94(3):846-52.
133. Pathak R, Bridgeman MB. Dipeptidyl peptidase-4 (DPP-4) inhibitors in the management of diabetes. *Pharm Ther.* 2010 Sep;35(9):509-13.
134. Brown NJ, Vaughan DE. Angiotensin-converting enzyme inhibitors. *Circulation.* 1998 Apr 14;97(14):1411-20.
135. Khairnar AK, Baviskar DT, Jain DK. Angiotensin II receptor blockers: an overview. *Int J Pharm Sci.* 2012;4:50-6.
136. Taylor F, Ward K, Moore TH, Burke M, Smith GD, Casas JP, et al. Statins for the primary prevention of cardiovascular disease. *Cochrane Database Syst Rev.* 2011 Jan 19;(1).
137. Feingold KR. Cholesterol Lowering Drugs. In: Feingold KR, Anawalt B, Boyce A, et al., editors. *Endotext* [Internet]. South Dartmouth (MA): MDText.com, Inc.; 2000 [cited 2022 Apr 5]. Available from: <https://www.ncbi.nlm.nih.gov/books/NBK395573/>.
138. Ward NC, Watts GF, Eckel RH. Statin toxicity: mechanistic insights and clinical implications. *Circ Res.* 2019 Jan 17;124(2):328-50.
139. Schrör K, editor *Aspirin and platelets: the antiplatelet action of aspirin and its role in thrombosis treatment and prophylaxis.* *Semin Thromb Hemost.* 1997;23(4):349-56.
140. Secco GG, Parisi R, Mirabella F, Fattori R, Genoni G, Agostoni P, et al. P2Y12 inhibitors: pharmacologic mechanism and clinical relevance. *Cardiovasc Hematol Agents Med Chem.* 2013 Jun 1;11(2):101-5.

141. Angiolillo DJ, Rollini F, Storey RF, Bhatt DL, James S, Schneider DJ, et al. International expert consensus on switching platelet P2Y₁₂ receptor–inhibiting therapies. *Circulation*. 2017 Nov 14;136(20):1955-75.
142. Cheng G, Hao H, Dai M, Liu Z, Yuan Z. Antibacterial action of quinolones: from target to network. *Eur J Med Chem*. 2013 Aug 1;66:555-62.
143. Leshner GY, Froelich EJ, Gruett MD, Bailey JH, Brundage RP. 1, 8-Naphthyridine derivatives. A new class of chemotherapeutic agents. *J Med Chem*. 1962 Sep 1;5(5):1063-5.
144. Andriole VT. The quinolones: past, present, and future. *Clin Infect Dis*. 2005 Jul 15;41(suppl_2):S113-9.
145. Aldred KJ, Kerns RJ, Osheroff N. Mechanism of quinolone action and resistance. *Biochemistry*. 2014 Feb 27;53(10):1565-74.
146. Brighty KE, Gootz TD. The quinolones. 3rd ed. Boston: Academic press; 2000. Chapter 2, Chemistry and mechanism of action of the quinolone antibacterials; p. 33-97.
147. Holmes B, Brogden R, Richards D. Norfloxacin. *Drugs*. 1985 Dec;30(6):482-513.
148. Pham TD, Ziora ZM, Blaskovich MA. Quinolone antibiotics. *Med Chem Commun*. 2019 Jun 28;10(10):1719-39.
149. Wagstaff AJ, Balfour JA. Grepafloxacin. *Drugs*. 1997 May;53(5):817-24.
150. Barman Balfour JA, Wiseman LR. Moxifloxacin. *Drugs*. 1999 Mar;57(3):363-73.
151. Saravolatz LD, Leggett J. Gatifloxacin, gemifloxacin, and moxifloxacin: the role of 3 newer fluoroquinolones. *Clin Infect Dis*. 2003 Nov 1;37(9):1210-5.
152. Garey KW, Amsden GW. Trovafloxacin: an overview. *Pharmacotherapy: J Hum Pharmacol Drug Ther*. 1999 Jan 2;19(1):21-34.
153. Viollet B, Guigas B, Garcia NS, Leclerc J, Foretz M, Andreelli F. Cellular and molecular mechanisms of metformin: an overview. *Clin Sci*. 2012 Mar 1;122(6):253-70.
154. Lewis RJ, Mohr JF. Dysglycaemias and fluoroquinolones. *Drug Saf*. 2012 Oct 19;31(4):283-92.

155. Telfer SJ. Fluoroquinolone antibiotics and type 2 diabetes mellitus. *Med Hypotheses*. 2014 Sep;83(3):263-9.
156. Aspinall SL, Good CB, Jiang R, McCarren M, Dong D, Cunningham FE. Severe dysglycemia with the fluoroquinolones: a class effect?. *Clin Infect Dis*. 2009 Aug 1;49(3):402-8.
157. El Ghandour S, Azar ST. Dysglycemia associated with quinolones. *Prim Care Diabetes*. 2015 Jun 1;9(3):168-71.
158. Liu HH. Safety profile of the fluoroquinolones. *Drug Saf*. 2010 May 1;33(5):353-69.
159. Sibiya HP, Mabandla MV, Musabayane CT. The effects of transdermally delivered oleanolic acid on malaria parasites and blood glucose homeostasis in *P. berghei*-infected male Sprague-Dawley rats. *PLoS One*. 2016 Dec 1;11(12):e0167132.
160. Halaby M-J, Kastein BK, Yang D-Q. Chloroquine stimulates glucose uptake and glycogen synthase in muscle cells through activation of Akt. *Biochem Biophys Res Commun*. 2013 May 20;435(4):708-13.
161. McGill JB, Johnson M, Hurst S, Cade WT, Yarasheski KE, Ostlund RE, et al. Low dose chloroquine decreases insulin resistance in human metabolic syndrome but does not reduce carotid intima-media thickness. *Diabetol Metab Syndr*. 2019 Jul 29;11(61):1-16.
162. Yabe K, Yamamoto Y, Suzuki T, Takada S, Mori K. Functional and morphological characteristics of pancreatic islet lesions induced by quinolone antimicrobial agent gatifloxacin in rats. *Toxicol Pathol*. 2019;47(1):35-43.
163. Yamada C, Nagashima K, Takahashi A, Ueno H, Kawasaki Y, Yamada Y, et al. Gatifloxacin acutely stimulates insulin secretion and chronically suppresses insulin biosynthesis. *Eur J Pharmacol*. 2006 Dec;553(1-3):67-72.
164. Tomita T, Onishi M, Sato E, Kimura Y, Kihira K. Gatifloxacin induces augmented insulin release and intracellular insulin depletion of pancreatic islet cells. *Biol Pharm Bull*. 2007;30(4):644-7.
165. Ghaly H, Kriete C, Sahin S, Pflöger A, Holzgrabe U, Zünkler BJ, et al. The insulinotropic effect of fluoroquinolones. *Biochem Pharmacol*. 2009 Mar 15;77(6):1040-52.

166. Maeda N, Tamagawa T, Niki I, Miura H, Ozawa K, Watanabe G, et al. Increase in insulin release from rat pancreatic islets by quinolone antibiotics. *Br J Pharmacol*. 1996 Jan;117(2):372-6.
167. Saraya A, Yokokura M, Gono T, Seino S. Effects of fluoroquinolones on insulin secretion and β -cell ATP-sensitive K^+ channels. *Eur J Pharmacol*. 2004 Aug 16;497(1):111-7.
168. Owens Jr RC, Ambrose PG. Antimicrobial safety: focus on fluoroquinolones. *Clin Infect Dis*. 2005 Jul 15;41(suppl_2):S144-57.
169. Frothingham R. Glucose homeostasis abnormalities associated with use of gatifloxacin. *Clin Infect Dis*. 2005 Nov 1;41(9):1269-76.
170. Yoshimatsu Y, Ishizaka T, Chiba K, Mori K. Usefulness of simultaneous and sequential monitoring of glucose level and electrocardiogram in monkeys treated with gatifloxacin under conscious and nonrestricted conditions. *Exp Anim*. 2018 Jan 3;67(2):281-90.
171. Catero M. Dysglycemia and fluoroquinolones: are you putting patients at risk? Consider an alternative in patients with specific risk factors. *J Fam Pract*. 2007 Feb;56(2):101-7.
172. Gajjar DA, LaCreta FP, Kollia GD, Stolz RR, Berger S, Smith WB, et al. Effect of multiple-dose gatifloxacin or ciprofloxacin on glucose homeostasis and insulin production in patients with noninsulin-dependent diabetes mellitus maintained with diet and exercise. *Pharmacotherapy*. 2000 Jun;20(6P2):76S-86S.
173. Grasela DM. Clinical pharmacology of gatifloxacin, a new fluoroquinolone. *Clin Infect Dis*. 2000 Aug;31(suppl_2):S51-8.
174. Biggs WS. Hypoglycemia and hyperglycemia associated with gatifloxacin use in elderly patients. *J Am Board Fam Pract*. 2003 Sep-Oct;16(5):455-7.
175. Lodise T, Graves J, Miller C, Mohr JF, Lomaestro B, Smith RP. Effects of gatifloxacin and levofloxacin on rates of hypoglycemia and hyperglycemia among elderly hospitalized patients. *Pharmacotherapy*. 2007 Nov;27(11):1498-505.
176. Mohr JF, McKinnon PS, Peymann PJ, Kenton I, Septimus E, Okhuysen PC. A retrospective, comparative evaluation of dysglycemias in hospitalized patients receiving

- gatifloxacin, levofloxacin, ciprofloxacin, or ceftriaxone. *Pharmacotherapy: The Journal of Human Pharmacology and Drug Therapy*. 2005;25(10):1303-9.
177. Vinh H, Anh VT, Anh ND, Campbell JI, Hoang NV, Nga TV, et al. A multi-center randomized trial to assess the efficacy of gatifloxacin versus ciprofloxacin for the treatment of shigellosis in Vietnamese children. *PLoS Negl Trop Dis*. 2011 Aug 2;5(8):e1264.
 178. Kennedy KE, Teng C, Patek TM, Frei CR. Hypoglycemia associated with antibiotics alone and in combination with sulfonylureas and meglitinides: an epidemiologic surveillance study of the FDA Adverse Event Reporting System (FAERS). *Drug saf*. 2020 Apr;43(4):363-9.
 179. Berhe A, Russom M, Bahran F, Hagos G. Ciprofloxacin and risk of hypoglycemia in non-diabetic patients. *J Med Case Rep*. 2019 May 12;13(1):142.
 180. Roberge RJ, Kaplan R, Frank R, Fore C. Glyburide-ciprofloxacin interaction with resistant hypoglycemia. *Ann Emerg Med*. 2000 Aug;36(2):160-3.
 181. Edmont D, Rocher R, Plisson C, Chenault J. Synthesis and evaluation of quinoline carboxyguanidines as antidiabetic agents. *Bioorg Med Chem Lett*. 2000 Aug 21;10(16):1831-4.
 182. Muluk R KP, Kulkarni G, Ingale P. Synthesis and evaluation of some novel benzimidazole and quinolone derivatives for their antifungal and antidiabetic activity. *World J Pharm Pharm Sci*. 2017 Dec 27;7(1):1263-78.
 183. Daina A, Michielin O, Zoete V. SwissADME: a free web tool to evaluate pharmacokinetics, drug-likeness and medicinal chemistry friendliness of small molecules. *Sci Rep*. 2017 Mar 3;7:42717.
 184. Bhutkar M, Bhise S. In vitro assay of alpha amylase inhibitory activity of some indigenous plants. *Int J Chem Sci*. 2012;10(1):457-62.
 185. Kuddus M. *Enzymes in Food Biotechnology*. Boston: Academic press; 2019. Chapter 1, Introduction to food enzymes; p. 1-18.
 186. Srinivasan B. Words of advice: teaching enzyme kinetics. *FEBS J*. 2021 Apr;288(7):2068-83.

187. Bowden AC. Fundamentals of enzyme kinetics. 3rd ed. MedTech; 2017.
188. Dougall IG, Unitt J. The Practice of Medicinal Chemistry. 4th ed. Boston: Academic press; 2015. Chapter 2, Evaluation of the biological activity of compounds: techniques and mechanism of action studies; p. 15-43.
189. Delaune KP, Alsayouri K. Physiology, noncompetitive inhibitor [Internet]. Treasure Island (FL): StatPearls Publishing; 2019 [cited 2022 Aug 4]. Available from: <https://europepmc.org/article/nbk/nbk545242>
190. Saboury A. Enzyme inhibition and activation: a general theory. J Iran Chem Soc. 2009 Jun;6(2):219-29.
191. Deodhar M, Al Rihani SB, Arwood MJ, Darakjian L, Dow P, Turgeon J, et al. Mechanisms of CYP450 inhibition: understanding drug-drug interactions due to mechanism-based inhibition in clinical practice. Pharmaceutics. 2020 Sep 4;12(9):846.
192. Ramsay RR, Tipton KF. Assessment of enzyme inhibition: a review with examples from the development of monoamine oxidase and cholinesterase inhibitory drugs. Molecules. 2017 Jul 15;22(7):1192.
193. Bhatia A, Singh B, Arora R, Arora S. In vitro evaluation of the α -glucosidase inhibitory potential of methanolic extracts of traditionally used antidiabetic plants. BMC Complement Altern Med. 2019 Mar 25;19(1):74.
194. Song YH, Uddin Z, Jin YM, Li Z, Curtis-Long MJ, Kim KD, et al. Inhibition of protein tyrosine phosphatase (PTP1B) and α -glucosidase by geranylated flavonoids from *Paulownia tomentosa*. J Enzyme Inhib Med Chem. 2017 Dec;32(1):1195-202.
195. Kazeem MI, Adeyemi AA, Adenowo AF, Akinsanya MA. Carica papaya Linn. fruit extract inhibited the activities of aldose reductase and sorbitol dehydrogenase: possible mechanism for amelioration of diabetic complications. Futur J Pharm Sci. 2020 Nov 22;6:96.
196. Kwon YI, Apostolidis E, Kim YC, Shetty K. Health benefits of traditional corn, beans, and pumpkin: in vitro studies for hyperglycemia and hypertension management. J Med Food. 2007 Jun;10(2):266-75.

197. Benzie IF, Strain JJ. The ferric reducing ability of plasma (FRAP) as a measure of “antioxidant power”: the FRAP assay. *Anal Biochem.* 1996 Jul 15;239(1):70-6.
198. Cruz-Bermúdez A, Laza-Briviesca R, Vicente-Blanco RJ, García-Grande A, Coronado MJ, Laine-Menéndez S, et al. Cisplatin resistance involves a metabolic reprogramming through ROS and PGC-1 α in NSCLC which can be overcome by OXPHOS inhibition. *Free Radic Biol Med.* 2019 May 1;135:167-81.
199. Henneberry MO, Engel G, Grayhack JT. Acid phosphatase. *Urol Clin North Am.* 1979 Oct;6(3):629-41.
200. Yang TT, Sinai P, Kain SR. An acid phosphatase assay for quantifying the growth of adherent and nonadherent cells. *Anal Biochem.* 1996 Oct 1;241(1):103-8.
201. Schmidtke P, Barril X. Understanding and predicting druggability. A high-throughput method for detection of drug binding sites. *J Med Chem.* 2010 Aug 12;53(15):5858-67.
202. Lipinski CA, Lombardo F, Dominy BW, Feeney PJ. Experimental and computational approaches to estimate solubility and permeability in drug discovery and development settings. *Adv Drug Deliv Rev.* 2001 Mar 1;46(1-3):3-26.
203. Samanen J. Similarities and differences in the discovery and use of biopharmaceuticals and small-molecule chemotherapeutics. *Introduction Biol Small Mol Drug Res Dev.* 2013 Jan 1:161-203.
204. Lipinski CA. Lead-and drug-like compounds: the rule-of-five revolution. *Drug Discov Today Technol.* 2004 Dec;1(4):337-41.
205. Neidle S. Therapeutic applications of quadruplex nucleic acids. Boston: Academic press; 2012. Chapter 9, Design principles for quadruplex-binding small molecules; p. 151-74.
206. Turner J, Agatonovic-Kustrin S. In silico prediction of oral bioavailability. In: Testa B, Van de Waterbeemd H, editors. *Comprehensive medicinal chemistry II.* Oxford: Elsevier; 2007. p. 699-724.
207. Armstrong D, Li S, Friauff W, Martus H, Reilly J, Mikhailov D, et al. Predictive toxicology: latest scientific developments and their application in safety assessment. In:

- Chackalamannil S, Rotella DP, Ward SE, editors. *Comprehensive medicinal chemistry III*. 3rd ed. Oxford: Elsevier; 2017. p. 94-115.
208. Gao Y, Gesenberg C, Zheng W. *Developing solid oral dosage forms*. 2nd ed. Boston: Academic press; 2017. Chapter 17, Oral formulations for preclinical studies: principle, design, and development considerations: p. 455-95.
209. Coimbra JT, Feghali R, Ribeiro RP, Ramos MJ, Fernandes PA. The importance of intramolecular hydrogen bonds on the translocation of the small drug piracetam through a lipid bilayer. *RSC Adv*. 2021 Jan 4;11(2):899-908.
210. Alex A, Millan DS, Perez M, Wakenhut F, Whitlock GA. Intramolecular hydrogen bonding to improve membrane permeability and absorption in beyond rule of five chemical space. *Med Chem Commun*. 2011 May 20;2(7):669-74.
211. O'Hagan S, Swainston N, Handl J, Kell DB. A 'rule of 0.5' for the metabolite-likeness of approved pharmaceutical drugs. *Metabolomics*. 2015 Apr;11(2):323-39.
212. Benet LZ, Hosey CM, Ursu O, Oprea TI. BDDCS, the Rule of 5 and drugability. *Adv Drug Deliv Rev*. 2016 Jun 1;101:89-98.
213. Al-Asri J, Wolber G. Discovery of novel α -amylase inhibitors using structure-based drug design. *J Cheminform*. 2014 Mar 11;6(supp_1):P50.
214. Giuberti G, Rocchetti G, Lucini L. Interactions between phenolic compounds, amylolytic enzymes and starch: An updated overview. *Curr Opin Food Sci*. 2020 Feb;31:102-13.
215. Nawaz M, Taha M, Qureshi F, Ullah N, Selvaraj M, Shahzad S, et al. Structural elucidation, molecular docking, α -amylase and α -glucosidase inhibition studies of 5-amino-nicotinic acid derivatives. *BMC Chem*. 2020 Jul 14;14:43.
216. Hawash M, Jaradat N, Shekfeh S, Abualhasan M, Eid AM, Issa L. Molecular docking, chemo-informatic properties, alpha-amylase, and lipase inhibition studies of benzodioxol derivatives. *BMC Chem*. 2021 Dec;15(1):40.
217. Apostolidis E, Kwon YI, Shetty K. Inhibitory potential of herb, fruit, and fungal-enriched cheese against key enzymes linked to type 2 diabetes and hypertension. *Inno Food Sci Emerg Technol*. 2007 Mar 1;8(1):46-54.

218. Etxeberria U, de la Garza AL, Campión J, Martínez JA, Milagro FI. Antidiabetic effects of natural plant extracts via inhibition of carbohydrate hydrolysis enzymes with emphasis on pancreatic alpha amylase. *Expert Opin Ther Targets*. 2012 Mar;16(3):269-97.
219. Park H, Hwang KY, Kim YH, Oh KH, Lee JY, Kim K. Discovery and biological evaluation of novel α -glucosidase inhibitors with in vivo antidiabetic effect. *Bioorg Med Chem Lett*. 2008 Jul 1;18(13):3711-5.
220. Chen JG, Wu SF, Zhang QF, Yin ZP, Zhang L. α -Glucosidase inhibitory effect of anthocyanins from *Cinnamomum camphora* fruit: Inhibition kinetics and mechanistic insights through in vitro and in silico studies. *Int J Biol Macromol*. 2020 Jan 15;143:696-703.
221. Wang SM, Pae CU. Biomarkers in bipolar disorders. Boston: Academic press; 2022. Chapter 23, Bipolar disorder and plasticity: a key target for new treatment; p. 439-57.
222. Maher S, Brayden DJ. Formulation strategies to improve the efficacy of intestinal permeation enhancers. *Adv Drug Deliv Rev*. 2021 Oct;177:113925.
223. Avogaro A, Dardano A, De Kreutzenberg S, Del Prato S. Dipeptidyl peptidase-4 inhibitors can minimize the hypoglycaemic burden and enhance safety in elderly people with diabetes. *Diabetes Obes Metab*. 2015 Feb;17(2):107-15.
224. Mourad AA, Khodir AE, Saber S, Mourad MA. Novel potent and selective DPP-4 inhibitors: design, synthesis and molecular docking study of dihydropyrimidine phthalimide hybrids. *Pharmaceuticals*. 2021 Feb 11;14(2):144.
225. Schwehm C, Li J, Song H, Hu X, Kellam B, Stocks MJ. Synthesis of new DPP-4 inhibitors based on a novel tricyclic scaffold. *ACS Med Chem Lett*. 2015 Jan 13;6(3):324-8.
226. Deacon CF. Physiology and pharmacology of DPP-4 in glucose homeostasis and the treatment of type 2 diabetes. *Front Endocrinol*. 2019 Feb 15;10:80.
227. Herman GA, Bergman A, Stevens C, Kotey P, Yi B, Zhao P, et al. Effect of single oral doses of sitagliptin, a dipeptidyl peptidase-4 inhibitor, on incretin and plasma glucose levels after an oral glucose tolerance test in patients with type 2 diabetes. *J Clin Endocrinol Metab*. 2006 Nov;91(11):4612-9.

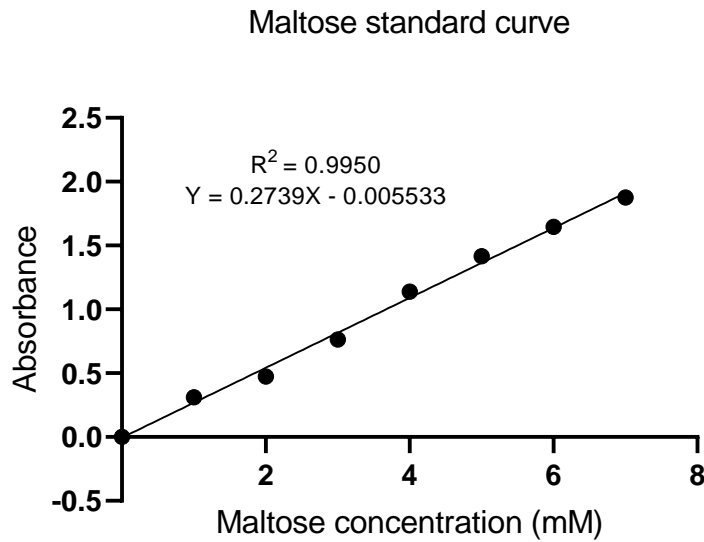
228. Pantaleão SQ, Philot EA, de Resende-Lara PT, Lima AN, Perahia D, Miteva MA, et al. Structural dynamics of DPP-4 and its influence on the projection of bioactive ligands. *Molecules*. 2018 Feb 23;23(2):490.
229. Rajapaksa NS, Lin X. Dipeptidyl peptidase-4 (DPP-4)-inhibiting amides for the treatment of diabetes. In: Lamberth C, Dinges J, editors. *Bioactive carboxylic compound classes: pharmaceuticals and agrochemicals*. Wiley-VCH; 2016. p. 177-96.
230. Kumar S, Mittal A, Mittal A. A review upon medicinal perspective and designing rationale of DPP-4 inhibitors. *Bioorg Med Chem*. 2021 Sep 15;46:116354.
231. Arulmozhiraja S, Matsuo N, Ishitsubo E, Okazaki S, Shimano H, Tokiwa H. Comparative binding analysis of dipeptidyl peptidase IV (DPP-4) with antidiabetic drugs—an ab initio fragment molecular orbital study. *PLoS One*. 2016 Nov 10;11(11):e0166275.
232. Zhao D, Sun L, Zhong S. Discovery of inhibitors targeting protein tyrosine phosphatase 1B using a combined virtual screening approach. *Mol Divers*. 2022 Aug;26(4):2159-74.
233. Johnson TO, Ermolieff J, Jirousek MR. Protein tyrosine phosphatase 1B inhibitors for diabetes. *Nat Rev Drug Discov*. 2002 Sep;1(9):696-709.
234. Deshpande T, Isshak M, Prierer R. PTP1B inhibitors as potential target for type II diabetes. *Curr Res Diabetes Obes J*. 2020;14:555876.
235. Liu R, Mathieu C, Berthelet J, Zhang W, Dupret J-M, Rodrigues Lima F. Human Protein Tyrosine Phosphatase 1B (PTP1B): From Structure to Clinical Inhibitor Perspectives. *Int J Mol Sci*. 2022 Jun 24;23(13):7027.
236. Zhi Y, Gao LX, Jin Y, Tang CL, Li JY, Li J, et al. 4-Quinolone-3-carboxylic acids as cell-permeable inhibitors of protein tyrosine phosphatase 1B. *Bioorg Medicinal Chemistry*. 2014 Jul 15;22(14):3670-83.
237. Roy D, Perreault M, Marette A. Insulin stimulation of glucose uptake in skeletal muscles and adipose tissues in vivo is NO dependent. *Am J Physiol Endocrinol Metab*. 1998 Apr;274(4):E692-9.

238. Honka MJ, Latva-Rasku A, Bucci M, Virtanen KA, Hannukainen JC, Kalliokoski KK, et al. Insulin-stimulated glucose uptake in skeletal muscle, adipose tissue and liver: a positron emission tomography study. *Eur J Endocrinol*. 2018 May;178(5):523-31.
239. DeFronzo RA. From the triumvirate to the ominous octet: a new paradigm for the treatment of type 2 diabetes mellitus. *Diabetes*. 2009 Apr;58(4):773-95.
240. López-García J, Lehocký M, Humpolíček P, Sába P. HaCaT keratinocytes response on antimicrobial atelocollagen substrates: extent of cytotoxicity, cell viability and proliferation. *J Funct Biomater*. 2014 May 8;5(2):43-57.
241. Steuber H, Heine A, Podjarny A, Klebe G. Merging the binding sites of aldose and aldehyde reductase for detection of inhibitor selectivity-determining features. *J Mol Biol*. 2008 Jun 20;379(5):991-1016.
242. El-Kabbani O, Wilson DK, Petrash M, Quijcho FA. Structural features of the aldose reductase and aldehyde reductase inhibitor-binding sites. *Mol Vis*. 1998 Sep 29;4:19.
243. Balestri F, Moschini R, Mura U, Cappiello M, Del Corso A. In Search of Differential Inhibitors of Aldose Reductase. *Biomolecules*. 2022 Mar 22;12(4):485.
244. Becker RC. Factor Xa inhibitors: critical considerations for clinical development and testing. *J Thromb Thrombolysis*. 2021 Aug;52(2):397-402.
245. Hitchings A, Lonsdale D, Burrage D, Baker E. The top 100 drugs: clinical pharmacology and practical prescribing. 2nd ed. Oxford: Elsevier; 2018. 325 p.
246. Pinto DJ, Smallheer JM, Cheney DL, Knabb RM, Wexler RR. Factor Xa inhibitors: next-generation antithrombotic agents. *J Med Chem*. 2010 Sep 9;53(17):6243-74.
247. Deichmann R, Lavie C, Andrews S. Coenzyme q10 and statin-induced mitochondrial dysfunction. *Ochsner J*. 2010;10(1):16-21.
248. Roche VF. Antihyperlipidemic statins: a self-contained, clinically relevant medicinal chemistry lesson. *Am J Pharm Educ*. 2005;69(1-5):546-60.
249. Istvan ES, Deisenhofer J. Structural mechanism for statin inhibition of HMG-CoA reductase. *Science*. 2001 May 11;292(5519):1160-4.

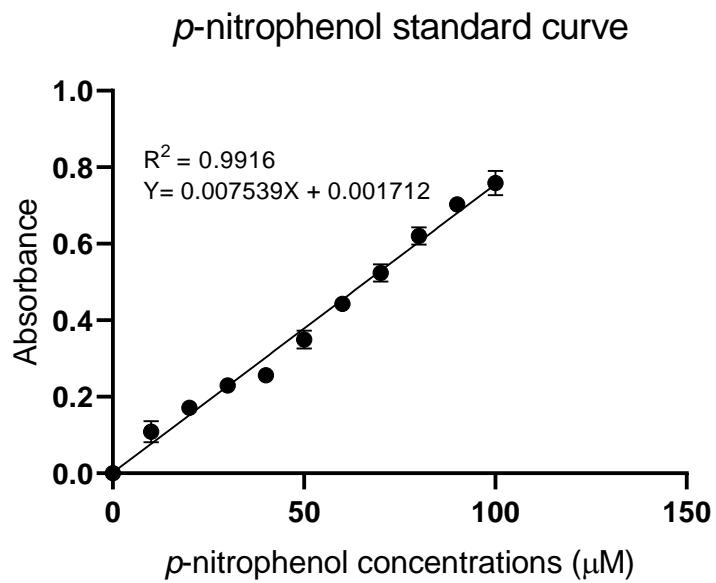
250. Prasad MV, Rao RH, Veeranna V, Chennupalli VS, Sathish B. Novel Quinolone Derivatives: Synthesis and Antioxidant Activity. Russ J Gen Chem. 2021;91(12):2522-6.

APPENDICES

Appendix 1: Maltose standard curve used to determine the kinetic mode of inhibition of alpha-amylase by QD4.

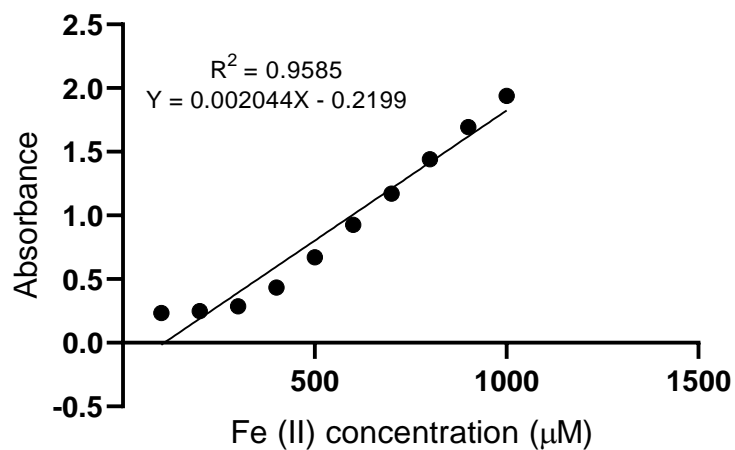


Appendix 2: *p*-Nitrophenol standard curve used to determine the kinetic mode of inhibition of alpha-glucosidase by QD1.



Appendix 3: Fe(II) standard curve used to determine the ferric reducing antioxidant power of quinolone derivatives.

Fe (II) standard curve



Appendix 4: Abstract of a published review article that was submitted to Current Reviews in Clinical and Experimental Pharmacology.

Curr Rev Clin Exp Pharmacol. 2022 Feb 18. doi: 10.2174/2772432817666220218101050.
Online ahead of print.

Fluoroquinolone-Induced Glycaemic Aberrations: Could Quinolones Be Repurposed To Serve As New Antidiabetic Agents?

Omobonlale Ayodele ¹, Setshaba Khanye ², Mamosheledi Mothibe ¹, Ntethelelo Sibiya ¹

Affiliations

PMID: 35184708 DOI: 10.2174/2772432817666220218101050

Abstract

Nalidixic acid is a synthetic antibiotic discovered in the 1960s during the synthesis of chloroquine, an effective drug for treating malaria. Nalidixic acid became the backbone for developing quinolones that are now widely used clinically for the treatment of various bacterial infections. The mechanism of action of quinolone involves the inhibition of topoisomerase II and topoisomerase IV. In attempts to improve the potency of fluoroquinolones, modifications were made; these modifications resulted in the emergence of newer generations of fluoroquinolones. Also, due to these modifications, several side effects were noted, including blood glucose control aberrations. Among fluoroquinolones that disrupt glucose homeostasis is gatifloxacin, which is in the third-generation category. Fluoroquinolones have been demonstrated to induce glycaemic aberrations by enhancing pancreatic cells' insulin secretion and interaction with antidiabetic agents via inhibition of cytochrome P 450 enzymes. Considering their ability to induce hypoglycaemia, few studies have reported repurposing of quinolones as an antidiabetic agent. Hyperglycaemia has also been reported, often preceding hypoglycaemia. Due to the ability to decrease blood glucose, it is not surprising that some authors have reported on novel quinolones derivatives with antidiabetic properties in experimental studies. However, there is still a paucity of data regarding the effect of quinolones derivatives on glycaemic control. Understanding how fluoroquinolones lower blood glucose concentration could serve as the basis in developing novel quinolone-derivatives with a sole purpose of lowering blood glucose concentrations. Although there are various conventional anti-hyperglycaemic agents, however due to their associated shortfalls as well as an increase in the prevalence of diabetes, the discovery and development of new antidiabetics is warranted.

Keywords: Quinolones; antidiabetic activity; diabetes mellitus; glycaemic; hyperglycaemia; hypoglycaemia.

Copyright© Bentham Science Publishers; For any queries, please email at epub@benthamscience.net.

Appendix 5: Abstract for a presentation that was presented during the Faculty of Pharmacy postgraduate research day 2022

Omobolanle Ayodele

– MSP candidate

INVESTIGATING THE EFFECT OF NOVEL QUINOLONE DERIVATIVE COMPOUNDS ON GLUCOSE UPTAKE IN SKELETAL MUSCLE AND HEPATIC CELL LINES

A OMOBOLANLE, N SIBIYA, SD KHANYE

¹Pharmacology Division,

²Pharmaceutical Chemistry Division

Background

DM is one of the major endocrine disorders found in every population and region of the world. Studies have reported that the number of people diagnosed with DM is steadily rising. The conventional treatment presents with side effects, and over time they become less effective. Therefore, there is a need to investigate novel compounds that will provide prolonged efficacy with minimal side effects.

Method

In this study, separate preparations of skeletal muscle (C2C12 myoblast) and hepatic (HepG2) cell lines in 24-well plates were exposed to quinolone derivatives (15, 30 and 60 µg/mL for 24 hours), after which glucose uptake and cell viability were assessed.

Result

The glucose uptake assay result showed that the compounds have no substantial effect on glucose uptake compared to the control group and the quinolone derivatives were non-cytotoxic in both cell lines.

Conclusion

The investigated quinolone derivatives exhibited a poor effect on glucose uptake. The lack of a substantial effect on glucose uptake cannot be attributed to a cytotoxic effect. Therefore, our compounds cannot work as insulin mimetics.